

2004

# Supervisory control of machine tool feed drives.

Rami. Shahin  
*University of Windsor*

Follow this and additional works at: <http://scholar.uwindsor.ca/etd>

---

## Recommended Citation

Shahin, Rami., "Supervisory control of machine tool feed drives." (2004). *Electronic Theses and Dissertations*. Paper 3669.

This online database contains the full-text of PhD dissertations and Masters' theses of University of Windsor students from 1954 forward. These documents are made available for personal study and research purposes only, in accordance with the Canadian Copyright Act and the Creative Commons license—CC BY-NC-ND (Attribution, Non-Commercial, No Derivative Works). Under this license, works must always be attributed to the copyright holder (original author), cannot be used for any commercial purposes, and may not be altered. Any other use would require the permission of the copyright holder. Students may inquire about withdrawing their dissertation and/or thesis from this database. For additional inquiries, please contact the repository administrator via email ([scholarship@uwindsor.ca](mailto:scholarship@uwindsor.ca)) or by telephone at 519-253-3000ext. 3208.

# **Supervisory Control of Machine Tool Feed Drives**

by

Rami Shahin

A Thesis

Submitted to the Faculty of Graduate Studies and Research  
through the Department of Industrial and Manufacturing Systems Engineering  
in Partial Fulfillment of the Requirements for  
the Degree of Master of Applied Science at the  
University of Windsor

Windsor, Ontario, Canada

2004

© 2004 Rami Shahin



Library and  
Archives Canada

Bibliothèque et  
Archives Canada

Published Heritage  
Branch

Direction du  
Patrimoine de l'édition

395 Wellington Street  
Ottawa ON K1A 0N4  
Canada

395, rue Wellington  
Ottawa ON K1A 0N4  
Canada

*Your file    Votre référence*

*ISBN: 0-612-96400-0*

*Our file    Notre référence*

*ISBN: 0-612-96400-0*

The author has granted a non-exclusive license allowing the Library and Archives Canada to reproduce, loan, distribute or sell copies of this thesis in microform, paper or electronic formats.

L'auteur a accordé une licence non exclusive permettant à la Bibliothèque et Archives Canada de reproduire, prêter, distribuer ou vendre des copies de cette thèse sous la forme de microfiche/film, de reproduction sur papier ou sur format électronique.

The author retains ownership of the copyright in this thesis. Neither the thesis nor substantial extracts from it may be printed or otherwise reproduced without the author's permission.

L'auteur conserve la propriété du droit d'auteur qui protège cette thèse. Ni la thèse ni des extraits substantiels de celle-ci ne doivent être imprimés ou autrement reproduits sans son autorisation.

---

In compliance with the Canadian Privacy Act some supporting forms may have been removed from this thesis.

Conformément à la loi canadienne sur la protection de la vie privée, quelques formulaires secondaires ont été enlevés de cette thèse.

While these forms may be included in the document page count, their removal does not represent any loss of content from the thesis.

Bien que ces formulaires aient inclus dans la pagination, il n'y aura aucun contenu manquant.

# Canada

# ABSTRACT

Currently industries are beginning to look at Reconfigurable Manufacturing Systems (RMS) concepts to be realized and attained possibly within the next few years. Unified Reconfigurable Open Control Architecture (UROCA) is a strategic research project carried out at the Intelligent Manufacturing Systems Centre (IMS) at the University of Windsor, which aims at unifying the reconfiguration aspects and managing the interaction amongst the different operating levels of individual machining control systems (CNC) which perform in a reconfigurable manufacturing system. The hierarchical control structure of UROCA demands the usage of a supervisory control scheme to manage servo controllers and their interactions with the machining process. The main function of the supervisory unit is to serve as a switching/reconfiguring logic amongst different available controllers, according to need, in order to maintain motion output within the permitted limits. Presumably, reconfiguration occurs due to emergent need well represented by change in either functionality or system capacity. Aspects of reconfiguration are numerous depicting continual changes in process functionality.

While motion control of machine tool feed drives is the targeted application. The goal of this study is to explore the relative performance potentials of supervisory control systems against the classical servo control systems; Reconfiguration aspects at the control level are the scope of this study.

One of the most essential nonlinear problems faced during modeling and control stages of the CNC machining systems is called backlash. Reversal of motion for each moving axis can lead to that area of disengagement where backlash occurs due to inherently unavoidable clearance between linkages of the machine tool feed drive system. Due to backlash, efficiency of machine tools will be undesirably turned down causing higher vibrations, lower contouring accuracy, and may draw the whole system into instability region. A Switching control scheme is designed to manage the control process where two different controllers with two different control functionalities, acting differently in two vital zones – one of them where the backlash lies, and the other when moving past the backlash – seem to be an important need. Each control



is activated at a time, under the supervision of an appropriate logic decision unit. The control functionality in the contact zone is dedicated to achieving the best possible tracking performance. While, in the backlash (non-contact) zone, the control functionality will be devoted to bring the system back in contact as fast and effective as it can. The contact-mode controller is to control the motor position with respect to the reference position, while the backlash-mode controller is to control the load position with respect to motor position.

Three switching schemes have been formulated, introduced and simulated. In our proposed switching schemes, results are successful findings for both position and feedrate outputs. Hence, it emphasizes that the output of this thesis depicts a reconfiguration aspect on the control process level for machine tools as perceived, investigated and resolved by the physical and control layers located at the left brain of UROCA architecture.

# ACKNOWLEDGEMENTS

God and My parents, in spite of circumstances, are naturally largely responsible for any of this happening to me in the first place. Much of the intensity of my experience at the University of Windsor, and the invaluable measures of achievement I can now be so proud of, will be remembered by a close circle of people whom I would like to recognize first and foremost. I love you all dearly, and I hope to make you proud.

Prof. Waguih ElMaraghy's unwavering support of my studies at the University of Windsor over the past three years has made this work possible. I am utterly unable to express in words the depth of my appreciation for this man's kind mentorship, his academic support, and also financial support throughout my Master's career. His unequivocal faith and devotion helped me through some of the most moments of professional growth I have experienced during my studies within the Department of Industrial and Manufacturing Systems Engineering. Thank you so much.

Within our excellent UROCA research group, Dr. ElSayed ElBeheiry, who helped me actualize a promising and exciting career in what I always wanted to pursue, but didn't even know could possibly be, who influenced and supported me greatly, with whom I shared moments of triumph and devastation, philosophical and technical inquiry, and numerous talks over good and frothy coffees. I learned a lot of this man, and he was never complaining about it. Thank you sp much. Ana Djuric, my friend and colleague who works at the parallel robotics application for UROCA, thank you for the good times we have spent together in lab B-24. Also, thanks to IMS research centre directors for giving me the chance to discuss points of interest with other fellow members through the regular meetings they kindly arranged for us. Special thanks to my colleague and friend Ahmad ElShennawy for his true friendship and support, may God bless you all.

# TABLE OF CONTENTS

<b>ABSTRACT.....</b>	<b>iii</b>
<b>ACKNOWLEDGEMENTS .....</b>	<b>v</b>
<b>LIST OF FIGURES.....</b>	<b>ix</b>
<b>NOMENCLATURE.....</b>	<b>xiv</b>
<b>CHAPTER</b>	
<b>1. INTRODUCTION .....</b>	<b>1</b>
1.1. NUMERICAL CONTROL TECHNOLOGY .....	1
1.2. MACHINE TOOL STRUCTURE.....	2
1.2.1. Mechanical Structure .....	2
1.2.2. Drives.....	3
1.2.3. Controls.....	3
1.3. CAM-CNC INTEGRATION CYCLE.....	4
1.4. RECONFIGURABLE MANUFACTURING SYSTEMS AND UROCA .....	6
1.5. SIMILARITIES AND DIFFERENCES AMONG CNC MACHINE TOOLS.....	12
1.5.1. Measures of Comparison .....	12
1.5.2. Positioning (Point-to-Point) and Contouring Systems.....	14
1.5.3. Open-Loop and Closed-Loop Systems .....	15
1.5.4. Machine Tool Joint Types .....	16
1.6. SWITCHING NEED: THE BACKLASH PROBLEM .....	19
1.6.1. Defintion of Backlash .....	20
1.6.2. Understanding Backlash .....	21
1.6.3. Trends of Backlash Research.....	21
1.7. MOTIVATION FOR THE STUDY OF BACKLASH.....	23
1.8. THESIS ORGANIZATION .....	24
<b>2. ASPECTS OF RECONFIGURATION IN CNC MACHINE TOOLS. 25</b>	
2.1. INTRODUCTION.....	25
2.2. SYSTEM LEVEL RECONFIGURATION .....	26

2.3. SOFTWARE LEVEL RECONFIGURATION .....	28
2.4. MACHINE LEVEL RECONFIGURATION .....	30
2.5. CONTROL LEVEL RECONFIGURATION .....	34
2.6. PROCESS LEVEL RECONFIGURATION .....	37
<b>3. MODELING OF CNC MACHINE TOOL FEED DRIVES .....</b>	<b>40</b>
3.1. INTRODUCTION.....	40
3.2. FEED DRIVE SYSTEMS.....	41
3.3. FEED DRIVE MODELING .....	45
3.3.1. Modeling from an Electrical Scope Perspective.....	45
3.3.2. Modeling from a Mechanical Scope Perspective.....	47
3.3.3. Stiffness Modeling.....	50
3.4. BACKLASH MODELS.....	52
3.4.1. Dead Zone Models.....	52
3.4.2. Describing Functions .....	54
3.4.3. The Hysteresis Model .....	55
3.5. MODELING FOR BACKLASH CONTROL .....	56
<b>4. CONTROLLING OF CNC MACHINE TOOL FEED DRIVES .....</b>	<b>59</b>
4.1. INTRODUCTION.....	59
4.1.1. Principles of Machine Tool Control .....	59
4.1.2. General Trends in CNC Machine Tools Research.....	60
4.2. REVIEW OF DIFFERENT BACKLASH CONTROL STRATEGIES.....	63
4.2.1. Conventional Linear Control .....	63
4.2.2. Switching Control.....	68
4.2.3. Adaptive Control.....	70
4.2.4. Other Types of Backlash Control .....	71
4.3. CONTROL DESIGN .....	72
4.3.1. Tracking Control Design Techniques.....	74
4.3.1.1. PID Controllers.....	74
4.3.1.2. Model-based Control for Contact Zone.....	76
4.3.2. Dead-Zone Control Design Techniques.....	78

4.3.2.1. Model-based Control for Backlash Zone.....	78
4.3.2.2. Rendezvous Problem .....	79
4.3.1. Switching Control.....	82
<b>5. TOOLS AND IMPLEMENTATION ISSUES.....</b>	<b>85</b>
5.1. MATLAB/SIMULINK OVERVIEW.....	85
5.2. PROPOSAL FOR HARDWARE-IN-THE-LOOP SYSTEM IMPLEMENTATION	87
<b>6. SIMULATION RESULTS .....</b>	<b>94</b>
6.1. FEED DRIVE TESTING PROCEDURE.....	94
6.2. PI CONTROL APPLICATION.....	95
6.3. MODEL-BASED CONTROL APPLICATION.....	105
6.4. SWITCHING CONTROL APPLICATION .....	109
6.4.1. Switching Control Scheme I.....	109
6.4.2. Switching Control Scheme II.....	113
6.4.3. Switching Control Scheme III .....	117
6.4.4. Results Discussion and General Comparison.....	121
<b>7. CONCLUSION .....</b>	<b>125</b>
<b>8. FUTURE WORK.....</b>	<b>127</b>

## APPENDIX A

<b>SWITCHING SCHEMES CONTROL ALGORITHMS.....</b>	<b>128</b>
<b>REFERENCES.....</b>	<b>140</b>
<b>VITA AUCTORIS .....</b>	<b>152</b>

# LIST OF FIGURES

<b>Figure 1.1.</b> Nature of information transfer of a CAM/CNC stage of product synthesis....	4
<b>Figure 1.2.</b> Machining of 2-D circular contours: a) convex, b) concave. ....	6
<b>Figure 1.3.</b> UROCA design methodology classification [ElBeheiry <i>et al.</i> , 2004].....	10
<b>Figure 1.4.</b> UROCA left brain at the intermediate (planning) and physical layer; the shaded area represents my scope of work [ElBeheiry <i>et al.</i> , 2004, <i>Reprod.</i> ].....	10
<b>Figure 1.5.</b> Supervisory control design for UROCA [ElBeheiry <i>et al.</i> , 2004].....	12
<b>Figure 1.6.</b> Schematic drawing for a turning machine tool.....	17
<b>Figure 1.7.</b> Schematic drawing for 5-axis milling machine ( <i>TTR-RT</i> ).. ....	18
<b>Figure 1.8.</b> Schematic drawing for 3-axis milling machine.....	18
<b>Figure 1.9.</b> Schematic drawing for 5-axis milling machine ( <i>TRR-TT</i> ).. ....	19
<b>Figure 2.1.</b> Aspects of reconfiguration chart [ <i>reprod. from</i> Mehrabi <i>et al.</i> , 2000].....	25
<b>Figure 2.2.</b> Development matrix of software versus hardware for machine tools [ <i>reprod. from</i> Mehrabi <i>et al.</i> , 2000].....	26
<b>Figure 2.3.</b> Possible system configurations with four machines.....	27
<b>Figure 2.4.</b> Machine tool controller principle as seen from an “open” point of view.....	29
<b>Figure 2.5.</b> Data interaction between the real-time database and controllers.. ....	30
<b>Figure 2.6.</b> An example of reconfigurable modules of machine tools [Pritschow <i>et al.</i> , 2003]... ..	31
<b>Figure 2.7.</b> Modularization of machine tool components as proposed by [Pritschow <i>et al.</i> , 2003].. ....	32
<b>Figure 2.8.</b> Communication system for a reconfigurable machine tool, [Pritschow <i>et al.</i> , 1997]... ..	35
<b>Figure 2.9.</b> Mapping theory vision for reconfigurable monitoring systems [ <i>reprod. from</i> Elijah Kannatey-Asibu].....	36
<b>Figure 2.10.</b> Definition of Fault domain and Sensor domain [Elijah Kannatey-Asibu]....	37
<b>Figure 2.11.</b> Ramp-up methodology [ <i>reprod. from</i> Mehrabi <i>et al.</i> , 2000].....	38
<b>Figure 3.1.</b> Schematic Diagram of a spindle system.....	41
<b>Figure 3.2.</b> Schematic diagram for a translational feed drive.....	42

<b>Figure 3.3.</b> Classification motors used in machine tools ( <i>Reprod. from Weck, 1984</i> ). ....	43
<b>Figure 3.4.</b> Generalized feed drive components .....	44
<b>Figure 3.5.</b> Schematic diagram demonstrates a rotational feed drive.....	45
<b>Figure 3.6.</b> Detailed dynamic model for a transverse feed drive ( <i>Reprod. from [Tsutsumi et al., 1996]</i> ).....	47
<b>Figure 3.7.</b> An extended-form block diagram for a feed drive system as conceived from [Tsutsumi et al., 1996] formulation.....	49
<b>Figure 3.8.</b> Stiffness model as proposed by [Ebrahimi et al, 2000]. .....	50
<b>Figure 3.9.</b> Feed drive mechanism plant block diagram.....	51
<b>Figure 3.10.</b> Backlash in two-inertia system.....	52
<b>Figure 3.11.</b> The dead zone backlash model.....	53
<b>Figure 3.12.</b> Backlash model within a feed drive system .....	57
<b>Figure 4.1.</b> A block diagram represents a general depiction of machine tool feed drives.....	59
<b>Figure 4.2.</b> Contour error as introduced by [Koren, 1980].....	61
<b>Figure 4.3.</b> Linear feedback from motor speed.....	64
<b>Figure 4.4.</b> Vision of our switching control for backlash compensation.....	73
<b>Figure 4.5.</b> Proportional-Integral (PI) control law for a 2-DOF feed drive model .....	75
<b>Figure 4.6.</b> Switching occurrences along the timeline defining all time values related to backlash zone .....	79
<b>Figure 5.1.</b> Simulink block structure.....	86
<b>Figure 5.2.</b> Hardware-in-the-Loop (HIL) vision for simulating a feed drive system within UROCA architecture.....	88
<b>Figure 5.3.</b> Plant control test distributed over several computation nodes.....	89
<b>Figure 5.4.</b> Categorization in Simulink model to be ready for RT-LAB usage.....	90
<b>Figure 5.5.</b> Addition of OpCom blocks to save real-time communication setup.....	91
<b>Figure 5.6.</b> Specialized block to represent ECU as implementation issue.....	92
<b>Figure 5.7.</b> Different possibilities of partitioning feed drive model into submodels and different paths along modules through simulation and/or real environment.....	93
<b>Figure 6.1.</b> Feed drive transient response (ramp input = 500 mm/min): a) without backlash. b) with 50 $\mu$ m backlash.....	96

<b>Figure 6.2.</b> Feed drive transient response (ramp input = 1000 mm/min): a) without backlash. b) with 50 $\mu$ m backlash.....	97
<b>Figure 6.3.</b> Feed drive transient response (ramp input = 2000 mm/min): a) without backlash. b) with 50 $\mu$ m backlash.....	98
<b>Figure 6.4.</b> Feed drive transient response (ramp input = 4000 mm/min): a) without backlash. b) with 25 $\mu$ m backlash.....	99
<b>Figure 6.5.</b> Feed drive transient response (ramp input = 8000 mm/min): a) without backlash. b) with 25 $\mu$ m backlash.....	100
<b>Figure 6.6.</b> Feed drive circular test (feedrate = 4000 mm/min): a) without backlash. b) with 25 $\mu$ m backlash.....	101
<b>Figure 6.7.</b> Feed drive circular test (feedrate = 6000 mm/min): a) without backlash. b) with 25 $\mu$ m backlash.....	102
<b>Figure 6.8.</b> Feed drive circular test (feedrate = 8000 mm/min): a) without backlash. b) with 25 $\mu$ m backlash.....	103
<b>Figure 6.9.</b> Feed drive circular test (feedrate = 8000 mm/min) with 25 $\mu$ m backlash.....	105
<b>Figure 6.10.</b> Position error of x-axis for a single controller set-up (no switching) with feedrate of 4000 mm/min.....	106
<b>Figure 6.11.</b> Position error of y-axis for a single controller set-up (no switching) with feedrate of 4000 mm/min.....	106
<b>Figure 6.12.</b> Position error of x-axis for a single controller set-up (no switching) with feedrate of 6000 mm/min.....	107
<b>Figure 6.13.</b> Position error of y-axis for a single controller set-up (no switching) with feedrate of 6000 mm/min.....	107
<b>Figure 6.14.</b> Position error of x-axis for a single controller set-up (no switching) with feedrate of 8000 mm/min.....	108
<b>Figure 6.15.</b> Position error of y-axis for a single controller set-up (no switching) with feedrate of 8000 mm/min.....	108
<b>Figure 6.16.</b> Position error of x-axis for switching controller I set-up with feedrate of 4000 mm/min.....	110



<b>Figure 6.17.</b> Position error of y-axis for switching controller I set-up with feedrate of 4000 mm/min.....	110
<b>Figure 6.18.</b> Position error of x-axis for switching controller I set-up with feedrate of 6000 mm/min.....	111
<b>Figure 6.19.</b> Position error of y-axis for switching controller I set-up with feedrate of 6000 mm/min.....	111
<b>Figure 6.20.</b> Position error of x-axis for switching controller I set-up with feedrate of 8000 mm/min.....	112
<b>Figure 6.21.</b> Position error of y-axis for switching controller I set-up with feedrate of 8000 mm/min.....	112
<b>Figure 6.22.</b> Position error of x-axis for switching controller II set-up with feedrate of 4000 mm/min.....	114
<b>Figure 6.23.</b> Position error of y-axis for switching controller II set-up with feedrate of 4000 mm/min.....	114
<b>Figure 6.24.</b> Position error of x-axis for switching controller II set-up with feedrate of 6000 mm/min.....	115
<b>Figure 6.25.</b> Position error of y-axis for switching controller II set-up with feedrate of 6000 mm/min.....	115
<b>Figure 6.26.</b> Position error of x-axis for switching controller II set-up with feedrate of 8000 mm/min.....	116
<b>Figure 6.27.</b> Position error of y-axis for switching controller II set-up with feedrate of 8000 mm/min.....	116
<b>Figure 6.28.</b> Position error of x-axis for switching controller III set-up with feedrate of 4000 mm/min.....	118
<b>Figure 6.29.</b> Position error of y-axis for switching controller III set-up with feedrate of 4000 mm/min.....	118
<b>Figure 6.30.</b> Position error of x-axis for switching controller III set-up with feedrate of 6000 mm/min.....	119
<b>Figure 6.31.</b> Position error of y-axis for switching controller III set-up with feedrate of 6000 mm/min.....	119

<b>Figure 6.32.</b> Position error of x-axis for switching controller III set-up with feedrate of 8000 mm/min.....	120
<b>Figure 6.33.</b> Position error of y-axis for switching controller III set-up with feedrate of 8000 mm/min.....	120
<b>Figure 6.34.</b> Comparison among the three switching schemes at a feedrate of 8000 mm/min.....	121
<b>Figure 6.35.</b> A zoomed view at switching schemes II and III at feedrate of 8000 mm/min.....	122
<b>Figure 6.36.</b> The overall feedrate output using switching scheme I.....	123
<b>Figure 6.37.</b> The overall feedrate output using switching scheme II.....	123
<b>Figure 6.38.</b> The overall feedrate output using switching scheme III.....	124

## Nomenclature

$s$	: The frequency-domain operator.
$J_m$	: Inertia of the motor (N.m.s <sup>2</sup> /rad).
$c_m$	: Damping of the motor (N.m.s/rad).
$V_m$	: Motor armature voltage (V).
$L_m$	: Motor armature inductance (H).
$R_m$	: Motor armature resistance ( $\Omega$ ).
$i_m$	: Motor current (A).
$e_m$	: Back electromotive voltage (V).
$K_b$	: Back e. m. v. conversion constant (V.s/m).
$K_t$	: Torque constant (N.m/A).
$\omega_m$	: Angular velocity of the motor (rad/s).
$\theta_m$	: Angular position of the motor (rad).
$\omega_l$	: Angular velocity of the load (table) (rad/s).
$\theta_l$	: Angular position of the load (table) (rad).
$T_m$	: Motor torque (N.m).
$K_\theta$	: Torsional stiffness of the ball screw (N.m/rad).
$J_b$	: Inertia of the ballscrew (N.m.s <sup>2</sup> /rad).
$\theta_b$	: Angular position beyond ballscrew torsional stiffness (rad).

$\frac{l}{2\pi}$	: Rotational-to-translational conversion factor (m/rad). where $l$ is the lead in (m).
$K_s$	: Axial rigidity of the supporting components (ballscrew, supporting bearings and brackets) (N.m/rad).
$X_s$	: Translational position beyond $K_s$ (m).
$M_b$	: Mass of the nut (kg).
$X_b$	: Linear position of the ballscrew (m).
$K_n$	: Axial rigidity between the ballscrew and the table (N.m/rad).
$M_t$	: Mass of the table (kg).
$X_t$	: Linear position of the table (m).
$c_t$	: Damping of the table (N.s/m).
$\theta_s$	: Shaft twist angle (due to flexibility) (rad).
$\theta_d = \theta_t - \theta_m$	: The displacement angle between the load and the motor (rad).
$\beta$	: The deterministic value of backlash (rad).
$\theta_\beta = \theta_d - \theta_s$	: The backlash angle where $-\beta < \theta_\beta < \beta$ (rad).
$J_t$	: Load inertia (N.m.s <sup>2</sup> /rad).
$c_m$	: Motor damping (N.m.s/rad).
$c_t$	: Load damping (N.m.s/rad).
$T_m$	: Motor torque (N.m).
$T_s$	: Shaft torque due to flexibility and damping (N.m).
$T_t$	: Load torque (N.m).

$k_s$	: Stiffness between motor and load (N.m/rad).
$c_s$	: Damping of the shaft between motor and load (N.m.s/rad).
$f_x$	: Feedrate in the $x$ -direction (mm/min).
$f_y$	: Feedrate in the $y$ -direction (mm/min).
$x_i$	: State $i$ as shown by state space representation..
$y$	: Output from a control system as shown by state space representation.
$\hat{x}_i, \hat{y}$	: Estimated or observed value of a state/output.
$u$	: Control input
$q, \hat{q}$	: Reference generalized coordinate and estimated reference generalized coordinate.
$\sigma$	: Switching signal.
$e$	: Tracking error – difference between reference and output.
$\varepsilon$	: Contouring error.

# **1. INTRODUCTION**

## **1.1. NUMERICAL CONTROL TECHNOLOGY**

Numerical Control (NC) equipment has been introduced by the Electronic Industries Association (EIA) as “A system in which actions are controlled by the direct insertion of numerical data at some point. The system may automatically interpret at least some portion of this data”[Koren, 1984].

The NC system replaces the manual actions of the conventional machine tool operator. In conventional machining, a part is produced by driving a handwheel-guided cutting tool along a workpiece by the operator. Contour cuttings are performed by a dexterous operator by sight. On the other hand, NC machine tools operators must not be skilled machinists. They only have to watch the operation of the machine, and usually replace the workpiece. All operations that require analysis, that were formerly done by the operator, are now contained in the part program.

The advent of the new technology in machine tools leads to increased productivity. There are many measures to evaluate a manufacturing system: productivity amongst of them can be identified and verified by production time.

Advantages of NC systems can be summarized as following:

- The need for a highly proficient and experienced operator is avoided.
- Full flexibility; features of a part can be changed via the part program.
- Accuracy is maintained through a quite wider range of speeds and feeds.
- Reduced production time.
- Enhancing contour machining manufacturability.
- Easy adjustment of the machine, which requires less time than with other manufacturing systems.
- The operator has more free time; can be utilized for looking after other machining operations.

Disadvantages of NC systems can be summarized as following:

- High initial investment in the machine.
- A long preparation time for each production cycle or tier.
- Inflexibility; since each machine is planned to make a certain fixed cycle of operation. If any of part features is changed, the machine configuration must be rebuilt or altered.
- A large stock of parts is required for the process, since a part is maintained in each machine.
- A relatively high operating cost.
- More complicated maintenance; a special maintenance crew is desirable.
- A highly skilled and properly trained part programmer is needed.

## **1.2. MACHINE TOOL STRUCTURE**

A machine tool system can be divided into three main groups of parts: mechanical structures, drives, and controls.

### **1.2.1. Mechanical Structure**

The structure consists of stationary and moving bodies. The stationary bodies include beds, columns, bridges, and gear box housings. They usually carry moving bodies, such as tables, slides, spindles, gears bearings, and carriages. The structural design of machine tool parts requires high rigidity, thermal stability, and damping. In general, the dimensions of machine tools are overestimated in order to minimize static and dynamic deformations during machining. The general design of machine tool structures will not be covered in this text. Instead, it is assumed that the relative static and dynamic compliance between the tool and the workpiece is measured experimentally or predicted with analytical methods. The effect of structural compliance on the accuracy of the machined workpiece and machining performance is presented.

### **1.2.2. Drives**

Moving mechanisms are grouped into spindle and feed drives in machine tools. The spindle drive provides sufficient angular speed, torque, and power to a rotating spindle shaft, which is held in the spindle housing with roller or magnetic bearings. Low- to medium-speed spindle shafts are connected to the electric motor via V-belts. There may be a single-step gear reducer and a clutch between the electric motor and spindle shaft. High-speed spindles ( $n > 15,000$  rev/min) may have electric motors that are built into the spindle to reduce the inertia and friction produced by the motor-spindle shaft coupling. In a typical and versatile machining center, the high and low speed spindles can be swapped in a short time period (i.e., one hour). The feed drives carry the table or the carriage. In general, the table is connected to the nut, and the nut houses a lead screw. The screw is connected to the drive motor either directly or via gear system depending on the feed speed, inertia, and torque reduction requirements. Conventional machine tools have numerous gear reduction steps in order to obtain a desired feed speed. Each feed screw has a dedicated drive motor in CNC machine tools. Very high speed machine tools may employ linear direct motors and drives without the feed screw and nut, thus avoiding excessive inertia and friction contact elements.

### **1.2.3. Controls**

The control parts include motors, amplifiers, switches, and computers that are used to supply the electrical parts in a controlled sequence and time. Conventional machine tools mostly contain relays, limit switches, and operator controlled potentiometers and directional control switches. CNC machine tools have power servo amplifiers, ON/OFF and limit switches, and a computer unit equipped with emergency, control, and operator interface units. The feed velocity and positioning accuracy of feed drives are dependent on the torque and power delivery of the servomotors and on the feed drive servo control algorithms executed in the computer numerical control (CNC) unit of the machine tool.



### 1.3. CAM-CNC INTEGRATION CYCLE

Computer-aided manufacturing (CAM) systems as well as computer numerical control (CNC) machine tools are invading every single corner in today's manufacturing industries. To machine the desired part, the CAM system generates the required tool path for the CNC machine tool so that it can cut the surfaces of the part. On the other hand, CAD/CAM integration considers the achievement of automatic production process from design specifications – well represented by a CAD model – to final product. Accordingly, the scope of motion controls of CNC machine tools covers three areas [Chou and Yang, 1991; 1992; Altintas, 2000; Koren, 1984], see Figure 1.1:

1. CAD model to cutter path conversion; involves feature recognition, geometry intersection, offsetting, etc.
2. Cutter path to motion trajectory conversion; referred also as command generation and it includes kinematics of coordinated motion, machine dynamics, and interpolators design.
3. Motion trajectory realization; Involves controllers design.

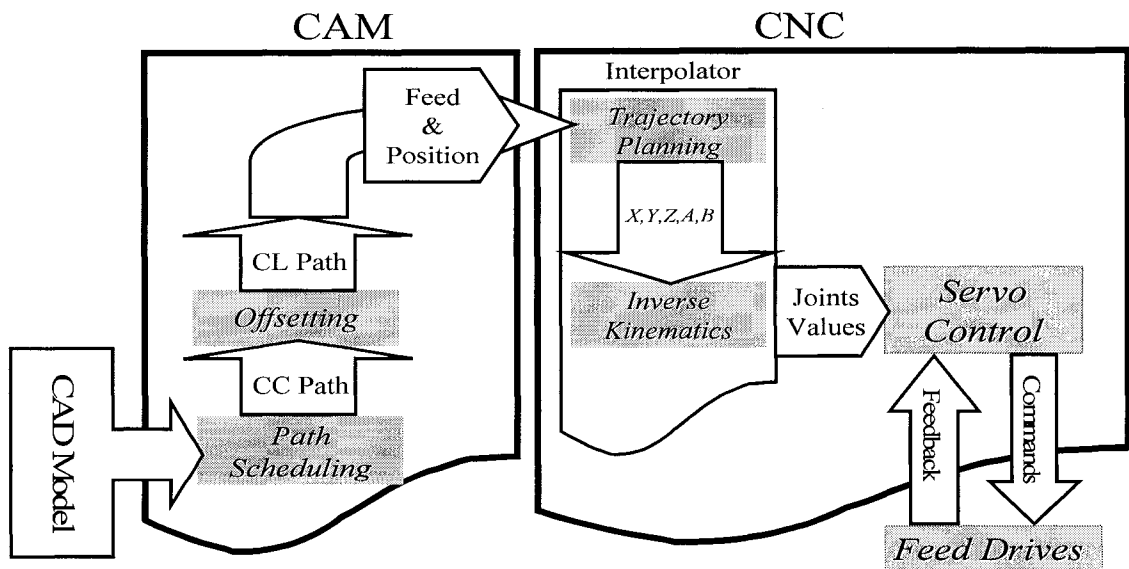


Figure 1.1. Nature of information transfer of a CAM/CNC stage of product synthesis.

Starting with the CAM role, it resolves the cutter contact (CC) points into cutter location points (CL) by offsetting the former depending on surface and geometry of the cutting tool. Cutter contact (CC) points are set of points on the machined surface where the tip of the tool pass. Scheduling the path between the CC points (CC path) will depend on the scallop height and forward (chordal) step size assigned to the operation. Most of the time, the isoparametric machining method will be applied which provide variable yet conservative scallop heights.

Cutter location (CL) points represent locations of the centre of tool via the path of cutting. CNC controllers deal with the CL path computationally while the output will apparently depict the CC path. On the other hand, CC velocity will depict the real feedrate by which more complexity will be added to the controller (interpolator) functions. After feeding the CL file, including CL path and velocity, into the CNC machine, the interpolator will either interpolate CL points to linear or curve trajectories in multi-axis machining depending on the type of interpolator (e.g., linear or curve interpolators). Linearly segmented tool path will cause fluctuation in feed rate while parametric curves are recommended to represent the tool path.

CC velocity and CL velocity are the same in linear motion. However, CC velocity will fluctuate in case encountering convex or concave surfaces since CL velocity is the parameter controlled as shown in Figure 1.2. This can be illustrated for a ball end mill via the following equation:

$$V_{CL} = V_{CC} \times \frac{R \pm r}{r} \quad (1.1)$$

Where  $R$  is the radius of the circular arc,  $r$  is the radius of the tool, and  $\pm$  depends whether the circular contour is convex or concave. Finally, our interest of the aforementioned areas within the CAM-CNC cycle is that of the servo control and the physical world where relative motion of the machine tool axes of motion is governed to guarantee a high-quality tool-workpiece interaction.

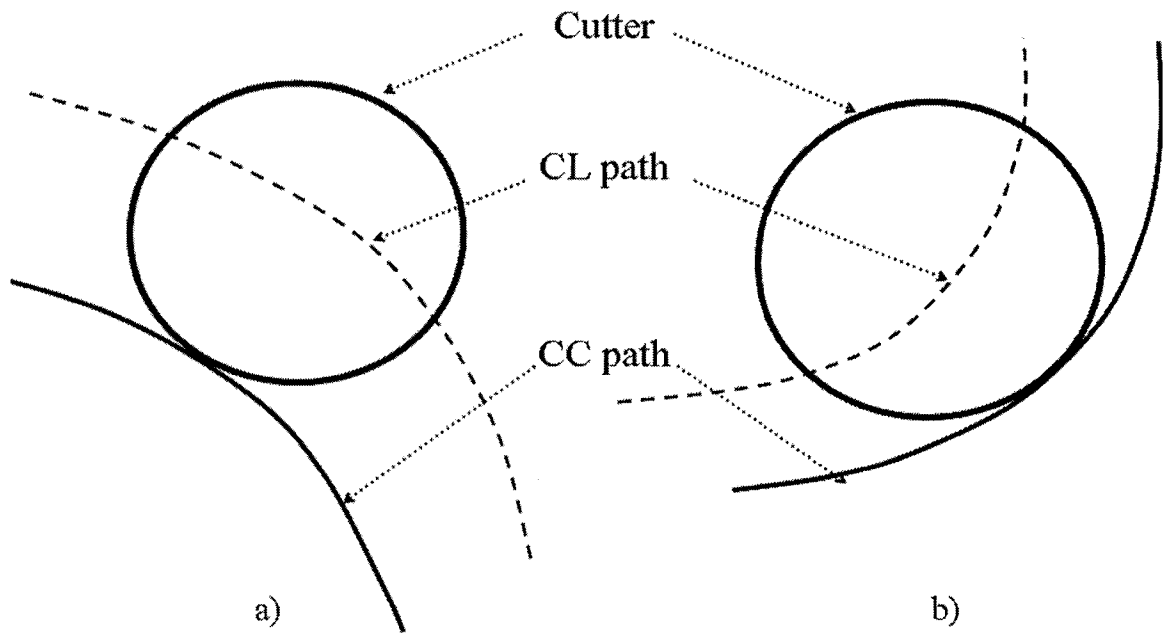


Figure 1.2. Machining of 2-D circular contours: a) convex, b) concave.

#### 1.4. RECONFIGURABLE MANUFACTURING SYSTEMS AND UROCA

As a start, let us define some crucial buzzwords and concepts that are highly demanding and competitive in the world of industry and manufacturing. A Flexible Manufacturing System is defined as the idea of using a set of machines to make a relatively wide variety of products, with automatic movement of products through any sequence of machines [Bredworth, 1991]. FMS often groups various CNC machines, robots, material transporters, automatic storage retrieving devices, and allow them to work flexibly. However, the FMS control software cannot be changed without high costs if new machines or parts to be added, or control algorithms to be manipulated due to change in functionality need.

As time goes on, product model lifetimes are decreasing and customer demands are constantly changing. In order for industries to survive in today's competitive market, their manufacturing systems must be able to respond effectively to these ongoing changes. With the rapidly changing manufacturing environment, the need for Reconfigurable Manufacturing Systems (RMS) is immense. A Reconfigurable

Manufacturing System (RMS) is one designed at the advent for rapid change in its structure, as well as its hardware and software components, in order to accommodate rapid adjustment of production capacity needed in response to new market circumstances, and functionality needed to produce a new part or overcome an emergent event. The National Research Council in a recently released study entitled Visionary Manufacturing Challenges for 2020 identified Reconfigurable Manufacturing Systems (RMS) as the number one priority technology in manufacturing for the Year 2020. The study also lists Reconfigurable Manufacturing Enterprises as one of the six grand challenges for the future of manufacturing. Proposed to the National Science Foundation (NSF) [Fact Sheets] in 1994 as a utopian, next generation technology, a living, evolving factory, Reconfigurable Manufacturing System (RMS) is increasingly recognized today as a requirement for industrial growth in a global economy [University of Michigan, ERC-NSF webpage].

The concept of Reconfigurable Manufacturing Systems (RMS) has been introduced with the aim of developing new methods for the design and implementation of manufacturing systems, which can be rapidly designed and reconfigured to provide exactly the production capacity and functionality needed when needed. Reconfiguration is a fast-paced expanding research field in manufacturing that propagates from system-level design issues to modular machines, reconfigurable control, and rapid ramp-up methods after reconfiguration [Mehrabi *et al.*, 1998].

Adaptable, integrated equipment processes, and systems that can be readily reconfigured for a wide range of customer requirements for products, features, and services is a priority technology. Hardware and software components, sub-processes, and subsystems will have to be adaptable and linked in easily programmable ways into higher-level processes and systems that span the entire product/service life cycle. Research opportunities to support the development of adaptable and reconfigurable manufacturing processes and systems fall into five broad areas [NRC, 1998]:

- Processes and tooling.
- Theoretical foundations.
- New manufacturing systems.
- Modeling and simulation.
- Control and communications concepts.

The production of various, customized-to-demand products will require the rapid reconfiguration of manufacturing operations, with the following capabilities:

- Systems models for all operations.
- Fundamental understanding of manufacturing processes.
- Synthesis and architecture technologies for converting information into knowledge.
- Unified communication methods and protocols for the exchange of information.
- Human-machine interfaces that enhance user performance.
- Adaptable and reconfigurable manufacturing processes and systems (e.g., biosynthetic processes and net-shape, programmable, flexible forming processes that do not require hard tooling).
- Sensor technology for precision process control.

Reconfiguration of manufacturing operations will involve different concepts and technologies than reconfiguration of enterprises or organizations. Here, the goal is to enable adaptation of manufacturing operations to make quick changes in the product or even to make different products. The realization of a reconfigurable factory requires tools that can combine basic operations in flexible ways to produce a set of processes; similar to the way linguistic primitives are combined using a flexible syntax to produce a rich variety of programs in a language. The degree of reconfigurability that can be achieved in this way far exceeds the degree of reconfigurability achieved by rearranging equipment.

One of the significant conditions of achieving RMS is to develop control systems that are reconfigurable. Previously developed control systems are unable to be

interchanged and reused effectively, and this can be extremely costly. To date, most control programs for manufacturing systems in industry are written in ladder logic and are implemented on programmable logic controllers (PLCs) which are proprietary and closed; they are vendor-specific control algorithms that cannot be changed or interchanged. For the aforementioned reason, switching mechanism, as proposed in this study, is considered unattainable based on FMS criteria, by which it has been designed depending on the requirements and concepts of RMS and the guidelines of UROCA project on which a brief insight is given in the next paragraphs.

Instead of dealing with closed proprietary control environment, Open software/hardware technology will be provided with the coming RMS. It targets at the development of a control architecture that supports multi-vendor, plug-and-play, modular criteria for machine tools, robotic systems and other components serving in manufacturing systems. Since there is variety of control architectures that engulf the hardware and software components/objects, they also differ to a high extent in concept and infrastructure due to the dissimilitude in applications, from which was the motivation for this project to launch, [ElBeheiry *et al.*, 2004].

Unified reconfigurable open control architecture (UROCA) is a research project, which aims at unifying the reconfiguration aspects and managing the interaction of individual machining control systems which perform in a reconfigurable manufacturing system. UROCA consists of two crucial parts – by which it resembles the human brain: deliberative left brain and reactive right brain, see Figure 1.3. UROCA is conceived as a tri-layer architecture, where the topmost layer represent the high level decision-making and task management where high-level-intelligence functions like: learning, knowledge building and data acquisition are embodied. The intermediate layer is the planning layer which is depicted by the presence of two planners: one at the deliberative part and the other at the reactive one. Each planning unit has its specific and distinctive information input that relies on the nature of the process; reactive responses needed for emergent and no-brainer actions – no intelligence is required, while deliberative responses needed after

fulfilling the decision cycle needed which involves erratic approaches on usage of intelligence.

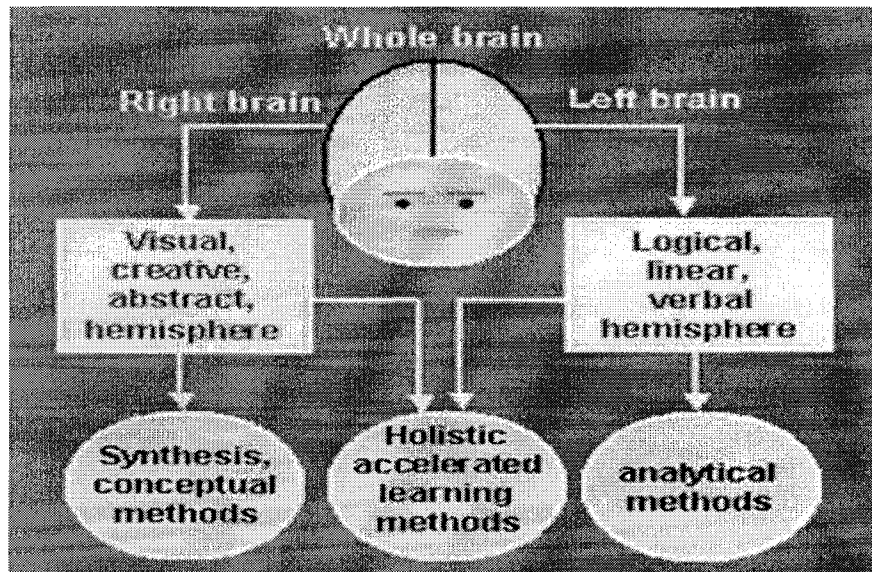


Figure 1.3. UROCA design methodology classification [ElBeheiry *et al.*, 2004].

All of this is connected to the lowermost layer of the architecture, namely, the physical controllers that guide and administer the required industrial entity, whether it is a CNC machine or a robot. This work is supposed to serve within the physical layer and, to an extent, some of the middle layer where the supervisory unit is attached, see Figure 1.4.

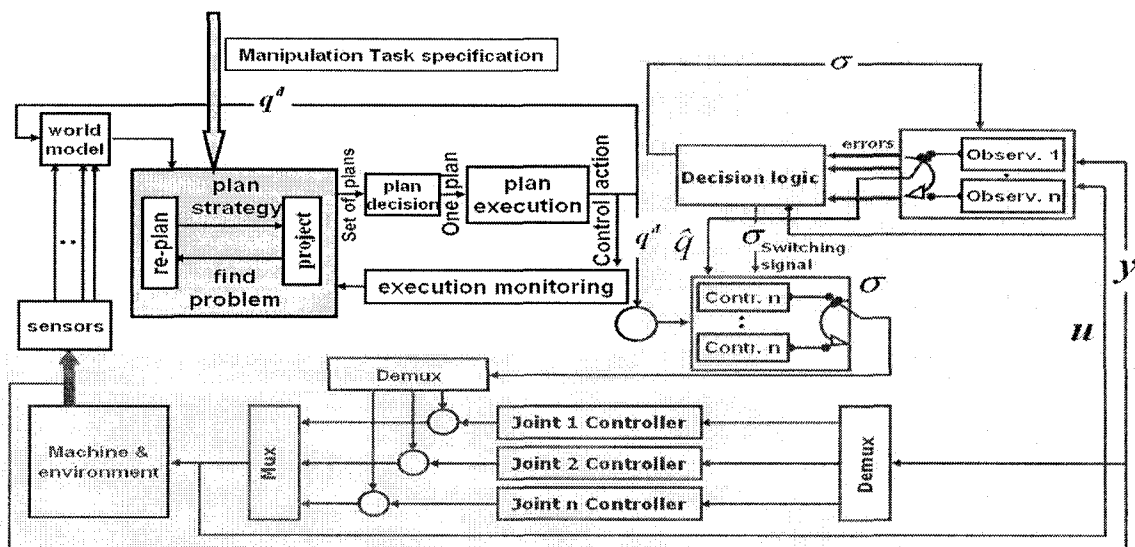


Figure 1.4. UROCA left brain at the intermediate (planning) and physical layer; the shaded area represents my scope of work [ElBeheiry *et al.*, 2004, *Reprod.*].

The hierarchical control architecture exploited by UROCA holds undoubted trade-off between centralized control attributes – optimized performance; yet hard to design and to reconfigure, and decentralized control attributes – easy to design and to reconfigure; yet lower performance is achieved. A good compromise has been depicted by hierarchical control architecture between reconfigurability and performance. CNC machine tools have usually decoupled and decentralized servo (position and speed) controllers to guard its axes movements. The presence of supervisory unit atop the servo controllers is the main resulting aspect due to UROCA. Planned trajectory after being processed within the planner is sent to the physical layer servo controllers to achieve the desired motion. This is considered to happen within the left brain structure where entities like: interpolators are embedded within the deliberative planner at the intermediate layer, and servo controllers within the physical layer of UROCA.

The existence of external disturbances, measurements inaccuracies, load variation, effects of inertia and flexibility and parasitic effects – such as backlash, friction, etc. – call for the use of intelligence and adaptability obtained by reconfigurable manufacturing systems. This would limit the use of the regular PID controllers which prevail in the world of CNC machine tools and industrial robots giving opportunity for other types of controllers to be implemented. Supervisory control has proven solid grounds at achieving foreseen goals of intelligence and adaptability. Supervisory control concept also supports the structure of hierarchical control as a mediator between the physical level and the more intelligent layers atop. Supervision, according to [ElBeheiry *et al.*, 2004] is of 3 types: pre-routed, estimator-based and performance-based supervision. The last one has been chosen since it provides good data inputs for system diagnosis and state estimation whenever needed for the operation of advanced controllers. Multiple controllers are available for the supervisor to switch over depending on the functionality needed. These controllers are designed based upon different dynamic models which necessarily changes according to the conditions that the supervisor is prepared to treat according to predetermined rules. In Figure 1.5, a conceptual schematic represents an observer-based supervisory unit connected to one 2-DOF axis of motion



that is going to be implemented within UROCA architecture. This concept is thoroughly discussed in Chapter 4.

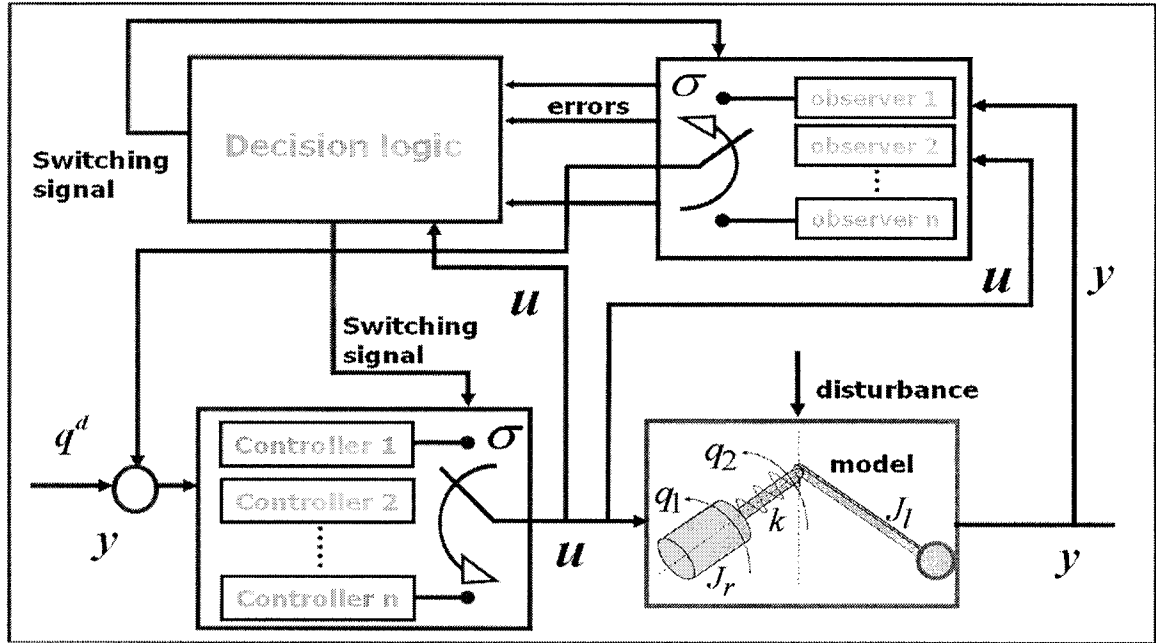


Figure 1.5. Supervisory control design for UROCA [ElBeheiry *et al.*, 2004].

Moreover, UROCA emphasizes the unification of reconfiguration aspects depending on the examining of similarities and differences in CNC machine tools. This has also a marginal effect on assisting the modular design of different levels of control architecture, encourages reusability and enhances the process of objects parameterization. A discussion of similarities and differences among machine tools to be performed through the next section.

## 1.5. SIMILARITIES AND DIFFERENCE AMONG CNC MACHINE TOOLS

### 1.5.1. Measures of Comparison

Machine tools are quite similar in their structures, designs and technology. Although we are comparing machines of different metal cutting processes, like turning, milling, and drilling, they are still having that common CNC function of managing the axes of motion to undergo positioning and contouring cutting processes. Basically, contouring systems are the super set that includes point-to-point systems (positioning) in terms of control aspects. This is regarded as one of the fundamental and essential

similarities that embody any design of the diverse controllers used in machine tools industry. Practically, the previous point can be seen in reality as you can use a milling centre to perform drilling for a hole on a surface. Milling involves side loading of the tool, in addition to end loading. This imposes different approaches towards metal cutting mechanics which plays a lively role in torque losses compensation. On the other hand, the main difference between a lathe and a mill is that on a lathe, the workpiece turns and the cutting tool is moving towards it, while on a mill, the tool turns and the workpiece is moved towards it. Actually, on a machining centre, we can see, nowadays, feed axes, either translational or rotational, are implemented on the tool (spindle) side.

Delimiting our scope within the CNC controller does not affect the way we study the model, since information included within that model must include the whole status of the machine. We have already agreed on taking the study of contemporary similarities and differences existing in the world of machine tools as the kernel and spine for the development of unified, reconfigurable and open architecture machine tool controllers. However, to study properly similarities and differences amongst machine tools, first of all, we have to state adequate and broad-spectrum measures, to which variability and diversity are clearly depicted, classified and compared. Accordingly, modeling, control and diagnosis generalization procedure is going to be conceived and blueprinted.

The measures, after revising the literature of basic and advanced machine tools scientific contributions, are:

- Class of use; local use, DNC or remote distributed systems.
- Type of motion of the tool; either positioning or contouring application.
- Type of metal cutting application(s) involved; milling, turning, drilling, etc.
- Type of programming; Incremental or absolute systems.
- Types of geometry processing units (interpolators); linear, circular, helical, etc.
- Type of control; open or closed loop control.
- Type of controllers; P, PI, PD, PID, Fuzzy, etc.

- Type of reference signal and computer degree of involvement; reference-pulse technique or sampled-data technique (i.e., pulse or binary word used as a reference).
- Other control aspects like adaptive control approach.
- Quality and quantity of degrees of freedom (joints) involved; number, type and location of axes of motion.
- Variance in machine feed drive components; coupling, motors, etc.

Actually these parameters are affecting each other in a way or another, for example, contouring systems require closed loop control and have also other impacts on other parameters. Some of these parameters are discussed in the next subsections.

### **1.5.2. Positioning (Point-to-Point) and Contouring Systems**

The most familiar example of a positioning NC machine tool is a drilling machine. In a drilling machine the workpiece is moved along the axes of motion until the center of the hole to be drilled is exactly under the drill. Then the drill is automatically moved toward the workpiece, the hole is drilled, and the drill moves out in a rapid traverse manner. The workpiece moves to a new point, and the same sequence of actions is repeated.

The workpiece is guided with respect to the cutting tool until it arrives at a numerically defined point. The cutting tool accomplishes the required task with the axes stationary. When the task is completed, the workpiece moves to the next point and the cycle is repeated.

In a positioning system, the path of the cutting tool and its feedrate while moving from one point to another is without any significance. The path from the starting point to the final position is not controlled. Therefore, this system would require only position counters for controlling the final position of the tool upon reaching the point to be drilled.

The data for each desired position is given by coordinate values, and the resolution depends upon the system's minimum measuring unit.

In contouring, or continuous-path, systems, the tool is cutting while the axes of motion are moving, as, for example, in a milling machine. All axes of motion might move simultaneously, each at a different velocity. When a nonlinear path is required, the axial velocity changes, even within the segment. For example, cutting a circular contour requires a sine rate change in one axis, while the velocity of the other axis is changed at a cosine rate. Also, the position of the cutting tool at the end of each segment together with the ratio between the axial velocities determines the desired contour of the part, and at the same time the resultant feed also affects the surface finish. Since, in this case, a velocity error in one axis causes a cutter path position error; the system has to contain continuous-position control loops in addition to the position counters.

### **1.5.3. Open-Loop and Closed-Loop Systems**

Every control system, including NC systems, may be designed as an open-loop or a closed-loop control. The term open-loop control means that there is no feedback and the action of the controller has no information about the effect of the signals that it produces.

The open-loop NC systems are of digital type and use stepping motors for driving the slides. A stepping motor is a device whose output shaft rotates through a fixed angle in response to an input pulse. The stepping motors are the simplest way for converting electrical pulses into proportional movement, and they provide a relatively cheap solution to the control problem. Since there is no feedback from the slide position, the system accuracy is solely a function of the motor's ability to step through the exact number of steps which is provided at its input. One of the major properties of a stepping motor is that its maximum velocity depends upon the load torque. The higher the load torque, the smaller the maximum allowable frequency to the motor. Stepping motors cannot be used with machines with inconsistent load torques, since an unexpected large load causes the motor to lose steps and eventually position error occurs.

The closed-loop control measures the actual position and velocity of the axis and compares them with the desired references. The difference between the actual and the desired values is the error. The control is designed in such a way as to eliminate or reduce, to a minimum, the error, namely the system is of a negative-feedback type. In contouring systems for machine tools, the cutting forces load the motors with torques depending on the cutting conditions, and therefore stepping motors are not recommended as drives for these contouring systems. They can be applied to laser-beam contour-cutting systems (in which only a mirror is moved) and to PTP drilling machines, where the loading torque on the motors is almost constant. Industrial robots and contouring systems such as lathes or milling machines require closed-loop control systems.

The design of the control system and the choice of the types of loop employed to meet performance and cost specifications, require knowledge of the nature of the controlled machine and loading torques. The allowable positioning error, accuracy, repeatability, and response time also have to be taken into consideration where an optimum performance is required.

#### **1.5.4. Machine Tool Joint Types**

After receiving position and feed commands from the controller, motion is produced by proper movements of the joints present in the machine tool. Taking into consideration that we are discussing conventional machine tool setup, i.e., serial kinematics machines only, the similarity with serial-joints manipulators are highly noticeable. Joints are either prismatic or revolute that produce both linear and rotational displacement, respectively. Linear joints are always orthogonal to each other, as well as axes of revolution of rotational joints; so that we can achieve the Cartesian coordinate configuration of  $X$ ,  $Y$ , and  $Z$ -axes; rotational axes denoted  $A$ ,  $B$  and  $C$ -axes are normally axes of rotation about  $X$ ,  $Y$ , and  $Z$ -axes, respectively. Also, position of the axis of motion is a point of variability among various machine tools, i.e., whether being placed in the tool side or workpiece side, see Figures 1.6, 1.7., 1.8. and 1.9.

Machining systems are diversified with respect to the number of degrees of freedom involved. The nature of the application adds or exempts an axis or more to the machine tool which considered as an important element of reconfigurability concept.

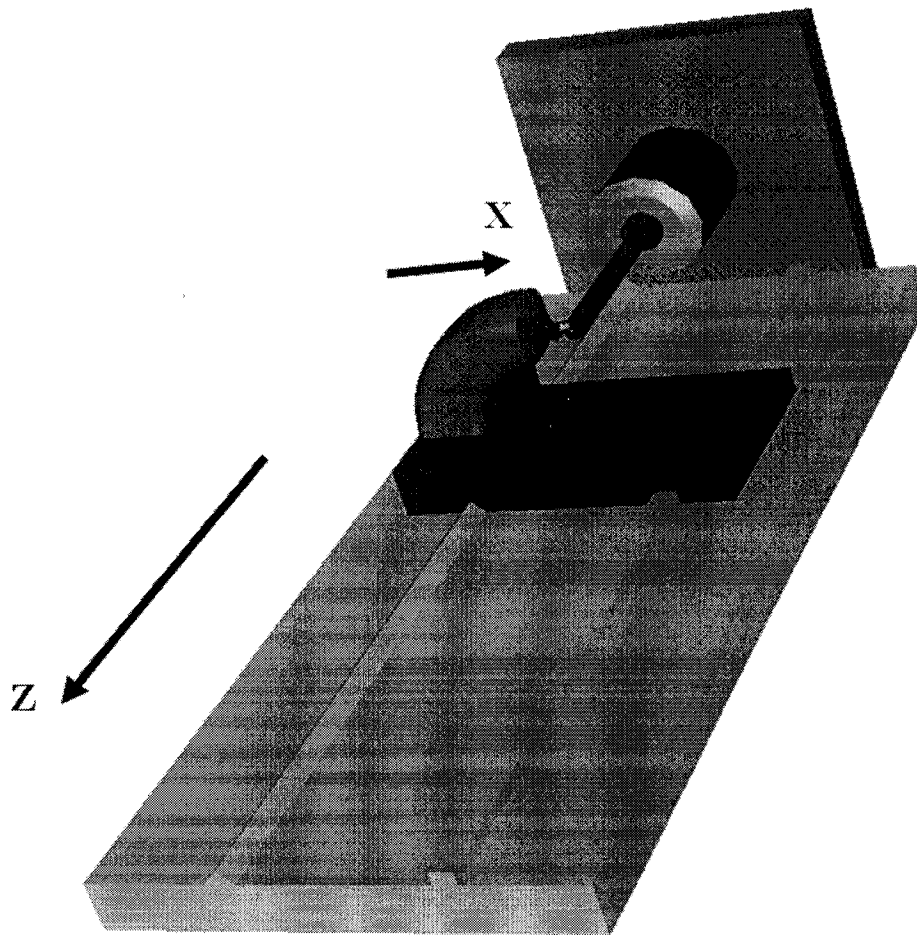


Figure 1.6. Schematic drawing for a turning machine tool.

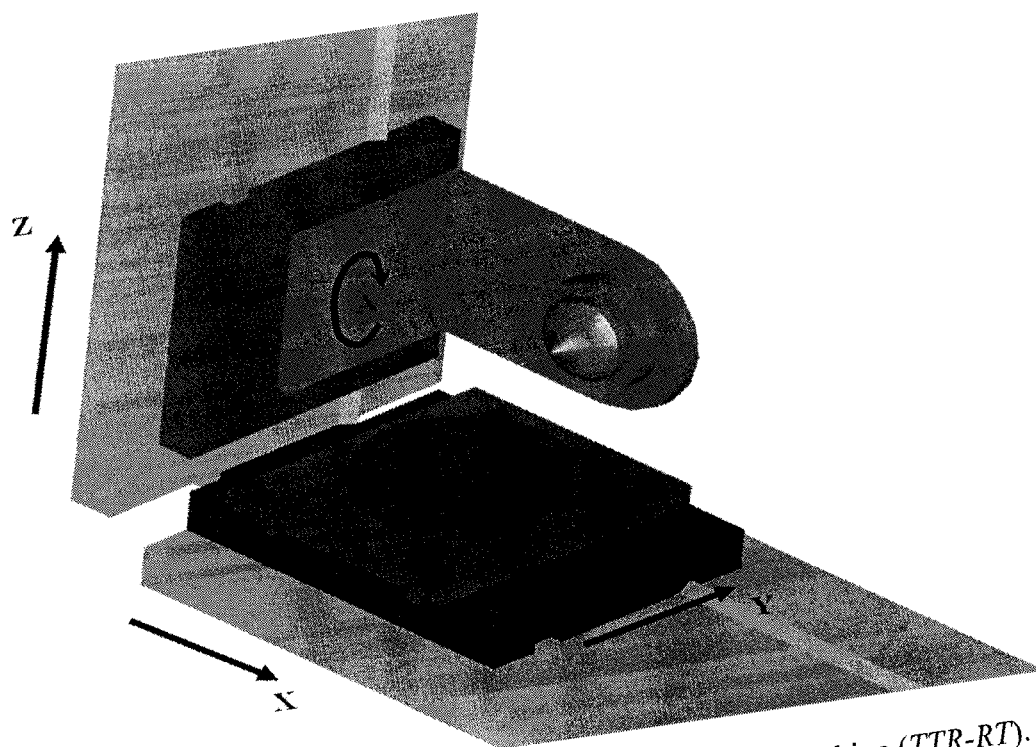


Figure 1.7. Schematic drawing for 5-axis milling machine (TTR-RT).

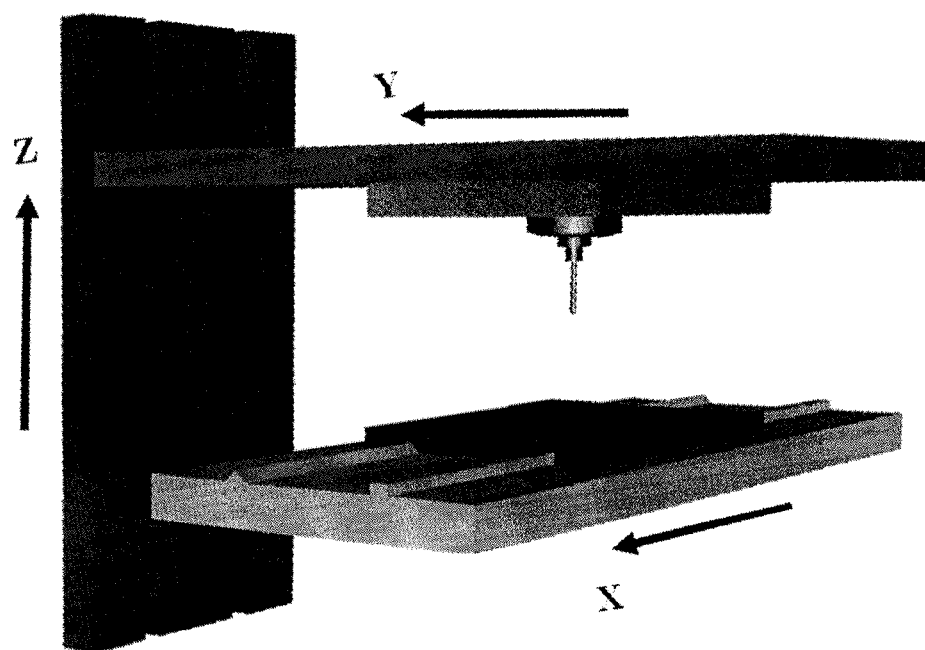


Figure 1.8. Schematic drawing for 3-axis milling machine.

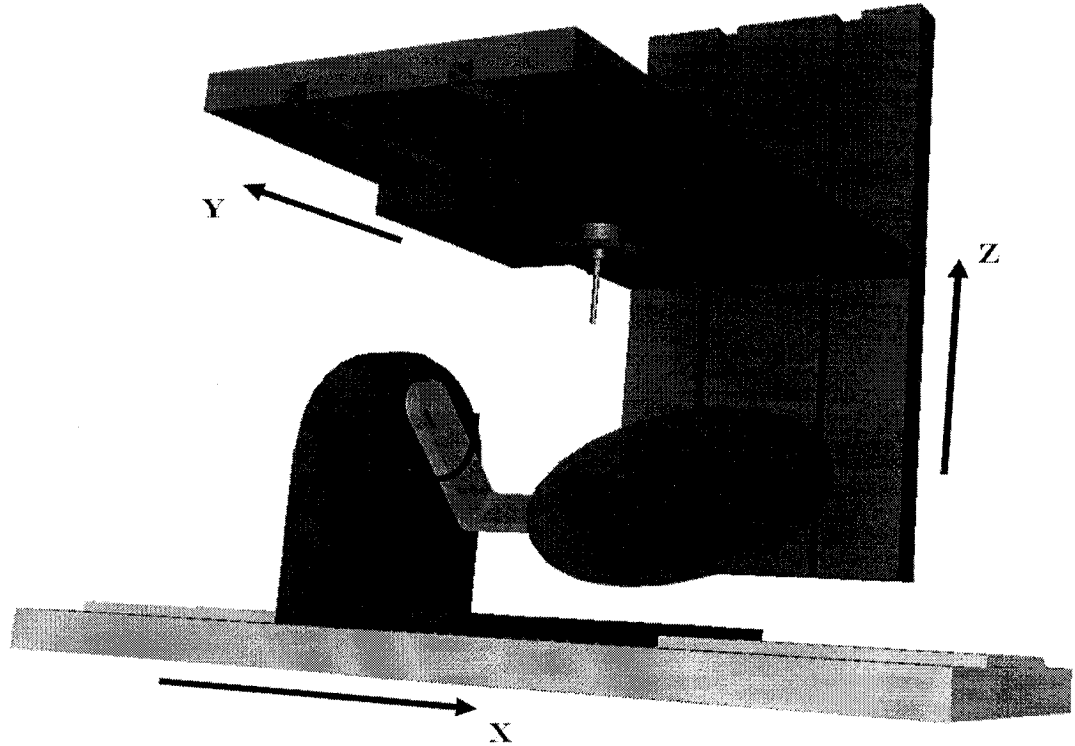


Figure 1.9. Schematic drawing for 5-axis milling machine (*TRR-TT*).

Also, the order of these axes, both in the tool side or workpiece side, which is depicted in the previous figures, can be different and of assorted combinations – it reaches 720 combinations for 5-axis milling machine tool; i.e., rotational and linear axes order with respect to each other. We have denoted translational joint by *T* and rotational joint by *R*, starting from the workpiece side to the tool side where the hyphen describes the discontinuity between workpiece and tool. However, such a difference is quite effective in more than 3-axis machining, where operating volume, machine rigidity, and efficiency are highly influenced. Location of rotational axes has its own importance to classify through the different multi-axis machine tools. They are either all placed on the tool side, all on the workpiece side, or distributed on both [Bohez, 2002].

#### 1.6. SWITCHING NEED: THE BACKLASH PROBLEM

Supervisory control unit occupies a strategic spot as an interface between the physical layer and the planning layer at the left brain of UROCA architecture. It takes the decision to resolve intermediate-level intelligence aspects and process-related hurdles, so



that the reconfiguration process takes place smoothly to achieve the ultimate goal: optimized process guaranteed. Taking the vision of real-time database – which is mentioned in chapter two – that contains all the controllers needed into consideration, to maintain a balanced and optimized machining process by choosing the right controller upon need. In our study, we are taking backlash as a trigger to induce the supervisory unit to maintain a smooth output for a machine tool represented by its axes of motion. In the next subsection, definition of backlash and its research trends are discussed thoroughly.

#### **1.6.1. Definition of Backlash**

Backlash was coined around 1815, and is a compound word denoting a backward lash (violent movement or reaction). In technical circles this has come to mean “the play between adjacent moveable parts (as in a series of gears),” or “the jar caused by this when the parts are put into action.” [McKechnie, 1983] Basically, backlash contains a mechanical hysteresis of the type commonly found in geared actuators and sensors, mechanisms employing lead or ball screws, and the like. Gears and screws provide machine tool engineers with a very useful means to adjust the ratio of applied force to resultant action and *vice versa* in machine mechanisms; however, backlash can confound the accuracy of such operations.

The component of backlash more familiar to the layperson is gearplay, which many of us are used to dealing with, for example, in the manual steering wheels of automobiles. The less familiar component is that of the “gnashing” of gears when put into sudden motion.

As illustrated by its figurative and literal dictionary definitions, backlash is composed of two salient features. In mechanical engineering terms these are mechanical hysteresis and impact phenomena between two relatively hard surfaces coming into contact. These features are both readily found in old-fashioned geartrains, where the gears fit loosely together and are usually made of a hard metal. Modern geartrains may be made of plastics, which are more pliant and thus impact with less power than do metals ones, and are also more likely to be manufactured and fit together with smaller tolerances

(and less free play). However, friction and wear can reduce tolerances in any kind of gears and also the axial truth of their spindles, potentially introducing appreciable backlash where originally it might have been negligible. Contrary to mechanical phenomenon like friction, backlash is a phenomenon which is fairly well-understood, and can be addressed, with varying degrees of detail, as mentioned extensively in chapter three.

### **1.6.2 Understanding Backlash**

Often, the impact is overlooked in machine design and control, with unhappy results. Typical sources of impact include: clearance between cams and followers; backlash or bearing clearances in mechanisms undergoing force or motion reversal; and mechanisms with components having large relative velocities. The study and control of impact phenomena is especially important for machine designers, since: firstly, all the major stresses in mechanical systems arise as a consequence of impact, and many serious machine failures are generated when impact forces are not properly recognized and controlled; Gear tooth failure (complete or near-complete shearing) will result in a sudden and highly significant increase in backlash, further compromising the mechanism accuracy and possibly causing damage to the machine as a whole. Secondly, useful short-duration effects, such as high stresses, rapid dissipation of energy, fast acceleration and deceleration, can be achieved from low energy sources by controlling the impact of bodies at low force levels. [Tornambè, 1996] Better precision, accuracy, speed and agility are demanded of modern machines. The range of precision currently demanded certainly approaches, and sometimes even exceeds, the composite precision of available mechanism components, requiring either a design modification or a special control strategy. The traditional deadzone model of backlash fails to address the full issue, so a more complete model must be brought to light.

### **1.6.3. Trends in Backlash Research**

Backlash is a highly nonlinear effect, and has the ability to excite high-order modes in a drive train, unlike nonlinearities such as compliance and friction; with the

aforementioned present, drive controllability is further undermined. A number of hysteresis models have been presented for approximating backlash, but further study is advised [Macki *et al.*, 1993]. Control strategies such as dithering have been applied with some success many years ago [Freeman, 1957, 1960], but relatively few researchers have pursued a better understanding of mechanical backlash over recent years. Recently, a state-of-the-art controls perspective was published in book form by the two main researchers in the field, Gang Tao of the University of Virginia and Petar V. Kokotović of the Center for Control Engineering and Computation at the University of California at Santa Barbara [Tao and Kokotović, 1996]. This work is based on numerous articles and proceedings of theirs over the past decade or so, an almost obscene number of which were printed in a small concentration of journals in 1995 alone [Tao, 1996, Tao and Kokotović, 1993, Tao, and Kokotović, 1995]. Particularly revealing is the observation that the titles for this flurry of articles are almost identical except for the random exchange of the key terms, backlash, dead-zone and hysteresis. This casual terminological exchange betrays, in spite of their great efforts, the consistent misrepresentation of backlash as a pure hysteresis or deadzone, as a convenient mathematical simplification necessary to obtain a convenient system-theoretic representation of the phenomenon. Hopefully their results will nonetheless retain some degree of usefulness in real systems, a standing question since they provide not a single example in neither their papers nor text. The importance of impact phenomena has in recently been exhorted by A. Tornambè of Terza Università di Roma, who ignores the work of Tao and Kokotović completely in his control design and simulations [Tornambè, 1996, Tornambè and Valigi, 1994]; A. Tustin had emphasized the same even as early as 1947 [Tustin, 1947A, 1947B].

Other scientists have made valuable contributions to modeling and control of backlash as well, in the areas of hysteresis modeling [Macki *et al.*, 1993, Nordin *et al.*, 1997, Pan *et al.*, 1995], phase-plane analysis [Owen, 1959], adaptive control [Lin, 1997, Recker, 1997, Sun *et al.*, 1992, Yang and Fu, 1996], neural control [Seidl *et al.*, 1995], robotic reflexing [Weng and Young, 1996, Youcef-Toumi and Gutz, 1994], numerical simulation of plastic collisions [Stein and Wang, 1998, Stewart and Trinkle,

1996], impact analysis [Dubowsky and Freudenstein, 1971A, 1971B, Gerdes and Kumar, 1995, Golnaraghi *et al.*, 1995, Harris and Crede, 1961], and even the *advantages* of backlash in control mechanisms [Olgac and Iragavarapu, 1995].

## 1.7. MOTIVATION FOR THE STUDY OF BACKLASH

As discussed at the outset, the study of this basic nonlinearity is chiefly motivated by the fact it is observed in almost any machine tool transmission, particularly in the sense of nonlinear disturbances on machine tool control. Commonly, the mathematical descriptions of machine dynamics are linearized to facilitate the dynamic analysis and control design; in such cases there will almost always be some observable, if not downright unacceptable, levels of nonlinearity caused by backlash. Even in nonlinear systems design, unmodeled, higher-order effects can sufficiently corrupt the desired actions of a machine when the nonlinearity descriptions are mathematically simplified. So in some cases, it is necessary to have a detailed understanding and commensurate model of backlash. As the desired precision of machine tools is pushed closer towards the boundaries of our design and manufacturing capabilities, a better understanding of transmission nonlinearity will be crucial to successful high tolerancing of consumer and industrial products, and hence, the quality and economy of those products. On the other hand, RMS as a challenging concept rises up as a vehicle to solve functionality problems; when needed functionality is changed with respect to time due to emergent condition such as backlash. We have chosen backlash as a cause of logical reconfiguration, for which change in control functionality need is required. From a backlash point of view, feed drive systems experience two different areas of operation: contact and backlash areas. The needed control functionality in the contact zone is dedicated to achieving the best possible tracking performance (tracking). While, in the backlash (non-contact) zone, the needed control functionality will be devoted to bring the system back in contact as fast and effective as it can (Regulating). Reconfiguring between the two specified controllers will operate according to the effect of backlash; this is firmly ascertained through the next chapters in terms of functionality and control.

## **1.8. THESIS ORGANIZATION**

After pointing out the basic and introductory basics beyond the area of research topic we have witnessed in Chapter One, aspects of reconfiguration for machine tools are discussed in general in Chapter Two to show the proper dimensions that pave the way for an acceptable and efficient process. In Chapter Three, modeling aspects of machine tool feed drive systems and backlash models are discussed thoroughly. In Chapter Four, control strategy to be discussed to solve and compensate for the effect of backlash. In Chapter Five, Tools and implementation of this study are comprehensively discussed showing variety of available software concepts and possibilities for future hardware implementation issues. In Chapter Six, simulation and results are shown for feed drive systems in machine tools with and without backlash, switching control results, and as well, comparison with the standard backlash compensation method using the well-known control techniques and diagrams. In Chapter Seven, conclusion is discussed extensively. And finally, future work is demonstrated in Chapter 8.

## 2. ASPECTS OF RECONFIGURATION IN CNC MACHINE TOOLS

### 2.1. INTRODUCTION

A reconfigurable manufacturing system (RMS) is founded for rapid change of production capacity and functionality in response to new market demands and new process technology [Koren *et al.*, 1999]. It has various distinct characteristics including: modularity, integrability, customizability, and diagnosability. Machine tools are almost the main player on the physical level for a modern manufacturing system where reconfigurability shall be introduced. In this chapter, we are explaining the aspects of reconfiguration on the system, software, control, machine, and process levels, see Figure 2.1. These levels are interrelated to a large extent specially when discussing reconfiguration. For example, a tangible kind of reconfiguration on machine physical level such as adding new functionality (e.g., add new axis of motion) will reflect on control and software levels subsequently.

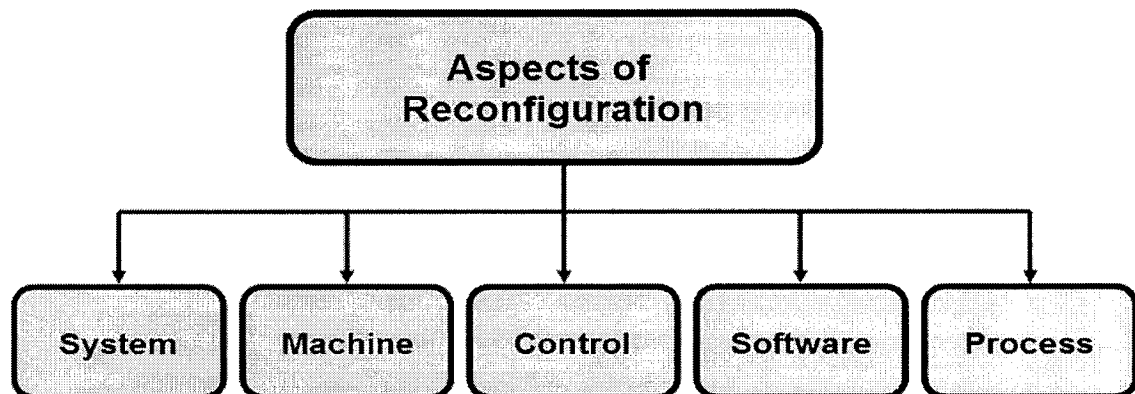


Figure 2.1. Aspects of reconfiguration chart [*reprod. from Mehrabi et al.*, 2000].

Technological impacts and variance among developed systems rely on the control level, as an intermediate environment; where receiving information from physical/machine and delivering to system level components. In Figure 2.2, systems are classified according to technological developments in software and hardware.

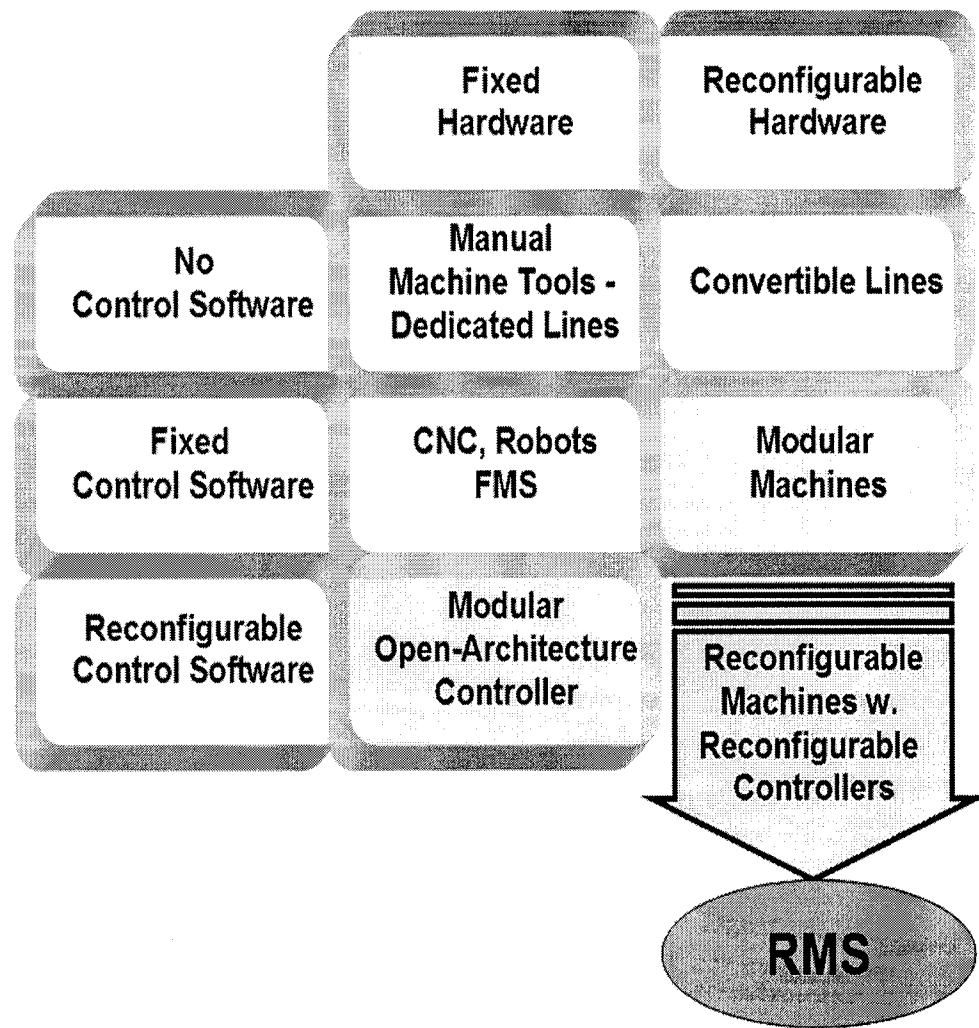


Figure 2.2. Development matrix of software versus hardware for machine tools [*reprod. from Mehrabi et al., 2000*].

## 2.2. SYSTEM LEVEL RECONFIGURATION

Considering the manufacturing cycle of a product, it passes through various stages to achieve the final product. It starts with product conceptualization and shifts into final product design, process planning, production system design, and process control. All of the previously mentioned steps are nicely computerized, yet still not collaboratively integrated.

At the system level, there can be a huge set of configurations for production of different types of products. These products can be of the same part family or of different

families of parts needed. When we say system level, it should comprehensively include the production line; however, it can partially cover a working cell of certain number of workstations.

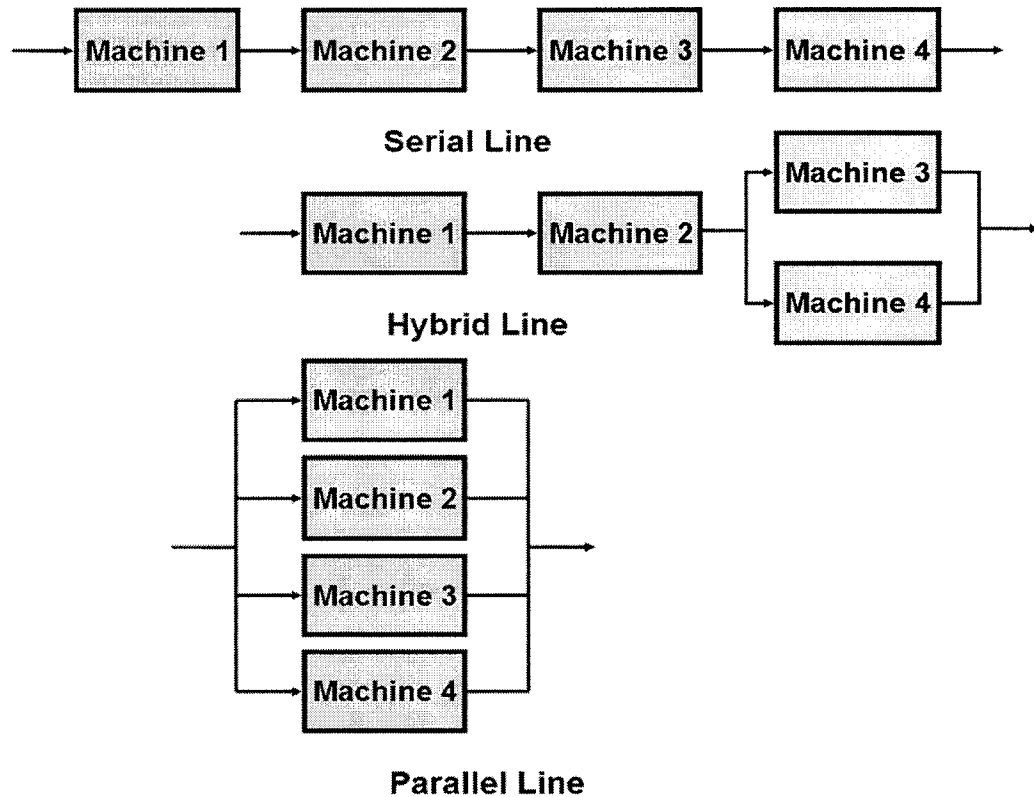


Figure 2.3. Possible system configurations with four machines.

These are the main types of system configurations; see Figure 2.3, where the machine tools are arranged in certain organization. Serial, parallel and hybrid are the main types of system configurations, however, sub-divisional types will be produced according to the nature of crossovers specially in parallel and hybrid types. The aforementioned types are all symmetric natured configurations, which are also referred to as “single-process”. In single-process configurations, each part goes through the same process plan and is executed on the same number of machines as all other parts, regardless of the path selected through the system. On the other hand, we have to define asymmetric configuration, which is also referred to as variable-process configuration. In variable-process configurations, a machined part may experience different process plans



executed on a varying number of machines, according to the path it follows through the system. An example of an asymmetric configuration is one part could be machined under 4 machines or 9 machines depending on the process plan undertaken.

There is no certain system-level design methodology has been undertaken so far to address and comprehensively portray the reconfiguration dimensions in a whole system.

### **2.3. SOFTWARE LEVEL RECONFIGURATION**

Since approximately 25% of the total initial cost of a machine tool is allocated to the software development, this depicts the importance of the software share of the effects of reconfigurability. Handling tasks at lower levels, such as control, monitoring and communications among mechanical, electrical and electronic components, and high level, such as process planning, user interface, process control, etc.

Attributes of the software components in a machine tool:

- Modularity; which facilitates addition/modification of machine tool components.
- Extensibility; which implies that these components are able to respond to new features, environments, and requirements.
- Reusability; which implies that software can be used in other different programs.
- Adaptability; which implies that these components can accommodate different configurations and support internal/external interactions of modules without modifications.
- Compatibility with the hardware.

The previous attributes can be provided via the implementation of open architecture principle and object oriented design guidelines. Openness might be acquired by having modular architecture and well defined interfaces, which allow third parties to develop and use these modules independently, see Figure 2.4. In addition to the hardware/software control modules, real-time database management systems are required to provide sharing data between the different controllers and sensors, and also provide a special domain for reusable modules to be maintained and extended thereafter.

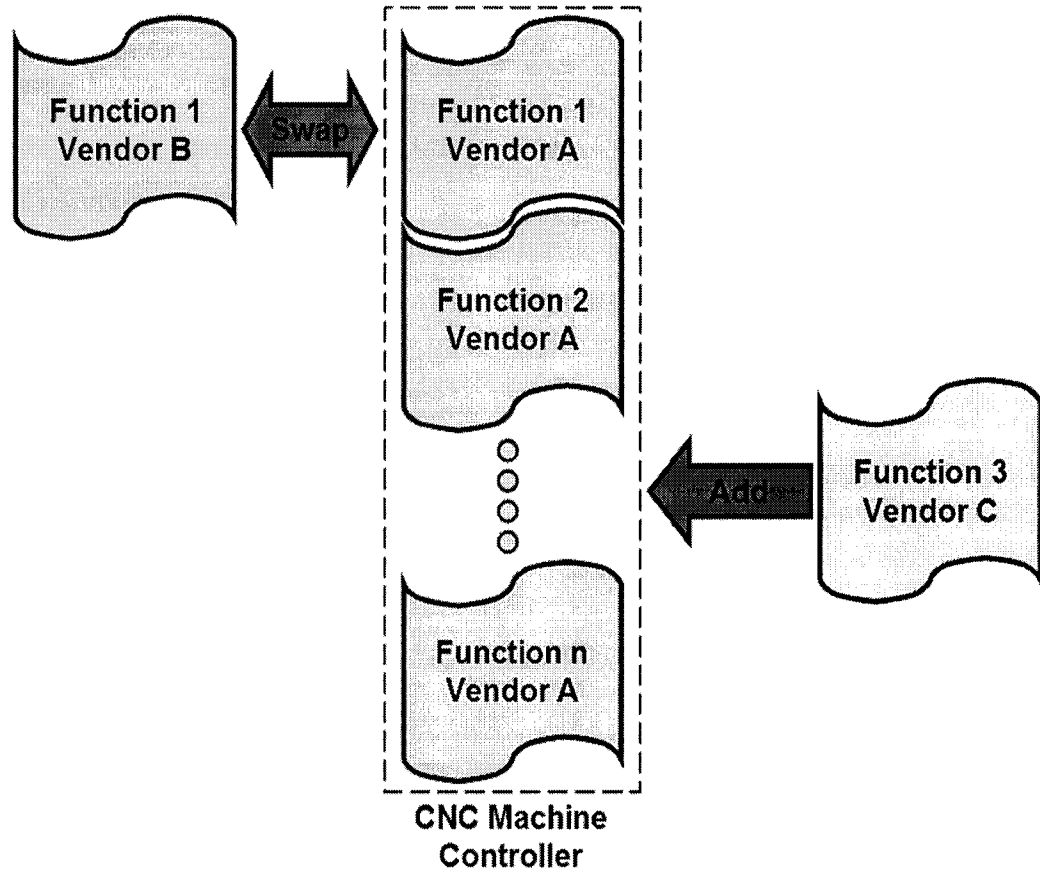


Figure 2.4. Machine tool controller principle as seen from an “open” point of view.

In Figure 2.5, Real time data base (RTDB) scheme as conceived by scientists [Zhou *et al.*, 1995] has been shown. Such a structure is essential to apply mapping theory between cause and effect, input and desired output which is discussed further in section 2.3.

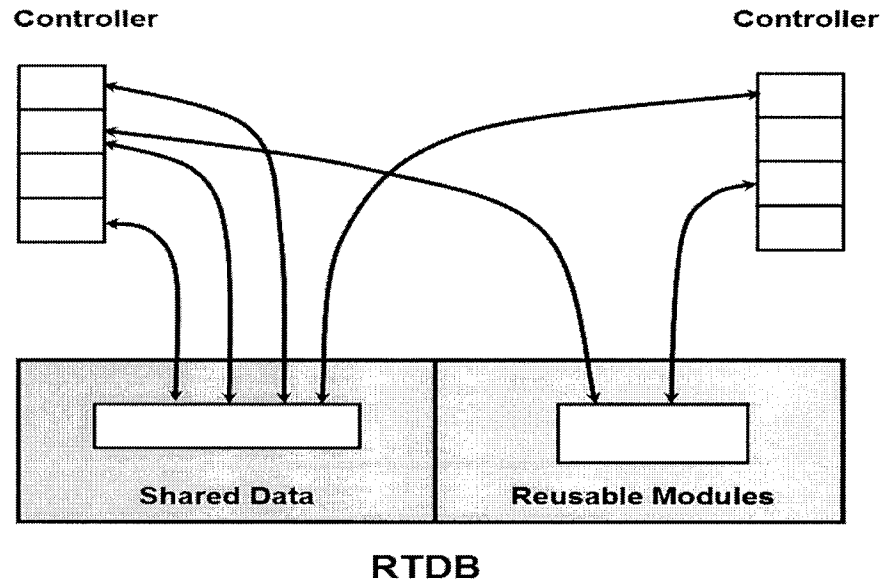


Figure 2.5. Data interaction between the real-time database and controllers.

#### 2.4. MACHINE LEVEL RECONFIGURATION

The most effective concept/key factor that haunts this area is modularity. How do we perfectly modularize the design of machine tool components? How can we ideally put down the map of granularity for machine tool to boost the process of reconfiguration? Answers for the previous questions are still susceptible to development and contributions from all over academia. There is no certain methodology to modularize physical components of machine tools.

Higher complexity will be achieved for reconfigurable machine tools due to considering the aspects of reconfiguration. For conventional machine tools, design has been optimized for certain process with defined and limited configurations. On the other hand, optimization of reconfigurable machine tool elements should consider the different configurations that expected to undergo. Also, clamping and fixturing processes are expected to be more complex and being of higher importance, although they are considered of the auxiliary functions of machine tools.

Machine tool modules are defined by electrical and mechanical interfaces, and co-operating input/output mechatronic components. Figure 2.6 (left) shows a slide as a component of a machine tool. The interfaces to the other machine components are easily screwable flange facings. The configurability within this component is possible, as three different workpiece mounting systems are integrable: Rigid clamping surface, switch shafts for discrete positioning or a NC-Axis. The respective mechanical interfaces are the blocks of the guides and the spindle nut. The core of a machine tool consists of the combination and assembly of such components. From inside outwards, the motion related components are usually added by process specific components (e.g. spindle), additional aggregates, tool- and palette changer, housing components.

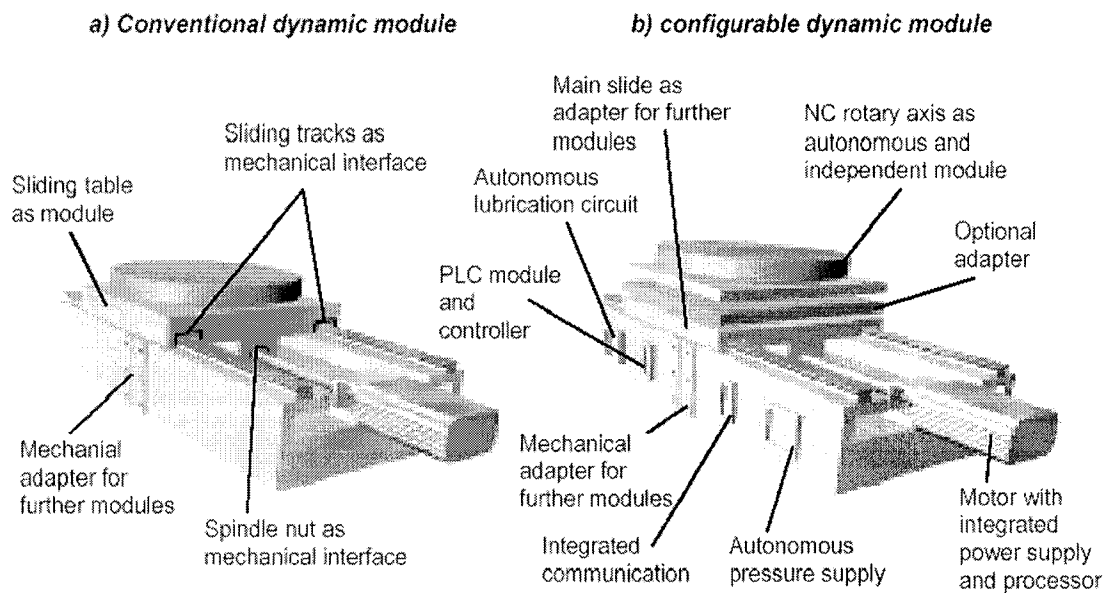


Figure 2.6. An example of reconfigurable modules of machine tools [Pritschow *et al.*, 2003].

To gather components into a module, boundaries of the module should be defined by having interfaces for the module. For reconfiguration purposes, mechanical adaptors can be included within these interfaces, or separately connected to them. Also, all services to the module should be built in as power supply, communication and control components (including PLC).

Figure 2.7 shows the basic design of a reconfigurable as proposed by [Pritschow *et al.*, 2003]. It is derived from the sequential aggregation of main and auxiliary functions to modules. The procedure of addition/omission of module(s) will reconfigure the present machine tool settings to perform different functionalities and processes.

Modules of machine tool components can be proposed as following:

- Motion module(s).
- Tool module.
- Workpiece manipulating module.
- Tool change module.
- Disposal units for auxiliary materials.
- Mechanical interfaces and adaptors.

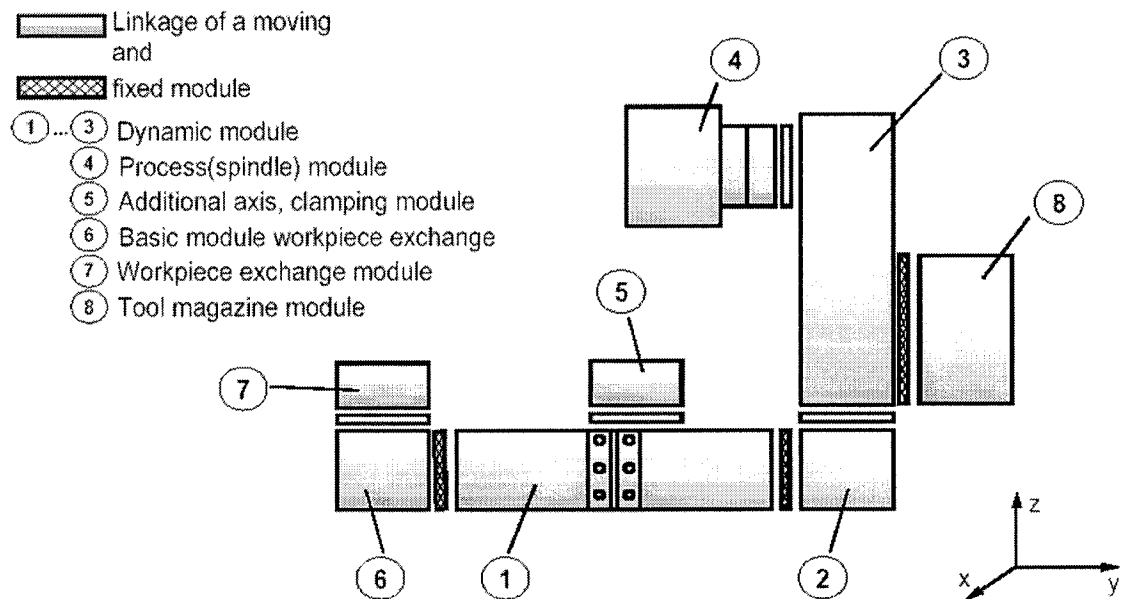


Figure 2.7. Modularization of machine tool components as proposed by [Pritschow *et al.*, 2003].

Reconfiguration of machine tools is accepted and taken into consideration if:

- The reconfiguration process can be carried out in a relatively short time (a few minutes up to hours).
- There are easy-to-use mechanical interfaces and adaptors.
- The interfaces for closing the supply systems for auxiliary energy, power. Communication and information handling are designed “plug-and-producible”.
- The controller automatically adapts to the new machine structure and functionalities.

Further reconfiguration will only gain practical success if:

- The cost for reconfigurable machine tools and the reconfiguration process are less than purchasing specialized machines.
- The producibility after a reconfiguration process can be checked and documented smoothly and automatically.

On the physical/machine level, the following objects can be defined to identify the reconfiguration process:

- The kinematic structure and geometrical sizes.
- The functionalities.
- The characteristics of the machines as a unit by feature modification of modules.

Reconfiguration of machine tools modules can be checked through several parameters:

- Feed.
- Path deviations.
- Stiffness of axes and frames.
- Dynamic behavior of active modules.
- Dynamic behavior of passive modules.

- Traversing range / work space.
- Metal removal rate, etc.

Reconfiguration of a machine tool would include:

- add/remove an axis/ axes of motion
- add/remove spindle(s)
- add/remove tool/workpiece palletes
- tool change
- motion module upgrade (e.g., upgrading the motor)

## **2.5. CONTROL LEVEL RECONFIGURATION**

Intelligent manufacturing systems require dynamic reconfigurability at all levels of all system components. Unfortunately, the majority of machine tools controllers (e.g., axis motion controllers) are closed with proprietary control structure (e.g., PID). This encompasses changes at the hardware, network communications, system software, and application software levels. And to be truly reconfigurable, machine tools built of machine modules require controllers built of control modules with the same level of granularity as the machine modules. The lowest-level control modules must contain both continuous servo control interacting with the mechanical hardware module via continuous-time signals, as well as discrete logic control interacting with other control modules.

In order to maintain optimal production processes the machining systems, including the controllers, must be adapted, when changes get too drastic. Control components include CNC, PLC, HMI (Human-machine interface) and communication tasks within a machine tool.

Commercial CNC systems contains primitive algorithm compared to those introduced by academia. Advanced control strategies like fuzzy logic, neural network, Petri nets, and many others are worked out through academic research during the last

decades. Also on-line tool wear and multi-sensor technology are employed to prevent many events which inevitable in industry nowadays.

Programmable logic controllers are also developing, though PLC has not changed potentially as a technology to assist the rise of reconfigurability. Research connected to PLC is tending to accrediting PC-based systems as a highly competitive alternative for future reconfigurable machine tool.

Complex modularity of machine tool can be overcome by having integrated control and communication system, see figure 2.8. Every module should be connected to the machine bus which considered the system boundary with machine level.

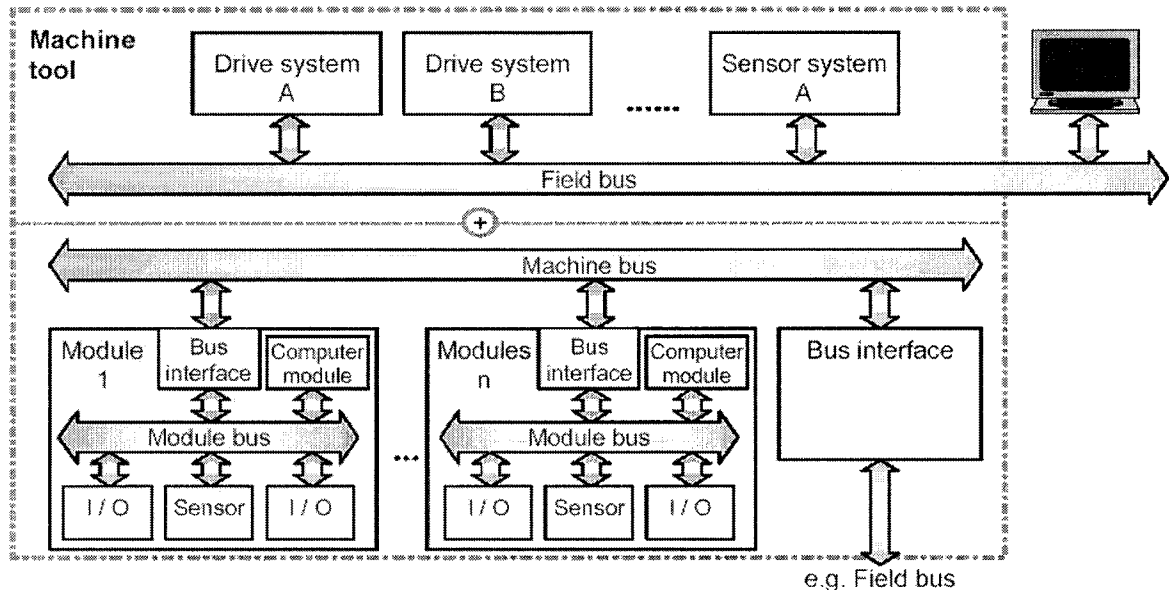


Figure 2.8. Communication system for a reconfigurable machine tool, [Pritschow *et al*, 1997].

Reconfiguring machine tools can be looked at as an adaptive process [Elijah Kannatey-Asibu]. The previous authors have investigated and tried to optimize the monitoring process when the reconfiguration appears. Since it includes a set of specific changes in software and hardware as well as total change in monitoring system, to facilitate changes occur in the nature of production. Multi-sensor monitoring is



paramount in reducing ramp-up time in such a system, since the system needs to be ramped up to full production each time it is reconfigured. This is to enable sources of process-related problems to be identified and corrective action taken in the early stages of system ramp-up.

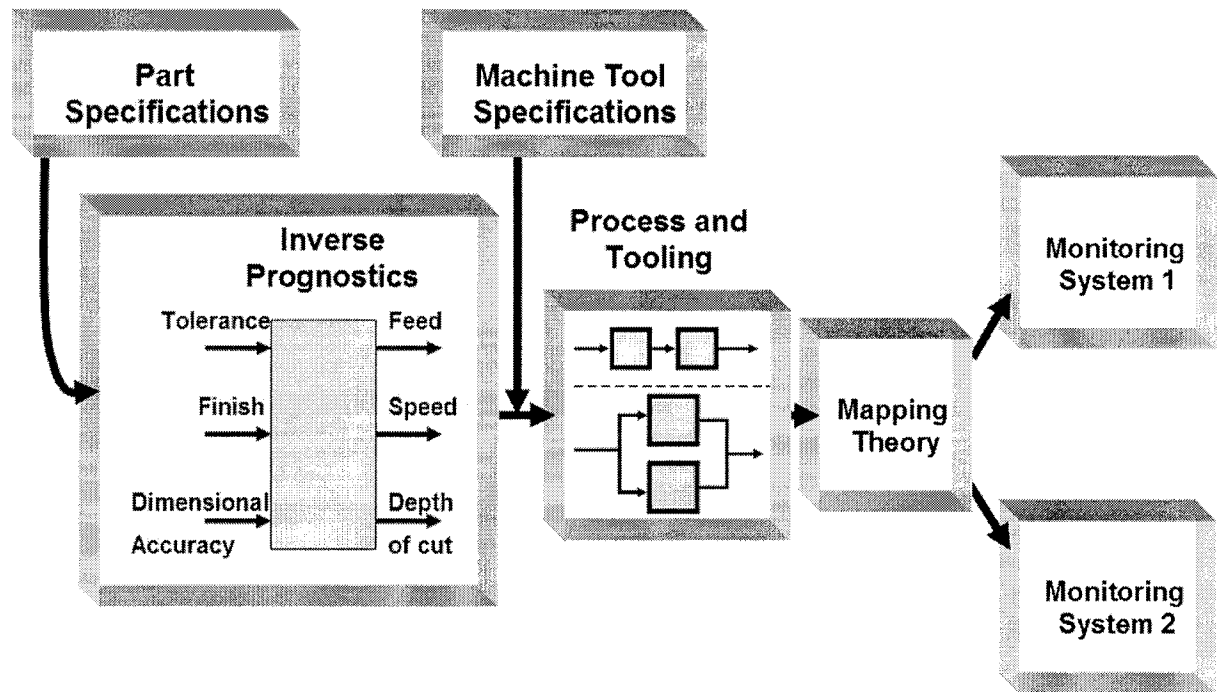


Figure 2.9. Mapping theory vision for reconfigurable monitoring systems [reprod. from Elijah Kannatey-Asibu, 1997].

An example might be a part whose production initially involves a face milling operation. And, due to product design changes, it becomes necessary to add a drilling operation; this could be done by implementing a spindle which is capable of drilling the necessary holes. Let us say that Figure 2.9 illustrates the reconfiguration process. For each product specification, inverse prognostics will be required to specify the machining operation(s). With the requisite process(es) specified, then the mapping theory can be used to specify an appropriate monitoring system. Figure 2.10 shows how mapping theory works for different types of faults for a machining process with many sensors involved. Fault and sensor domains should be defined for such a system for corrective action to be justified and triggered.

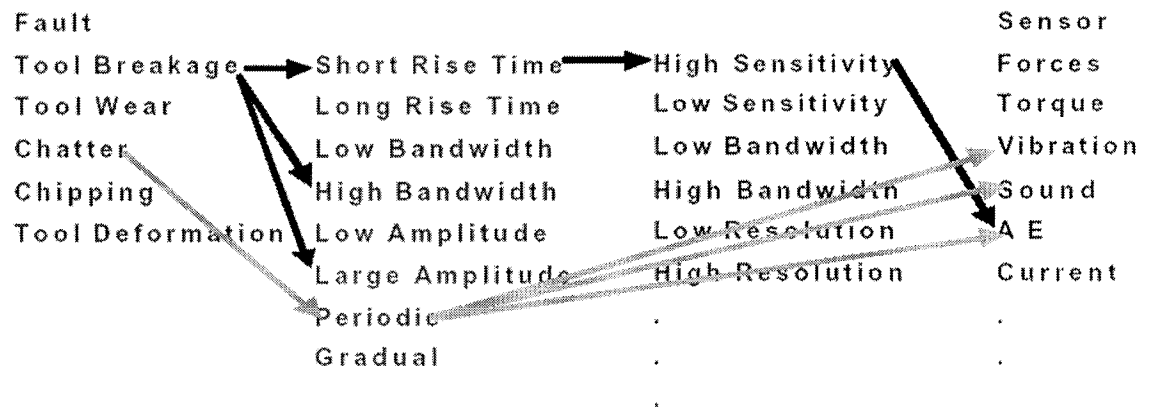


Figure 2.10. Definition of Fault domain and Sensor domain [Elijah Kannatey-Asibu, 1997].

## 2.6. PROCESS LEVEL RECONFIGURATION

Although automatic monitoring and control of machining operations at the process level has been shown to provide substantial economic benefits, the transition of this technology from the laboratory to industry has been slow. One reason for this slow transition is the closed software/hardware architecture of conventional CNC systems. This problem has motivated a growing interest in the design of open-architecture machining platforms. Open-architecture machining platforms will provide the capability to implement complex configurations of process monitoring and control functionalities and to change frequently these configurations. These functionalities must perform well in a wide variety of situations to be feasible for industrial use. This challenge has motivated research in the area of supervisory machining control.

Since the purpose of this thesis is focusing within the process control reconfiguration, we are going to give a different example from the study undertaken. After reconfiguration of the machine tool, production must be “fine-tuned” before it consistently produces at the required quality and production volume. This is referred to as ramp-up, and it takes a long time (months or even years) with traditional machining

systems. In Figure 2.11 ramp-up methodology is explained by which it is used to reduce ramp-up time for new and reconfigured RMS

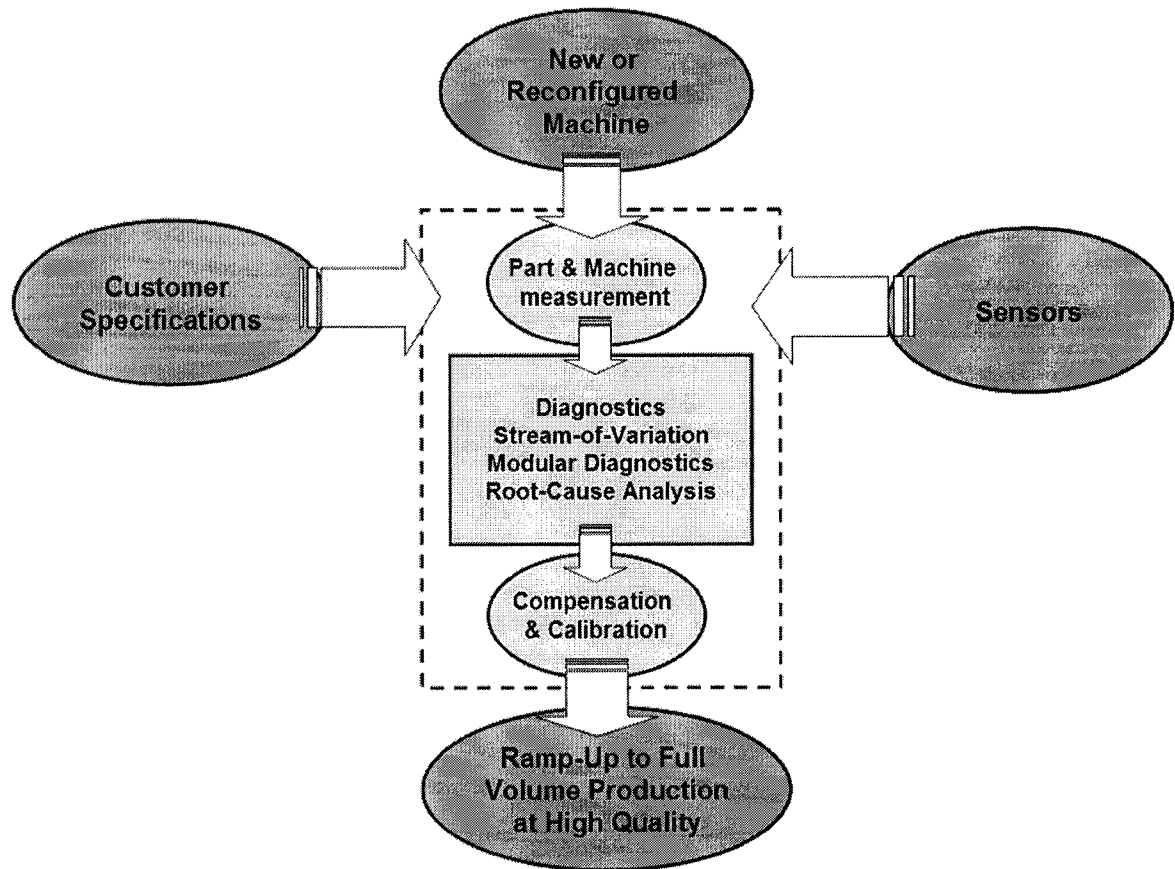


Figure 2.11. Ramp-up methodology [*reprod. from Mehrabi et al., 2000*].

As more and more plant-floor networks become integrated with enterprise networks, Ethernet is encouraging IT departments to get involved in the configuration and selection of components at the process level. However, with their knowledge of the special demands faced, process automation managers should not abdicate control of their networks to the IT function. All of this leads us to e-manufacturing concept. E-Manufacturing is a transformation system that enables the manufacturing operations to achieve predictive near-zero-downtime performance as well as to synchronize with the business systems through the use of web-enabled and wireless infotronics technologies. It integrated information and decision making among data flow from machine/process

level, information flow from factory and supply system level, and cash flow from business system level. E-Manufacturing is a business strategy as well as a core competency for companies to compete in today's e-business environment. It is aimed to complete integration of all the elements of a business- including suppliers, customer service network, manufacturing enterprise and plant floor assets with connectivity and intelligence brought by the infotronics technologies and intelligent computing to meet the demands of e-business/e-commerce practices that gained great acceptance and momentum over the last decade. E-Manufacturing is a transformation system that enables e-Business systems to meet the increasing demands through tightly coupled supply chain management (SCM), enterprise resource planning (ERP), and customer relation management (CRM) systems as well as environmental and labor regulations and awareness.

### **3. MODELING OF CNC MACHINE TOOL FEED DRIVES**

#### **3.1. INTRODUCTION**

Dynamic modeling of a system is quite essential to build the cornerstone of the design of a control system. CNC machine tools are considered one of the dynamical systems that constitute of electrical and mechanical components. The system dynamic model often determines whether performance requirements are met. Two schools of thoughts haunt the world of dynamic systems design modeling: the physical-principle methods and black-box approach.

The physical-principle methods employ the basic physics of the system to derive a dynamic model. It forms a practical application of the well-known and well-structured theories – such as Newton’s laws of motion, Kirchhoff’s law, conservation of energy and many of other fundamental physical rules – where the system elements and their interconnections are known to obey. The assumed model constructed by the above technique also depends on the physical parameters of the system; e.g., mass, stiffness, etc. If the system parameters are not available, then parameter identification method can be utilized.

The black-box approach is primarily statistical in nature. This approach generates a model that best fit the system to be modeled. In depth, the system is exposed to certain input while the response or output is recorded. Accordingly, analysis of the input-output relationship leads to a representing model. Time series analysis, as an example, often assumes a stochastic system. Under this technique, methods like Neural Networks are classified.

The type of model sought will depend both on the objective of the engineer and the tools for analysis. If a pencil-and-paper analysis with parameters expressed as unknowns, a relatively simple model will be needed where secondary parameters to be neglected. On the other hand, numerical analysis can be held on a computer where a

comprehensive model with both primary and secondary elements discussed and showed in the model.

### 3.2. FEED DRIVE SYSTEMS

As a matter of fact, the CNC controllers are generally coordinating relative motion between the tool and the workpiece. This should be done to fulfill a certain cutting process. It substantially confines the problem of searching odds and commons of various machine tools to a smaller area, i.e., spindle and feed drive systems. Spindle system, see Figure 3.1, is the regulated output of an electric actuator, which is highly similar in variant machine tools. For a spindle, what makes a real difference is only whether the spindle surrounding the tool or the workpiece. Consequently, this will affect the scope of cutting mechanics contribution to the design of controller. The main target of control here is spindle on/off task, clockwise/counterclockwise rotation and rotational velocity variation tasks. This task as other switching tasks (e.g. coolant on/off) is supervised by the PLC unit of a CNC controller [Song, D.-J; Weck, 1984].

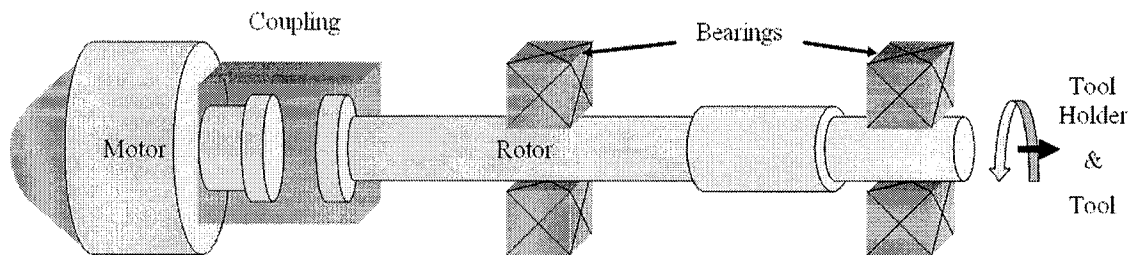


Figure 3.1. Schematic Diagram of a spindle system.

Machine tool feed drives control the positions and velocities of machine tool slides or axes in accordance with commands referenced by CNC interpolator. Due to the inertia, stiffness and damping of the different components of feed drive systems, the feed drive maximum delivered torque should be sufficient to undergo an acceptable cutting operation. An example of a feed drive for a CNC machine is shown in Figure 3.2.

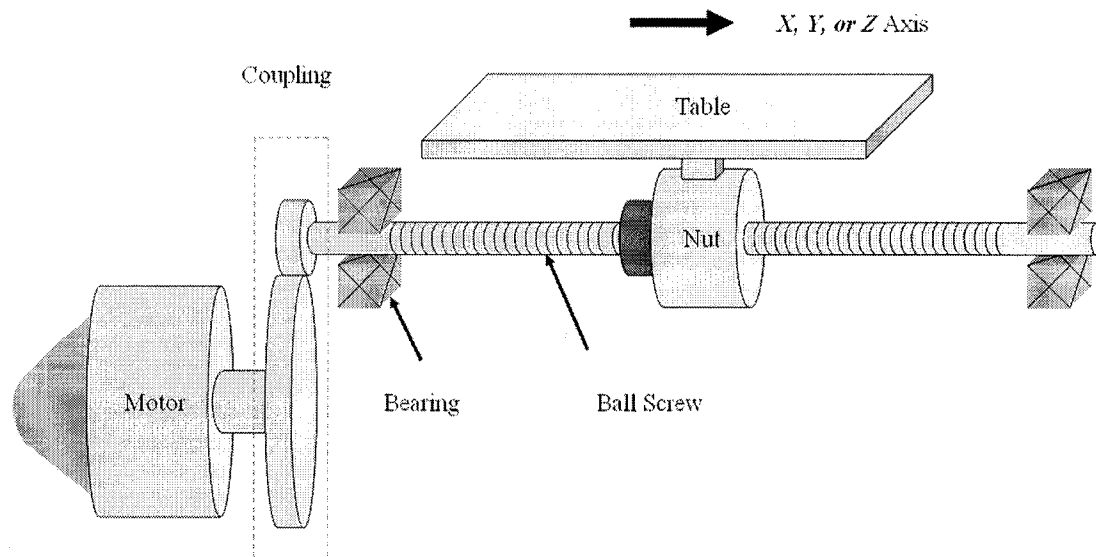


Figure 3.2. Schematic diagram for a translational feed drive.

The four main requirements of feed drives [Srinivisan and Tsao, 1997]:

- Good dynamic design. Changes in feed rate undergone by machine tool moving components should not exceed a time delay of 20-30 ms.
- Immediate signal transmission. Issues like damping and backlash should be taken care of to reduce the vibration of mechanical components during motion.
- Eradication of interference factors. High static and dynamic stiffness to minimize friction and cutting forces effects and vibration caused.
- Matching of individual axes. More rapidly reacting drives should be matched to the slower ones in multi-axis machining.

Electric motors actuate the drives of a machine tool creating motions in three dimensions and causing the tool to cut through the workpiece. Feed drives are usually actuated by motors of several types and specifications which depend on the application of the machine tool, manufacturer, etc. Mainly, motors are of two types: electric motors and hydraulic motors (Figure 3.3.). Both of them provide motion of the main drive systems of

the machine tools which include the motion of the main spindle in lathes, milling machine, drilling machines, etc. Choosing a motor type is affected by the nature of application and requirements needed. Hydraulic motors offer a reduction in weight for a given power and a better acceleration; usually used for high-torque applications. Electric motors are more common in industry in the mean time. They feature longer life, higher efficiency, less maintenance and reduced heat generation.

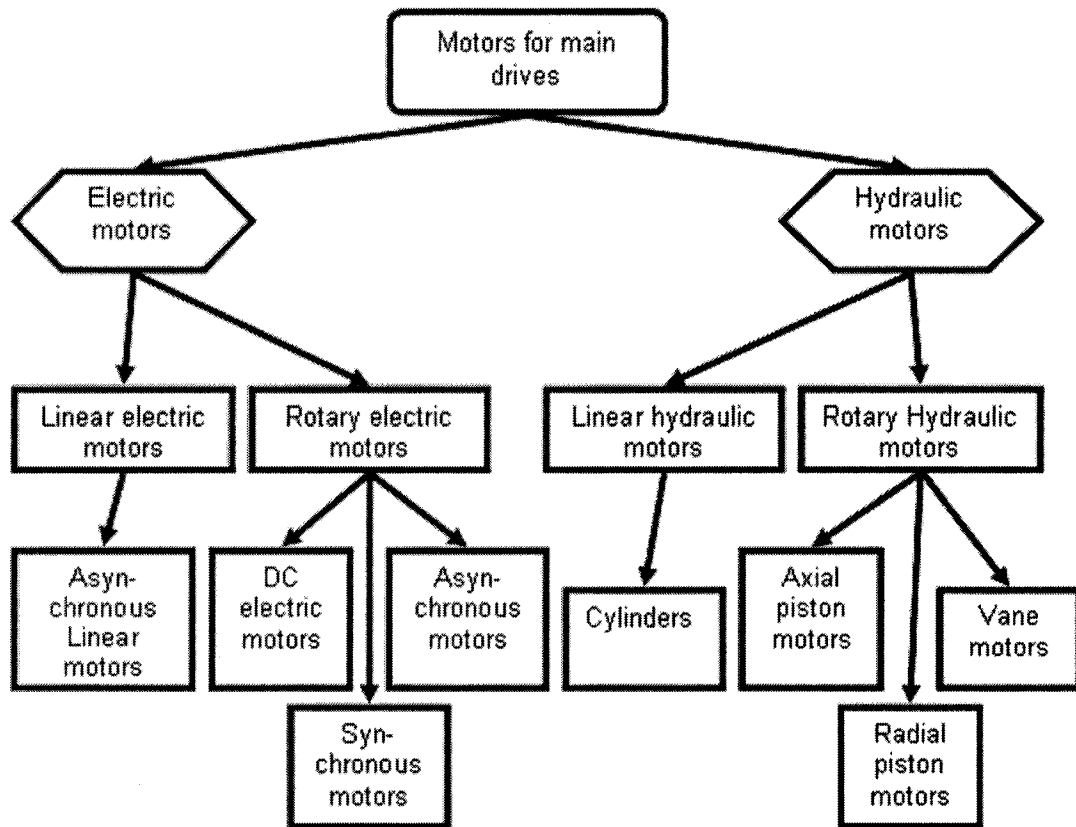


Figure 3.3. Classification motors used in machine tools [Reprod. from Weck, 1984].

Motion is transferred to rest of the mechanical structure which includes a velocity reduction component (e.g. gear box, pulleys) and, in case of transverse feed drive, a rotary-to-transverse conversion component is needed (e.g. leadscrew and nut, rack and pinion, etc) which is connected to the sliding table [Weck, 1984; Koren, 1984; Altintas, 2000].



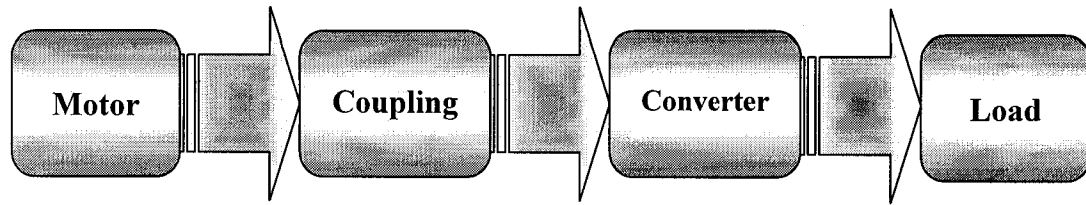


Figure 3.4. Generalized feed drive components.

In Figure 3.4., the above components form the universal model that represents most of feed drive systems, which is mentioned in most of machine tool literature.

Although machine tool designs vary immensely, the mechanical configurations of feed drives are largely standardized. In almost all cases, the recirculating ball screw has established itself as the solution for converting the rotary motion of the servomotor into linear slide motion. Its bearing takes up all axial forces of the slide. The servo-motor and ball screw drive are usually directly coupled. Toothed-belt drives are also widely used to achieve a compact design and better adapt the speed. For position measurement of feed axes on NC machine tools it is possible to use either linear encoders or recirculating ball screws in conjunction with rotary encoders.

Feed drives used in CNC machine tools are either linear or rotational, see Figure 3.4. Also, exemption of a certain component of the above model will introduce a specific type of a feed drive, for example:

- Eliminating the converter/ball screw represents a rotary axis.
- Eliminating the coupling and ball screw represents a linear-motor-driven feed system, i.e., direct linear feed system is employed.
- The load component can be reconfigurable using a very flexible cutting mechanics module.

Rotary and indexing tables are the main types of rotational feed drives. Where rotary tables are considered as a full new axis added to the machine tool, indexing table is considered half-axis due to the fact that its resolution is quite low (360 positions, i.e., 1

degree per movement) and it moves separately from the simultaneous movement of machine's other axes of motion.

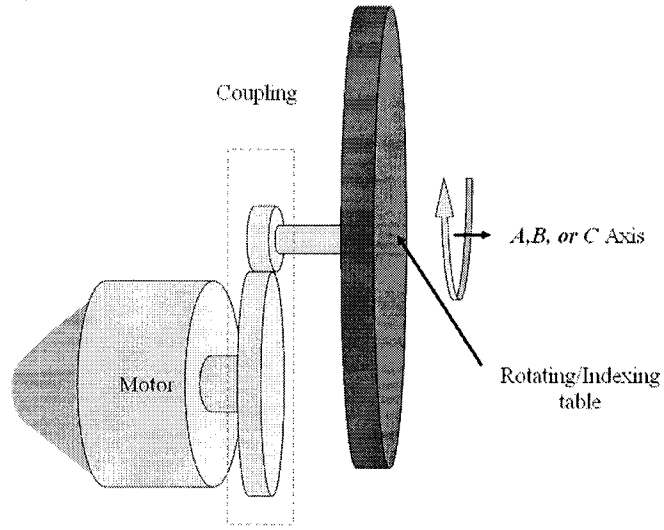


Figure 3.5. Schematic diagram demonstrates a rotational feed drive.

### 3.3. FEED DRIVE MODELING

#### 3.3.1. Modeling from an Electrical Scope Perspective

The three governing equations for a DC motor are the back electromotive force, the electric circuit, and the load:

$$e_b = K_b \omega \quad (3.1)$$

$$V_m = L_m \frac{di_m}{dt} + R_m i_m + e_b \quad (3.2)$$

$$J_m \ddot{\theta} + c_m \dot{\theta} = K_t i_m \quad (3.3)$$

Solving in the frequency domain for  $i_m$  in equation (3.2):

$$i_m(s) = \frac{J_m s^2 \theta(s) + s c_m(s)}{K_t} \quad (3.4)$$

Solving in the frequency domain for  $V_m$  in equation (3.2) and substitute equations (3.1) in (3.2):

$$V_m(s) = L_m s i_m(s) + R_m i_m(s) + K_b s \theta(s) \quad (3.5)$$

$$\begin{aligned} V_m(s) = & \frac{L_m s [J_m s^2 \theta(s) + c_m s \theta(s)]}{K_I} \\ & + \frac{R_m [J_m s^2 \theta(s) + c_m s \theta(s)]}{K_I} \\ & + K_b s \theta(s) \end{aligned} \quad (3.6)$$

$$V_m(s) = \frac{s \theta(s)}{K_I} ( [J_m s + c_m] [L_m s + R_m] + K_b K_I ) \quad (3.7)$$

The transfer function for a DC motor from voltage applied to the armature to angular position acquired on the rotor:

$$\frac{\theta(s)}{V_m(s)} = \frac{K_I}{s ( [J_m s + c_m] [L_m s + R_m] + K_b K_I )} \quad (3.8)$$

Inductance can be neglected, so the transfer function can be shown as following:

$$\frac{\theta(s)}{V_m(s)} = \frac{K_I / R_m}{s \left[ J_m s + \left( c_m + \frac{K_b K_I}{R_m} \right) \right]} \quad (3.9)$$

The state-space formulation of the previous transfer function can be shown as following:

$$\begin{bmatrix} \dot{\theta} \\ \dot{\omega} \end{bmatrix} = \begin{bmatrix} 0 & 1 \\ 0 & -\frac{1}{J_e} \left[ B_e + \frac{K_b K_I}{R_m} \right] \end{bmatrix} \begin{bmatrix} \theta \\ \omega \end{bmatrix} + \begin{bmatrix} 0 \\ \frac{K_I}{J_e R_m} \end{bmatrix} \quad (3.10)$$

### 3.3.2. Modeling from a Mechanical Scope Perspective

Accurate modeling and identification of feed drive dynamics is a paramount stage in formulating a high performance CNC machine tool control. Parameters like friction of its different types (coulomb, static), damping and inertia should be identified. The way of estimating the plant is quite sensitive, by which, determines the accuracy of the model and consistency of the controller as a result of that. Feed drive components cannot be dealt with as a complete rigid body, yet full elasticity represented by FEA methods could be time consuming specially in a real time environment such that of controllers. Models of machine tool feed drive systems are of various natures depending on the number of degrees of freedom considered. Most traditional machine tool controllers are of the closed loop type where feedback signal is taken from the motor side [Altintas, 2000; Koren, 1984; Renton and ElBestawi, 2001]. The plant model is usually of two-degrees-of-freedom nature [Matsubara *et al.*, 1997].

A schematic diagram of a dynamic model for the generalized linear feed drive system is shown in Figure 3.6 [Tsutsumi *et al.*, 1996]. The following nomenclature will be needed to discuss next feed drive model:

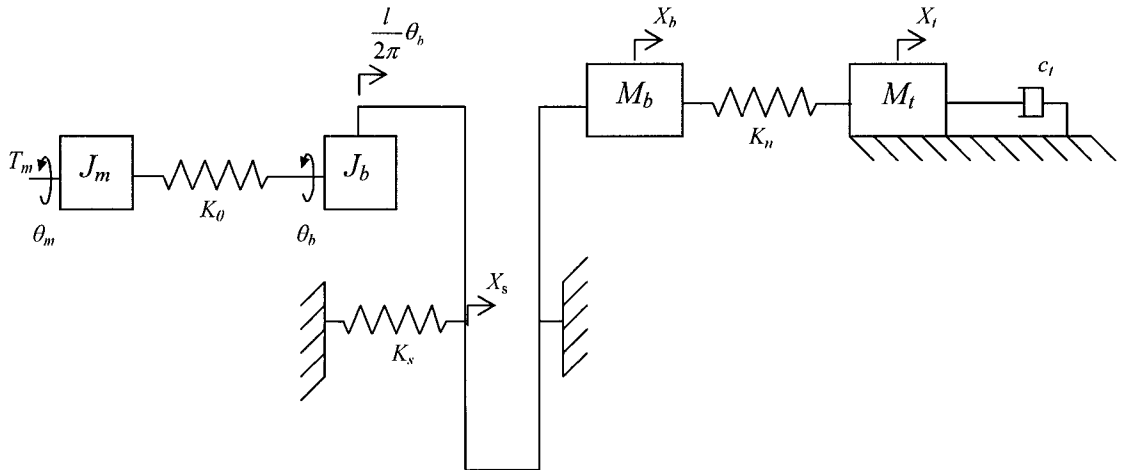


Figure 3.6. Detailed dynamic model for a transverse feed drive (*Reprod. from* [Tsutsumi *et al.*, 1996]).

The Dynamic equations are taken from [Tsutsumi, 1995]; ignoring frictional forces amongst the various modeled components, depicting a system of four degrees of freedom:

$$\begin{aligned}
J_m \ddot{\theta}_m + K_\theta [\theta_m - \theta_b] &= T_m \\
J_b \ddot{\theta}_b + K_\theta [\theta_b - \theta_m] + \frac{l}{2\pi} K_s \left[ \frac{l}{2\pi} \theta_b - X_b \right] &= 0 \\
M_b \ddot{X}_b + K_s \left[ X_b - \frac{l}{2\pi} \theta_b \right] + K_n [X_b - X_t] &= 0 \\
M_t \ddot{X}_t + c_t \dot{X}_t + K_n [X_t - X_b] &= 0
\end{aligned} \tag{3.11}$$

They have modeled this system dividing the machine tool feed drive system into 4 main components, the trajectory generation, servo controller, the actuator system and the table mechanism. Having such a widely demonstrated model will help in minimizing errors and energy leaks in the system. Although not shown here, frictional forces were assigned for each and every component discussed.. In Figure 3.7, we can see the block diagram of feed drive system with a ballscrew as conceived from [Tsutsumi *et al.*, 1996]. The most interesting point about this model is involving machine structure components in the form of stiffness, though, not the whole machine structure has been considered; only surrounding and supporting members.

Depending on the previous model, rotary axis can modeled as following:

$$\begin{aligned}
J_m \ddot{\theta}_m + K_\theta [\theta_m - \theta_t] &= T_m \\
J_t \ddot{\theta}_t + K_\theta [\theta_t - \theta_m] &= 0
\end{aligned} \tag{3.12}$$

The latter formulation for a rotational feed drive system (e.g., rotating tables, indexing tables) is achieved after eliminating the ballscrew component to maintain an angular output similar to that of motor. Generally, the gear ratio component (coupling) is assumed to be unity in our study.

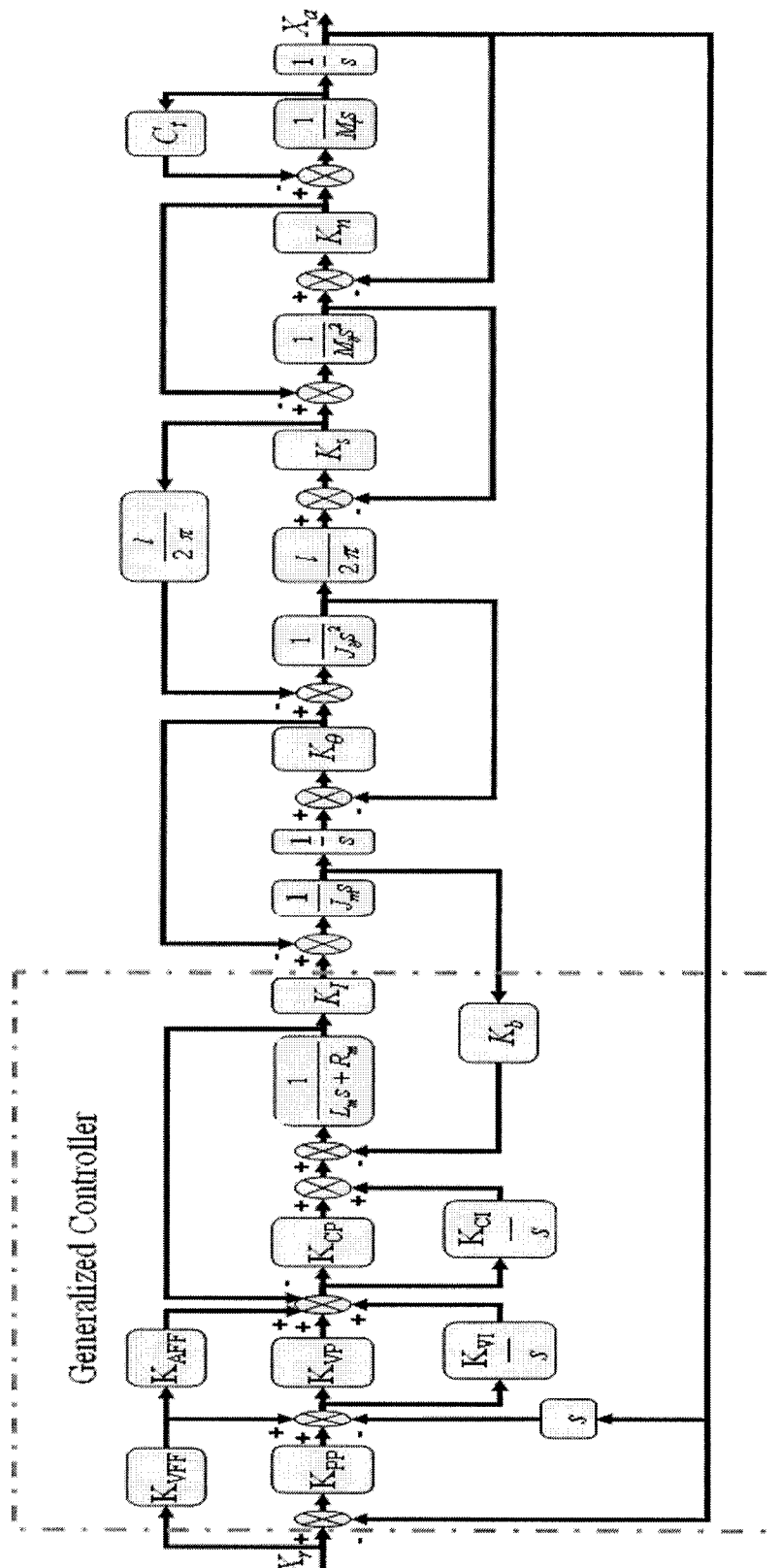


Figure 3.7. An extended-form block diagram for a feed drive system as conceived from [Tsutsumi *et al.*, 1996] formulation.

### 3.3.3. Stiffness Modeling

In [Ebrahimi and Whalley, 2000], the authors have dealt with the modeling of feed drive systems in a very comprehensive way on the basis of the work of researchers like: [Chen and Tlustý, 1995; Lauderbaugh and Ulsoy, 1988; Koren, 1978; Kulkarni and Srinivasan, 1991], and others. Moreover, they have included stiffness of the mechanical components and backlash of the ball-screw in their study (Figure. 3.8). Coulomb and viscous friction are included for the different mechanical structures and the motor as well. However, they assumed dealing with lumped elasticities in the feed drive system when dealing with inertia and friction in particular. Although the study was devoted to the analysis of stiffness in feed drive systems but they have manifested a generic dynamic model of a feed drive system.

In Figure 3.8., axial and angular deflections are taken into consideration in the concerned mechanical structures, which will cover a significant portion of error calculations for axes of motion of a machine tool, hence; improve the functionality of the dependent controllers. A detailed block diagram of the drive model is shown in Figure 3.9.

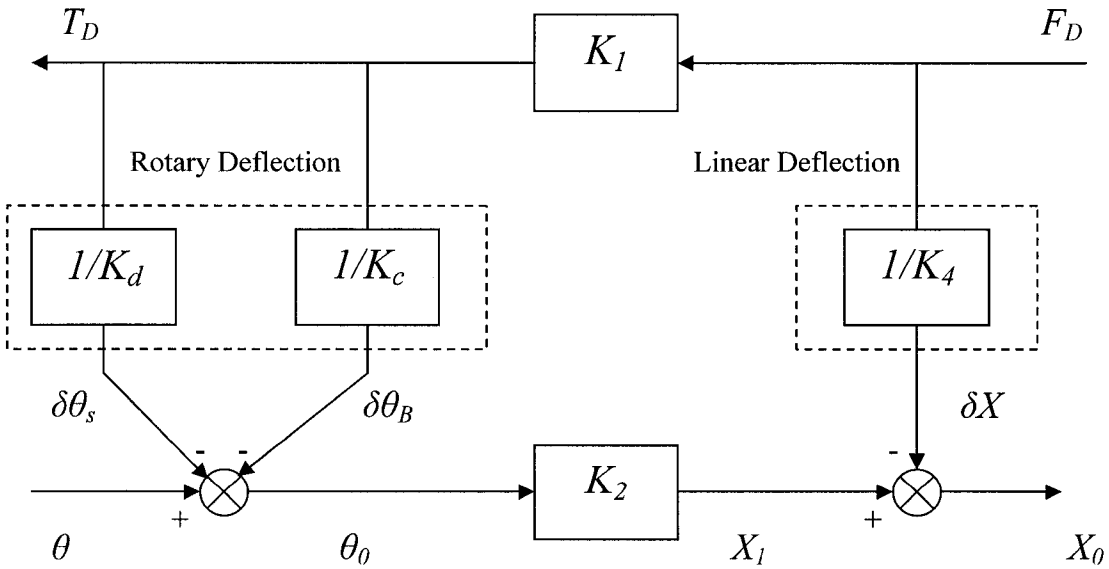


Figure 3.8. Stiffness model as proposed by [Ebrahimi *et al*, 2000].

Where:

- $K_d$  : the angular stiffness of ball-screw
- $K_c$  : the angular stiffness of velocity reduction component (pulley, gear, etc)
- $K_1$  : torque-to-force conversion constant (pitch/ $2\pi\zeta$ )
- $K_2$  : angular displacement-to-transverse displacement conversion constant
- $K_4$  : overall axial stiffness of the structure

The overall stiffness produced from the previous detailed description of machine tool feed drive flexibilities will be plugged in the following Figure, which shows the model of a whole plant, at  $K_f$  :

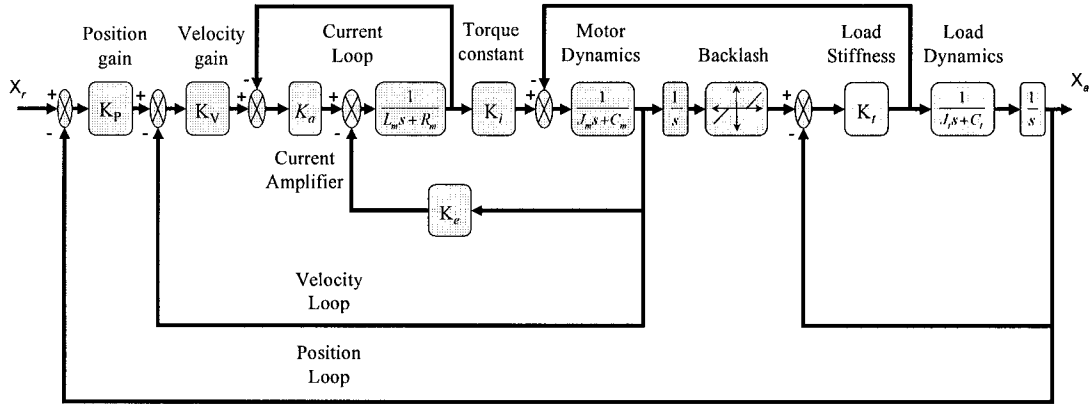


Figure 3.9. Feed drive mechanism plant block diagram.

A 2-inertia system is the most widely-used and numerically efficient for controller design. After searching the literature, we have found that nonlinear problems are mostly discussed and analyzed using this model as an experimentation vehicle. Next, in our



simulation, this model is essentially implemented to establish our study and achieve the results needed.

### 3.4. BACKLASH MODELS

Many motion control systems are of interest. The following are the known models that deal with backlash; the first one will be implemented in our design [Nordin *et al.*, 2002]:

#### 3.4.1. Dead Zone Models

The most widely-used model used to interpret the backlash, and also considered the simplest form that embodies that intrinsic problem. It can be shown in its most preliminary way by equation (3.13) where damping coefficient is considered zero (i.e., inertia-free spring with no internal damping). First, we are going to define the related nomenclature, see Figure 3.10 for further depiction of values mentioned below:

$$T = \begin{cases} k_s(\theta_d - \beta) & |\theta_d| < \beta, \\ 0 & |\theta_d| < \beta, \\ k_s(\theta_d + \beta) & \theta_d < -\beta \end{cases} \quad (3.13)$$

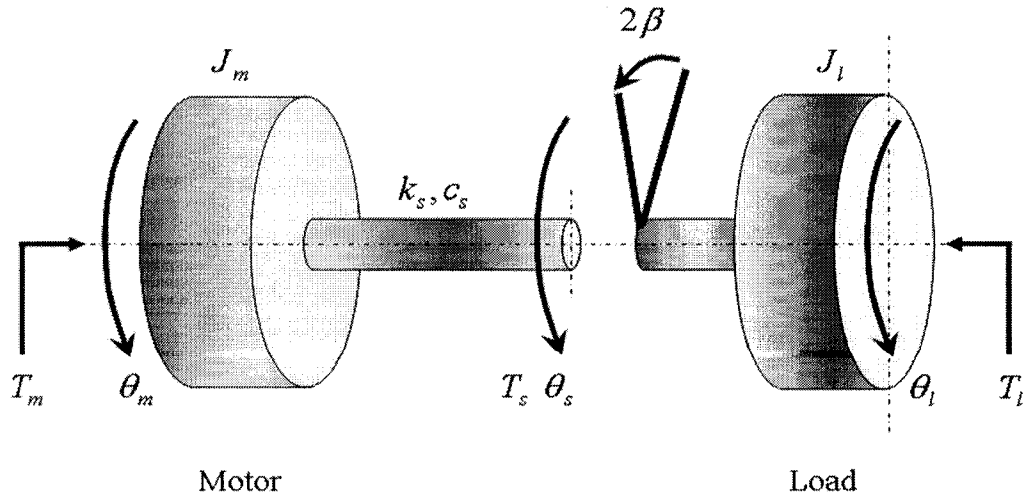


Figure 3.10. Backlash in two-inertia system.

If internal damping is introduced, a typically used modification of the dead-zone model which can be shown in the following form:

$$T' = \begin{cases} k_s(\theta_d - \beta) + c_s\dot{\theta}_d & \theta_d > \beta, \\ 0 & |\theta_d| < \beta, \\ k_s(\theta_d + \beta) + c_s\dot{\theta}_d & \theta_d < -\beta \end{cases} \quad (3.14)$$

To define the system in a more realistic manner, exemption of non-physical torque component produced due the damping term when opposing the direction of motion:

$$T = \begin{cases} 0 & \text{if } T' < 0 \text{ \& } \theta_d > 0 \text{ or if } T' > 0 \text{ \& } \theta_d < 0, \\ T' & \text{else} \end{cases} \quad (3.15)$$

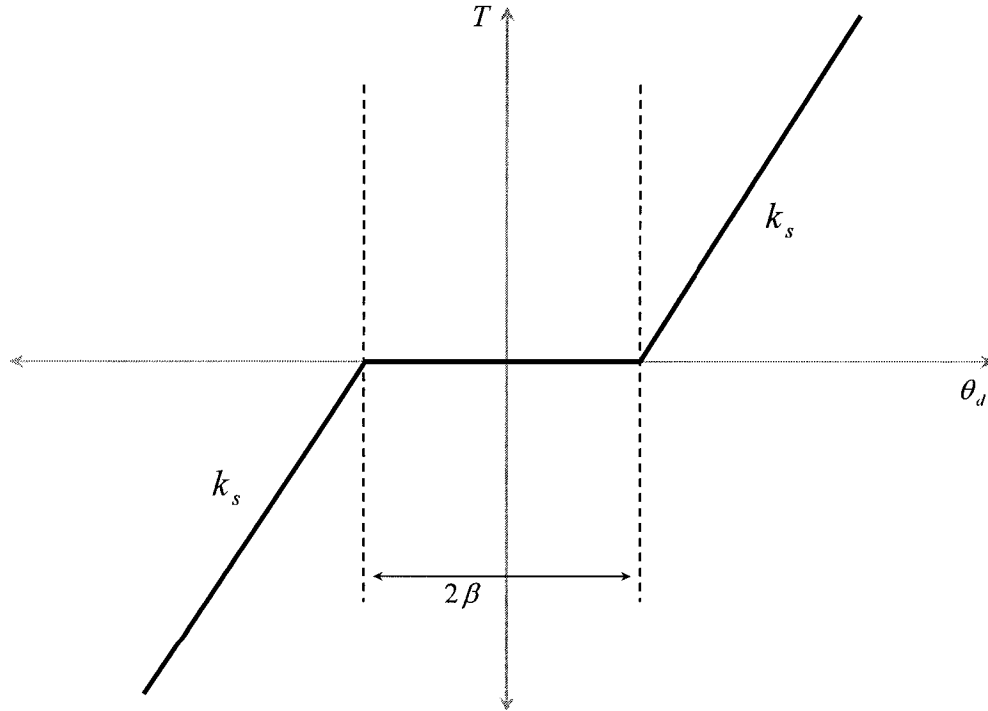


Figure 3.11. The dead zone backlash model.

Also, there is more comprehensive model which is called the exact or physical model [Nordin *et al.* 2002]:

$$T_{exact} = k_s(\theta_d - \theta_\beta) + c_s(\dot{\theta}_d - \dot{\theta}_\beta) \quad (3.16)$$

$$\dot{\theta}_\beta = \begin{cases} \max\left(0, \dot{\theta}_d + \frac{k_s}{c_s}(\theta_d - \theta_\beta)\right) & \theta_\beta = -\beta \\ \dot{\theta}_d + \frac{k_s}{c_s}(\theta_d - \theta_\beta) & |\theta_\beta| < \beta \\ \min\left(0, \dot{\theta}_d + \frac{k_s}{c_s}(\theta_d - \theta_\beta)\right) & \theta_\beta = \beta \end{cases} \quad (3.17)$$

In this model, flexibility of the shaft has been taken into account, producing more accurate description of backlash by taking the twist angle component out of consideration. Excluding the previously mentioned feature, this model is considered identical to the modified dead zone model.

### 3.4.2. Describing Functions

The describing function approach can be implemented to solve non-linear problems, taking into the considerations that the output of this nonlinear system is dominated by the first harmonic of a Fourier series when exposed to a sinusoidal input. Numerous researchers and scientists have used describing functions as means to depict backlash behavior in mechanical systems. Most of servo systems inner components act like low-pass filters which diminish higher harmonics effects. As pointed out by [Brandenburg and Schäfer, 1987; Brandenburg and Schäfer, 1989], a constant output torque,  $T_o$ , to represent the operating point for a system with backlash consideration. a sinusoidal input with an amplitude value  $A$  and offset value  $B$  can be expressed in the following form:

$$\theta_d(t) = A + B \sin(\omega t) \quad (3.18)$$

The output is approximated by a constant offset and the first harmonic:

$$T_s(\theta_d, \dot{\theta}_d) \approx N_B B + AN_p \sin(\omega t) + AN_q \cos(\omega t) \quad (3.19)$$

To solve for the output torque denoted  $T_o$ , the dual-input describing function (DIDF) technique is used to solve for the previous equations 2.18 and 2.19. After that, the following equation is considered:

$$T_o = BN_B(A, B, \omega) \quad (3.20)$$

This procedure is applied to the dead zone model to obtain the describing function for a mechanical system considering backlash in its model.

### 3.4.3 The Hysteresis Model

This model mainly considers the relationship between the motor and load outputs,  $\theta_m$  and  $\theta_l$ , respectively, assuming the presence of a stiff shaft in between. Two classifications for hysteresis models in the case of backlash have been introduced in the literature: friction-driven and inertia-driven hysteresis models. The latter model assumes the driven member (load) holds its position in place, as if hurdled by high friction, when the system is experiencing backlash. Contrarily, the former model zeroes the value of the friction causing the system to move with constant velocity, i.e.,  $\ddot{\theta}_l = 0$ . Considering load torque disturbances are equal to zero, and gear ratio between motor and load shaft equals to one, the following two equations resemble the friction-driven and inertia-driven hysteresis models respectively:

$$\dot{\theta}_l(t) = \begin{cases} \dot{\theta}_m(t) & \text{if } \dot{\theta}_m(t) > 0 \quad \theta_l(t) = \theta_m(t) - \beta, \\ \dot{\theta}_m(t) & \text{if } \dot{\theta}_m(t) < 0 \quad \theta_l(t) = \theta_m(t) + \beta, \\ 0 & \text{otherwise,} \end{cases} \quad (3.21)$$

$$\begin{aligned}
\dot{\theta}_l(t) &= \dot{\theta}_m(t) & \text{if } \dot{\theta}_m(t) > 0 & \theta_l(t) = \theta_m(t) - \beta, \\
\dot{\theta}_l(t) &= \dot{\theta}_m(t) & \text{if } \dot{\theta}_m(t) < 0 & \theta_l(t) = \theta_m(t) + \beta, \\
\ddot{\theta}_l(t) &= 0 & \text{otherwise,} &
\end{aligned} \tag{3.22}$$

One of the features of hysteresis models in general is absence of damping component in mathematical formulation, similar to dead-zone models. Moreover, the shaft is assumed totally stiff,  $k_s = \infty$ .

### 3.5. MODELING FOR BACKLASH CONTROL

We are using the two-inertia system with backlash and stiffness which can be described as following:

$$J_m \ddot{\theta}_m + c_m \dot{\theta}_m = u - \mathcal{G} \tag{3.23}$$

$$J_l \ddot{\theta}_l + c_l \dot{\theta}_l = \mathcal{G} \tag{3.24}$$

Where the subscripts,  $m$  and  $l$ , stands for motor side and load side, respectively,  $u(t)$  is the control input,  $\mathcal{G}$  is the spring force between the two masses. For convenience, the mathematical model of the feed drive is put down in terms of torsional inertia and stiffness. i.e., the translational movement of the table is transformed into an equivalent rotary movement, and due to which the mass of the table is converted into an equivalent inertia. The spring force  $\mathcal{G}$  is function of the motor position,  $\theta_m(t)$  the load position,  $\theta_l(t)$  and backlash,  $\delta(\theta_d)$ .

$$\mathcal{G} = k_s \delta(\theta_d) \tag{3.25}$$

Where  $k \geq 0$ , is the spring stiffness, and  $\delta(\theta_d)$  is a dead-zone characteristic used to model the backlash effect:

$$\delta(\theta_d) = \begin{cases} (\theta_d - \beta) & \theta_d > \beta, \\ 0 & |\theta_d| < \beta, \\ (\theta_d + \beta) & \theta_d < -\beta \end{cases} \quad (3.26)$$

With  $\beta \geq 0$  which is the dead-zone width. The viscous friction is shown in both sides; motor and load, of the feed drive system by  $c_m$  and  $c_l$ , respectively. The block diagram of this system is shown in Figure 3.11 [Sugie, H. *et al.*, 2000].

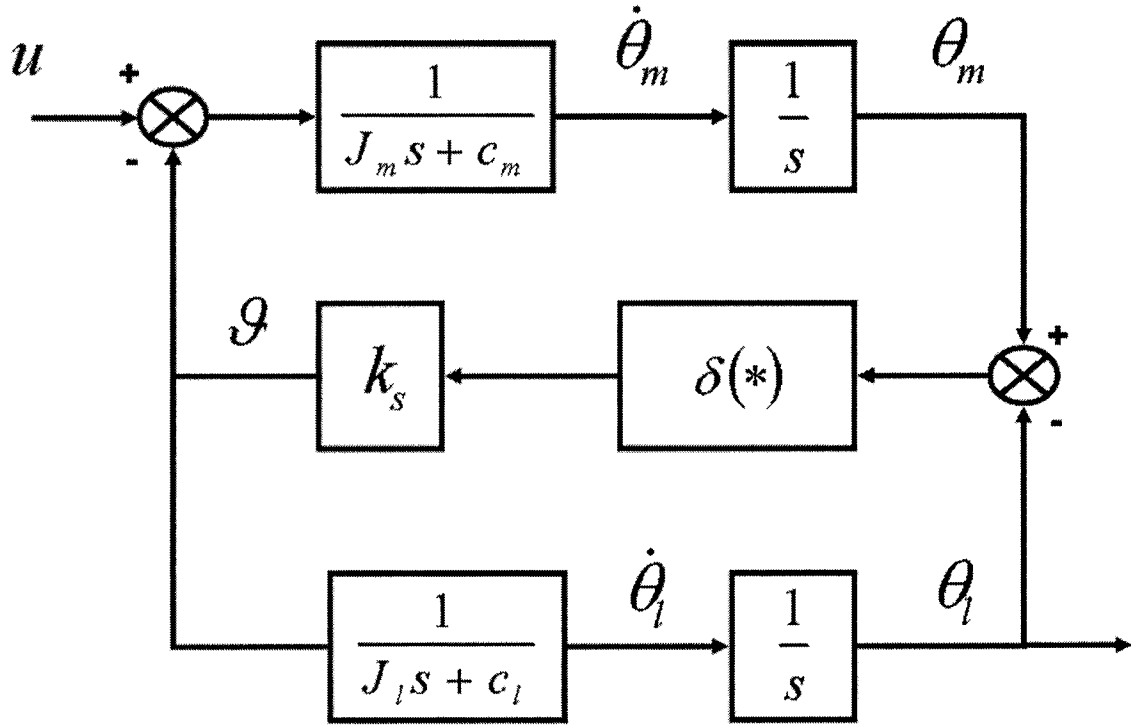


Figure 3.12. Backlash model within a feed drive system.

This system can be formulated into state-space representation as following:

$$\dot{x}_m(t) = A_m x_m(t) + B(u(t) - g(t)) \quad (3.27)$$

$$\dot{x}_l(t) = A_l x_l(t) + B_l g(t) \quad (3.28)$$

Where the two equations show the states of motor and load, respectively, are

$$x_m^T = [\theta_m \quad \dot{\theta}_m], \quad x_l^T = [\theta_l \quad \dot{\theta}_l], \quad A_m = \begin{bmatrix} 0 & 1 \\ 0 & -\frac{c_m}{J_m} \end{bmatrix}, \quad A_l = \begin{bmatrix} 0 & 1 \\ 0 & -\frac{c_l}{J_l} \end{bmatrix}, \quad B = \begin{bmatrix} 0 & 1/J_m \end{bmatrix}^T$$

$$\text{and } B = \begin{bmatrix} 0 & 1/J_l \end{bmatrix}^T.$$

The control process involves two main modes of operation, in which two controllers are to be interchanged; backlash-phase and contact controllers. In backlash phase,  $\mathcal{G}(t) = 0$ , the load and motor dynamics represented by equations (2.9 & 2.10) are decoupled. Physically, this phenomenon is obviously sensed, due to the fact that the motor does fail to supply motion to the load in that instant. When  $\mathcal{G}(t) \neq 0$ , the feed drive system halves are brought back to a coupling condition, i.e., is in the contact phase.

For this system, stiffness  $k$  and backlash angle  $\beta$  are the main critical parameters which affect accuracy of the output desired. The more the flexibility of the system, the more the system prone to control difficulties.

## 4. CONTROLLING OF CNC MACHINE TOOL FEED DRIVES

### 4.1. INTRODUCTION

#### 4.1.1. Principles of Machine Tool Control

A typical block diagram of a control system used in machine tool feed drives is shown in Figure 4.1. Generally, in multi-axis machine tools, each axis of motion is driven by a separate control loop. However, control as a whole process task is achieved concurrently by working out all axes of motion involved. The controlled variable, which is the actual axial position  $P$ , is measured by having an encoder or a resolver connected conventionally to the motor, however, research labs deal with feedback from the load side. The actual position is fed back and compared with the reference signal, which is the required position  $R$ . The resulting error signal  $e$  is fed into the control resulting into generating of control signal  $u$ . Consequently, this leads into generation of driving torque  $T$  by which the feed drive is actuated. The controller aims at eliminating the error signal itself, i.e., eliminating tracking error and nearly equating  $P$  with  $R$  [Koren, 1984; Altintas, 2000].

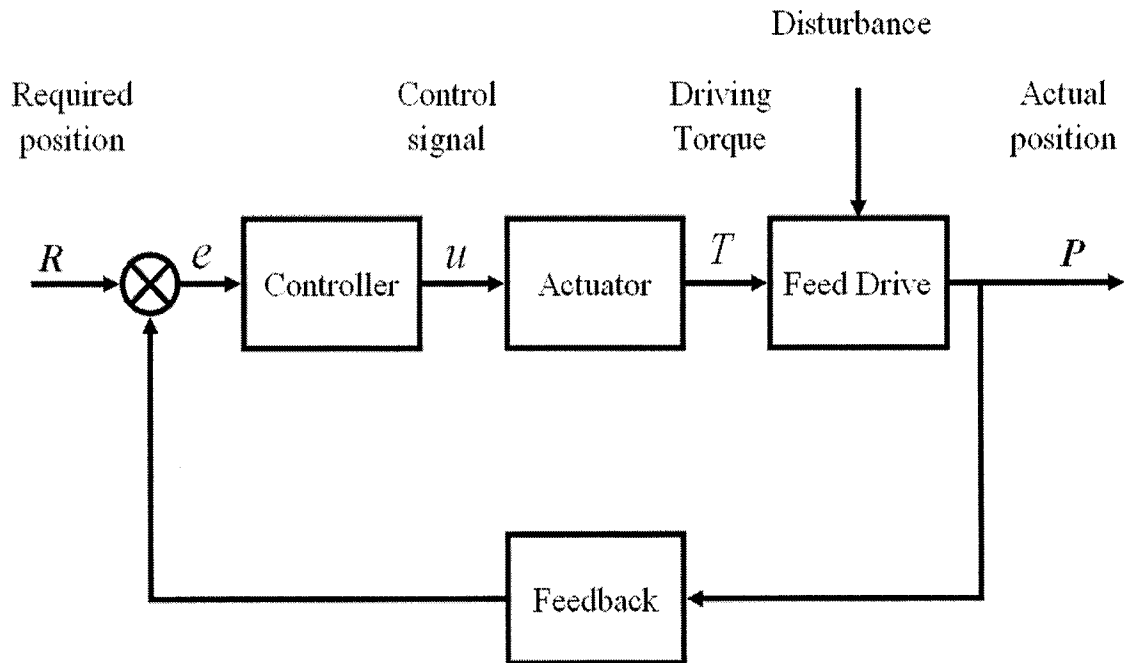


Figure 4.1. A block diagram represents a general depiction of machine tool feed drives.



There are two main types of CNC systems: point-to-point, and contouring systems. The latter requires a good axial positioning accuracy at the desired points; usually a proportional (P) control can accomplish this task quite satisfactorily. The former introduces movement in three dimensional space where the entire path is paramount as a resulting continuous output and the trajectory as a whole is compared with the desired one, e.g., milling. Speaking in terms of feedback, contouring systems essentially have feedback in their control loop in contrary to point-to-point systems where they are open-loop controlled. In the literature, they always refer to contouring systems in their studies as a superset, taking into consideration that point-to-point operations (drilling, boring, etc) are being included within machining centers due to their continuous economic feasibility.

#### **4.1.2. General Trends in CNC Machine Tools Research**

Among those who are concentrating their research efforts in machine tools, particularly, in drive nonlinearity, certain investigators stand out of the crowd. Kato, who has touched upon friction in many areas of research, considered stick-slip in the slideways of a workpiece table [Kato *et al.*, 1972]. Also, Tomizuka has shown the problems which friction can cause in machine tool contouring accuracy under both low- and high-speed operation [Suzuki and Tomizuka, 1991; Tung *et al.*, 1993a; Tung *et al.*, 1993b], and has developed pulse-width modulated (PWM) control techniques to compensate for them [Yang and Tomizuka, 1987; Yang and Tomizuka, 1988]. Tarn and his associates have since developed and tested controllers for both the stiction [Tarn and Cheng, 1995] and backlash [Kao *et al.*, 1996] problems individually as found in a computerised numerically-controlled (CNC) drill press and lathe. Other researchers are involved with a number of machine tool projects, including control [Alter and Tsao, 1996a; Alter and Tsao, 1996b; Brown and Parkin, 1998]. Some investigators are looking at mechatronic solutions to improve machine tool precision and accuracy.

The purpose of having a controller for any electromechanical system is to overcome errors and stabilize the system. Sources of errors are numerous for machine tools. We can classify errors into the following groups [Koren and Lo, 1992]: machine

structure induced errors, disturbances due to cutting forces and controller and plant dynamics. In contouring application, the term “contouring error” has been introduced to denote the orthogonal error component with respect to the desired path shown in Figure 4.2. This error is of two-dimensional nature since it requires two axes of motion to be depicted. Contour errors are quite the concern for many scientists [Koren, 1980; Koren, 1984; Poo *et al.*, 1972]. However, error values given by manufacturers as machine tool specifications are, unfavorably, axial tracking error values.

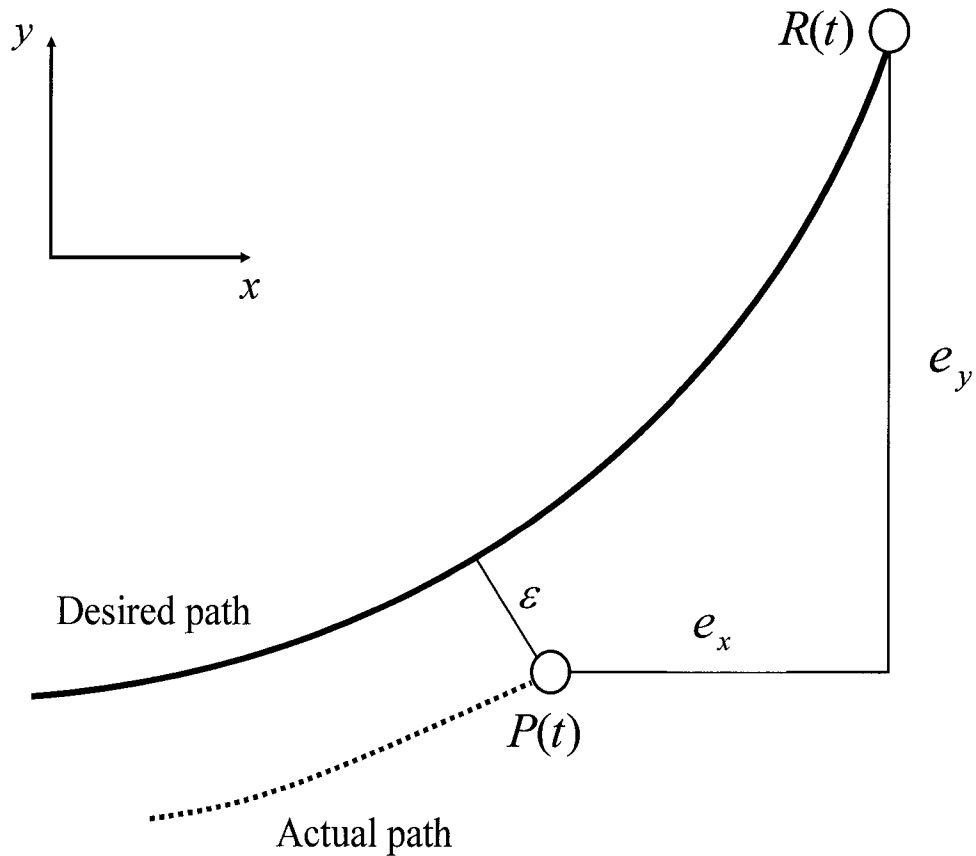


Figure 4.2. Contour error as introduced by [Koren, 1980].

Where  $\varepsilon$  denotes the contour error,  $P(t)$  and  $R(t)$  the desired and actual tool positions, at time  $t$ , respectively,  $e_x$  and  $e_y$  denote the tracking errors in  $x$ - and  $y$ -directions, respectively. Contour errors are induced by various causes. The most common

cause is the one due to contour shape itself. Producing nonlinear trajectories requires nonlinear inputs to the system. In cases of circular contouring, the following  $x$  and  $y$  input equations are introduced:

$$x = r(1 - \cos(\omega t)) \quad (4.1)$$

$$y = r \sin(\omega t) \quad (4.2)$$

Where  $r$  is a circle radius,  $\omega = f / r$  and  $f$  denotes the overall feedrate along the circle. Such a sinusoidal input produces primary transients before reaching a steady similar sinusoidal output. Consequently, phase lag in addition to the usual wave amplitude difference (steady-state error) occur which inherently depends on the value of  $\omega$ . Therefore, the contour error is a function of  $\omega$ . For a circular path, the following formulation represents the contour error [Koren, 1992]:

$$\frac{\varepsilon}{r} = 1 - \frac{1}{\sqrt{1 + (2\xi\omega / \omega_n)^2 - 2(\omega / \omega_n)^2 + (\omega / \omega_n)^4}} \quad (4.3)$$

Where  $\xi$  and  $\omega_n$  are the damping factor and the natural frequency for any machine tool feed drive control loop, respectively.

[Koren, 1980] has explained the contouring error due to parameter mismatch in controller gains at steady state of  $x$ - and  $y$ -axes as following:

$$\varepsilon_{ss-mismatch} = \left( \frac{f_x f_y}{f} \right) \left( \frac{K_y - K_x}{K_x K_y} \right) \quad (4.4)$$

Where  $f_x$  and  $f_y$  denotes the required feedrates in both  $x$ - and  $y$ - axes, respectively,  $f$  is the overall feedrate, which equals  $\sqrt{f_x^2 + f_y^2}$ ,  $K_x$  and  $K_y$  are the open-loop gains for  $x$ - and  $y$ -axes, respectively. Other sources of contour errors are

mainly due to cutting force disturbances. Depending on all of the previous information, the idea of cross coupling control have evolved and paved the road for such an improvement to establish a new branch of machine tool control science.

## **4.2. REVIEW OF DIFFERENT BACKLASH CONTROL STRATEGIES**

### **4.2.1. Conventional Linear Control**

Academia has been dealing with the non-linear problem of backlash since quite a while. Naturally, usage of conventional linear techniques for motion control systems would be the first refuge for researchers to tackle this prominent hurdle.

Literature findings in our study are organized starting with the least-precision cases all the way to position control systems, considering chronological order. Almost all the papers we found on speed control assume feedback from the motor side only. This is the most relevant case from an industrial point of view since often it is impossible or very expensive to measure the velocity of the environmentally harsh load side. However, It is surprising that feedback from the load side for speed controlled systems seems to be very scantily treated in the literature. [Brandenburg, Geissenberger, Kink, Schall, & Schramm, 1999] is an exception, since in many important systems there are sensors on the load side, e.g., the wheel speed in trucks and cars is measured, or the end effector in robots may contain several sensors.

Linear feedback from the measured motor speed, see Figure 4.3, is the most common control configuration. The following 2-inertia linear model to be considered:

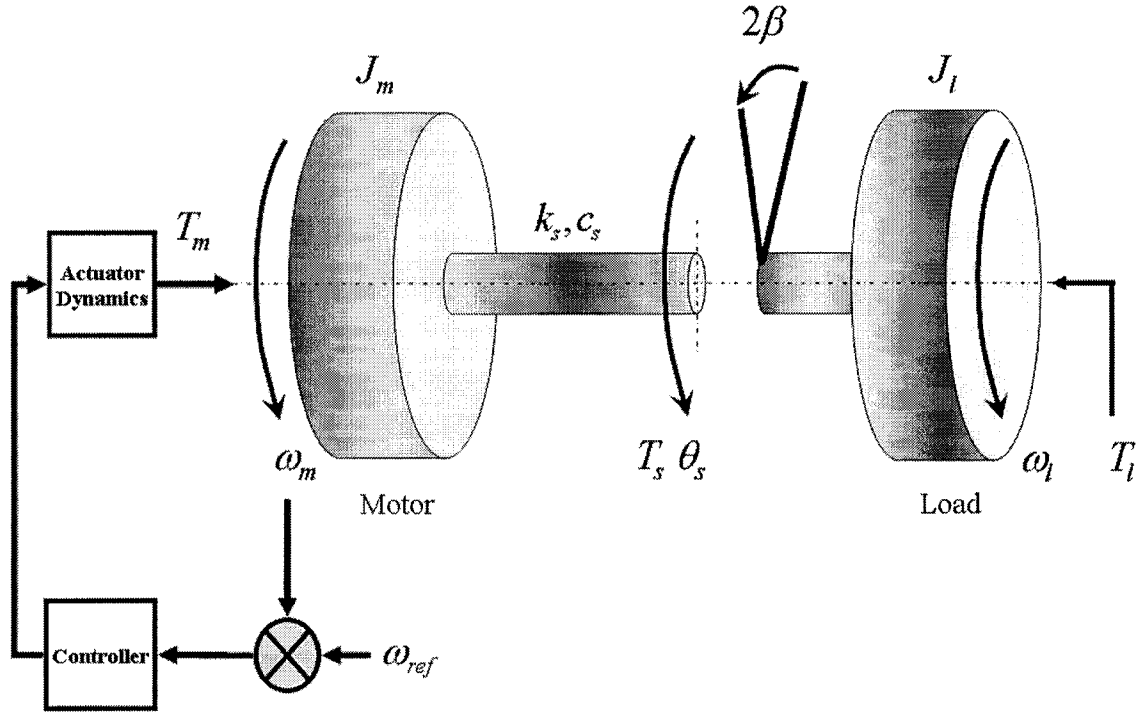


Figure 4.3. Linear feedback from motor speed.

In [Brandenburg,1986] and [Brandenburg *et al.*,1986] the describing function of the dead zone backlash model is used to ascertain the PI-control of the model mentioned previously, with backlash may cause limit cycles whose amplitudes depend on the size of the load torque disturbance  $T_l$ . A supplementary shaft torque observer with partial torque compensation may make the closed loop system asymptotically stable with a transient response similar to that of a linear system.

In [Dhaouadi *et al.*1994], a three mass system is considered: motor, gear, and load, with a backlash between the motor and the gear. The backlash is modeled as a dead zone. The controller contains an integral term, partial feedback from a gear torque observer, and state feedback from a two-mass-model reduced-order observer that estimates the second shaft torque, the load torque disturbance, and the load angular velocity. The reduced order observer and state feedback gains are turned by pole placement. The backlash is replaced by an uncertain gain, which is equivalent to using the describing function of a shaft modeled as a pure spring, integrated into the frequency

function of the linear part of the open loop; see [Nordin *et al.*, 1997]. Experiments show that feedback from the gear torque observer suppresses the high frequency limit cycle that appears otherwise, at the price of a higher overshoot and longer settling time of a step response on the load side.

In the simulation study [Cohen and Cohen, 1994], a worm gear is considered in place of the backlash element, modeled as  $T_s$ , is multiplied by a gear ratio that depends on the direction of motion. The controller includes a shaft torque compensator, together with a pole placement design using the Diophantine equation [Astrom & Wittenmark, 1984]. In [Nordin, 2000], it is demonstrated how to use Quantitative Feedback Technique (QFT) for uncertain systems with backlash, described by a static function of  $\theta_d$  and  $\omega_d$ , see previous chapter for modeling parameter definitions.

A mechanical solution to the backlash problem in high precision position control systems is the so called anti-backlash gear that contains two cog wheels on the motor side connected with a stiff spring, such that the backlash gap is always closed. The price for this solution is the appearance of an additional resonance that limits the achieved closed-loop bandwidth.

Linear controllers that shall handle systems with backlash must be robust enough to handle this nonlinearity. A few different approaches have been reported in literature. Many of the results use describing functions as a stability analysis method. The most straightforward control method for systems with backlash is to use a basic PID-controller that is tuned not to excite oscillating modes originating from the backlash or shaft flexibility [Hori *et al.*, 1994; Nakayama *et al.*, 2000].

One of the earliest papers using the describing function technique is [Chestnut, 1954]. A generalized describing function is used for the dead zone model of backlash together with the equations of a two-mass system with position feedback either from the motor or from the load. Conditions for limit cycles are clearly analyzed.

In [Freeman, 1957], Freeman analyzes the transients of his system, considering also non-linear friction. In [Freeman, 1959], Freeman analyzes, using the generalized describing method [Slotine & Li, 1991], a two-mass system with linear friction, modeled as a second-order system, with a stiff axis and backlash (modeled as a dead zone) and feedback from the load position and/or motor position, or velocity. The analysis is compared with simulations on an analog computer. With the chosen model, limit cycles were found for all cases where the load position was measured. In [Freeman, 1960] he continues to propose measuring both the motor position, and the load position and apply a preload in form of an extra step signal at each backlash separation in order to close the backlash gap. An analog computer study shows that limit cycles are reduced if the preload is smaller than the backlash gap.

In [Ahmad, 1985], the reference signal to the motor position PID controller is complemented with an offset, or preload, to compensate the backlash gap such that the load position will presumably be correct in steady state. No dynamic effects are considered. The backlash compensation is thus done in open loop, since there is no feedback from the load position. Under the assumption that the motor loop is fast, the backlash compensation is similar to inverse compensation of a backlash at the plant input, as proposed in [Tao and Kokotović, 1996]. A very useful idea is presented in [Choi, Nakamura and Kobayashi, 1996] to replace the mechanical anti-backlash gear: let the gear be driven by two motors with preloads of opposite signs such that the backlash gap is closed. The price for this solution is increased energy usage in steady state. Experiments show that the limit cycle disappears and that the steady state position error is zero.

Speed controlled systems treated in [Brandenburg, 1986; Brandenburg *et al.*, 1986; Brandenburg and Schafer, 1987] showed that a load observer together with either cascaded motor position PI-control, or P-control with inner motor speed P-control, avoids high-frequency limit cycles produced. Describing function analysis, using the dead zone model, reveals in the no-load disturbance case  $T_l = 0$ , there might still appear low-frequency low-amplitude limit cycles. These were, however, never discovered neither in

simulations nor in experiments, and, in any case will be “destroyed” by any non-zero load disturbance that is always present in real systems; e.g. due to friction. It is also shown in [Brandenburg and Schafer, 1987] that the circle criterion demands much larger load disturbance than the describing function analysis as a sufficient condition for limit cycle avoidance. [Odai and Hori, 1998; Nakayama *et al.*, 2000; Shahruz, 2000] followed the same approach undertaken by Brandenburg research group. The resulting control system can often be rewritten as a PID-controller. In [Odai and Hori, 1998], the result is in the form of a PID-controller with modified parameter values and with more derivative action on the feedback than on the reference signal.

Oldak *et al.*, [1994], developed a QFT scheme for uncertain systems with backlash. He used the describing function technique for backlash representation, which was modeled as a dead zone, to augment the plant value set. Moreover, the deviation of the backlash from a linear function is seen as a disturbance that gives rise to a disturbance rejection specification. A simulated example demonstrates a closed loop system without limit cycles. In [Azenha and Machado, 1996], first- and second- order Variable Structure Controllers (VSS) are tested with position feedback from the load side. In this case the variable structure controllers turn out to be saturated first and second-order controllers. By implementing describing function analysis of the VSS's, and for the inertia driven hysteresis model for the backlash, the existence of limit cycles is indicated and findings are corroborated by simulation. This comes as no surprise, since it is known that linear feedback from load side results either in limit cycles or a steady-state error if the controller contains an integrator [Thomas, 1954; Oldak *et al.*, 1994]. If all states are measurable, a state feedback controller can be used. If load or motor signals are measured, a state observer and state feedback can be used. An application of the latter is presented in [Hori *et al.*, 1994], where motor speed is measured. In [Hori *et al.*, 1994], a simulation study shows that PI-control of a two-mass, or three-mass system with each backlash between the masses modeled as a dead zone is accompanied by limit cycles on the load side. If the PI is compensated with feedback from observed states, the limit cycle is eliminated.



A linear controller can be designed using some of the existing robust design methods. The backlash nonlinearity is modeled as a suitable uncertainty, fitting into the used design method's framework. Examples of robust design methods are  $H_\infty$  [Green and Limebeer, 1995] and QFT [Horowitz, 1991]. QFT can be used for MIMO systems, but in its simplest form it can be viewed as a SISO loop-shaping design method. The result is a controller consisting of a series of SISO filters. Applications of QFT synthesis to backlash systems are [Yang, 1992; Nordin and Gutman, 1995].

A frequently used approach in handling backlash is to treat it as a torque disturbance, which enters the system at the location of backlash. The system is then treated as linear, and the controller is supposed to compensate for the torque disturbance. With this system model, a torque observer can be used, which estimates the torque disturbance. The torque is then compensated for in an inner feedback loop. In an outer parallel loop, a PID or other controller is used to control a “backlash-free” system.

#### **4.2.2. Switching Control**

The controllers in this group consist of two separately designed controllers (often linear): One is designed for the system in backlash mode, and the other for contact mode. The overall controller is then switching between the two controllers according to prescribed switching criterion. Switching controllers detect when backlash mode is entered, and try to quickly get back to contact mode. Note the difference between active and passive switching controllers that passive switching controllers get more cautious when backlash mode is entered.

In [Nordin, 2000], a continuous gain scheduling is used between two controllers designed by QFT. The controller's output signal is used as scheduling variable. The linear controller used at low torques is tuned to be cautious so that no oscillations arise. Switching between two state feedback control laws is described in [Friedland, 1997]. The switching is based on the backlash angle.

Next, we are going to discuss the later works by Tao and his colleagues, this group had numerous publications on the field of backlash in mechanical systems. [Ezal *et al.*, 1997] uses a linear (PD) controller for the contact mode. The goal is to traverse backlash as fast as possible but with “soft landing” on the other side. This problem is formulated as a rendezvous problem, solved by optimal control. An open-loop optimal control law is first presented, but is then reformulated as a feedback controller. The model includes a traditional dead-zone backlash model with damping term.

[Ling and Tao, 1999] extends the optimal control results for backlash mode from [Ezal *et al.*, 1997] into a  $2 \times 2$  system. In [Tao *et al.*, 2001], these results are applied to a gun-turret application. In contact phase, feedback linearization is used. In backlash phase, the optimal control results from [Ling and Tao, 1999] and [Ezal *et al.*, 1997] are used.

[Tao, 1999] presents two different results. First, the inverting results from [Taware and Tao, 2000] are presented, see above. Secondly, a control strategy for backlash feedback systems is developed. For these systems, a switched controller structure, with one impact phase and one backlash phase PD-controller, is suggested. The state of the backlash and its size is assumed known. The simplified dead-zone model without damping and compliance is used. The results are interesting due to their simplicity. However, the model structure has not included a switching criterion between the two controllers.

Other switching studies have been examined by [Yang and Fu, 1996], where the system switches between an adaptive controller in impact mode, and a simple controller with a reference angle in backlash mode. The adaptive controller stops adaptation in backlash mode. The simple controller is not described in the paper. [Boneh and Yaniv, 1999] uses two cascade QFT-designed controllers, each one having a feedback controller block and a setpoint pre-filter block. In contact mode, the inner loop controller is bypassed. In backlash mode, this controller positions the motor for smooth contact with the load, while the outer loop gives the desired direction of backlash closure.

### 4.2.3. Adaptive Control

Many authors have used adaptive control as a complement to other control strategies. The system performance is then enhanced by the parameter adaptation mechanism. This mechanism makes the controller nonlinear, but if the remaining part of the controller is linear, the controller type is considered as linear anyway. The motivation for this is that the transients due to backlash are much faster than the adaptive mechanism.

In [Brandenburg and Shafer, 1987], they have extended their earlier work on disturbance observers, with a model reference adaptive controller (MRAC). In [Brandenburg and Schafer, 1989], the first author complements his previous works by considering systems with backlash and friction, claiming that model reference adaptive control with adaptation of disturbance model is of great benefit both for speed and position control: A PI disturbance controller, active only when a disturbance occurs, compensates for steady-state speed and position errors on the motor side, in such a way that it suffices to use a linear speed controller of P rather of PI-type. Thus reducing the order of closed-loop system and achieving a faster response. Similar ideas to those of [Johansson and Rantzer, 1997; Johansson and Rantzer, 1998; Johansson, 1999; Indri and Tornambè, 1997] are used in [Nordin, 2000] to prove set convergence when viscous friction shaft damping, and actuator dynamics are present, with a deadzone backlash model, and a switched high-order controller. By using smart switching between two linear controllers, one tuned optimally for the system without backlash, and one tuned for robust performance for the system with backlash, almost the same performance as for the system without backlash can be achieved [Nordin, 2000; Nordin & Gutman, 2000]. A similar solution was suggested by [Shafer, 1993] where two linear observers were used for the system with open and closed backlash, respectively, and switched according to the state of the backlash element.

Two non-linear schemes are also proposed in [Shafer, 1993]: if only a motor sensor is available, a compensation of steady-state error due to the backlash is recommended using a simple hysteresis element in the controller. If there is a second

sensor at the load side, a solution is suggested in which, at the instant of the backlash opening, a trajectory is predicted which ensures that the backlash closes smoothly, and a limit cycle free operation results. Dynamic errors due to backlash are reduced. This method required utmost fast calculations and a high sampling frequency if the backlash angle is small [Schafer & Brandenburg, 1991].

#### 4.2.4. Other Types of Backlash Control

The controllers in this group can be represented by several subgroups, such as, Dithered controllers and Sinusoidal input describing function (SIDF) inversion controllers.

A dither is a periodic high frequency signal, added to the control signal into a nonlinear system, in order to improve system performance. [Desoer and Shahruz, 1986] applies this method to the control of backlash systems. [Taylor and Strobel, 1985] presents a method to decrease the amplitude sensitivity of nonlinear systems, called “describing function inversion”. The resulting controller is a nonlinear PID-controller where the functions  $f_p(e)$ ,  $f_I(e)$ ,  $f_D(e)$  are chosen so that the dynamics of the open loop of controller and system is independent of the amplitude of sinusoidal input  $e$  :

$$u = f_p(e) + \int_0^t f_I(e) dt + \frac{d}{dt} f_D(e) \quad (4.5)$$

The method is also applied to a gun turret testbed in [Taylor and Lu, 1993].

Another type of control is called inverting control, it includes an explicit inverse model corresponding to the nonlinearity in the system. Tao and his colleagues have many results on ‘inverting control’ of systems with hard nonlinearities at the input or output [Tao and Kokotović, 1993; -1994; -1995c; -1995b; -1995a; -1996]. Most results are devoted to backlash nonlinearities, but also friction and hysteresis are discussed. The controllers utilize a nonlinearity inverse, and adaptive schemes are partly used to adjust the parameters of the inverse. The book [Tao and Kokotović, 1996] summarizes and

extends the articles' results. For example, systems with input and output nonlinearities are treated. [Ma and Tao, 2000] combines an adaptive inverse of an input nonlinearity with feedback linearization control for the remaining dynamics, which may be smoothly nonlinear. This is a generalization of some results from [Tao and Kokotović, 1996] for actuator nonlinearities.

Inverting control of sandwiched nonlinearities is treated in [Taware and Tao, 1999, 2000]. The approach is to use an inner loop controller to “cancel” the input dynamics. In [Taware and Tao, 1999], the cancellation is done in continuous time, by state feedback or by measuring the nonlinearity input signal. In [Taware and Tao, 2000] the inner loop is a discrete time controller that replaces the input dynamics by a delay. It is assumed that the nonlinearity input or output is measured. In both cases, the nonlinearity is then inverted and the output dynamics can be controlled.

[Dean *et al.*, 1995] makes an experimental validation of the results in [Tao and Kokotović, 1993]. Their results are discouraging, which the authors explain by measurement noise problems in the system. The system has a significant amount of friction, which is not taken into account in the controller design. This could also be an explanation of the bad experimental results. In [Su *et al.*, 2000], the backlash is approximately modeled as a differential equation. Its analytic solution is used to construct a backlash inverse and a controller for backlash systems. [Tarng *et al.*, 1997] describes backlash compensation in CNC-machines. A compensation of the desired trajectory is used to get correct machine movements. The optimal trajectory compensation is found by simulated annealing optimization.

#### **4.3. CONTROL DESIGN**

A feed drive system can be modeled as a multi-inertia system with the inertias connected by dampers and springs; two-mass system is mainly used when backlash is the main interest of analysis. When dealing with backlash as a scope of analysis, it has two distinct operational areas where control of feed drives changes its approach of having a stable process. The control functionality in the contact zone is dedicated to achieving the

best possible tracking performance. While, in the backlash (non-contact) zone, the control functionality will be devoted to bring the system back in contact as fast and effective as it can. The contact-mode controller is usually a simple PID or a model-based controller, while the backlash-mode controller is usually designed by the use of an appropriate control design method (e.g., linear control techniques, optimal control, etc.) by which the property of bringing the system's disturbed state back to its initial value is guaranteed.

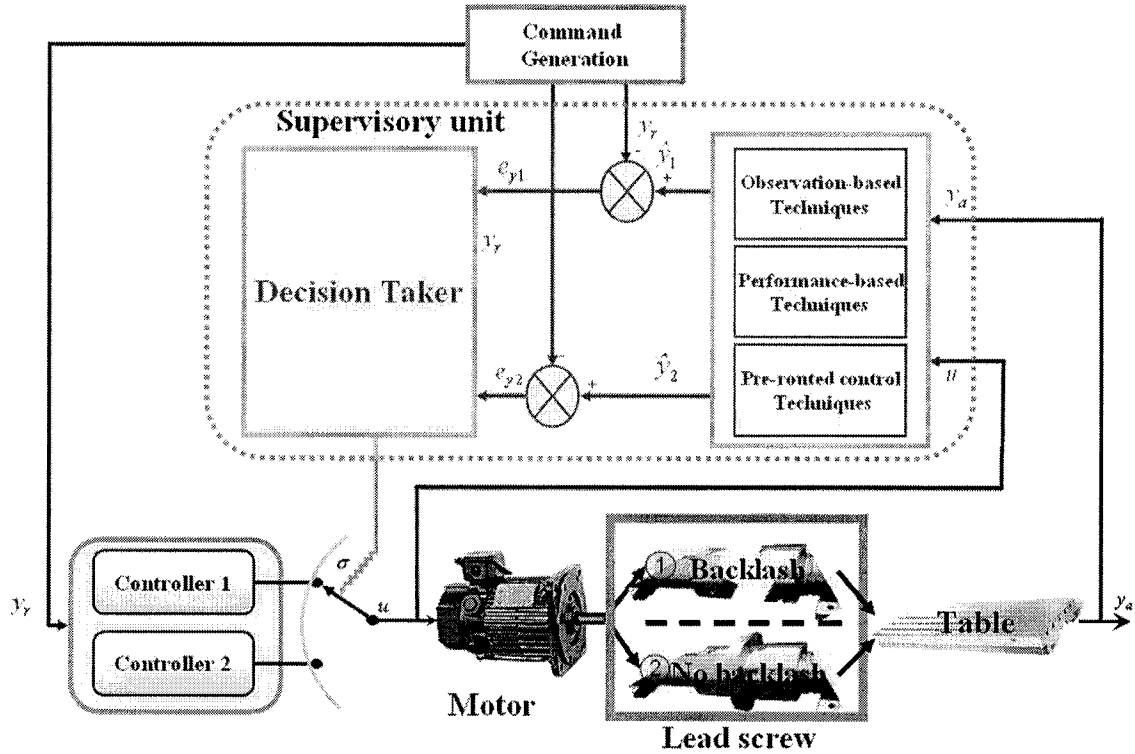


Figure 4.4. Vision of our switching control for backlash compensation.

The supervisory control concept also supports the structure of hierarchical control as a mediator between the physical level and the more intelligent layers atop. Supervision, according to [Elbeheiry *et al.*, 2004] is of 3 types: pre-routed, estimator-based and performance-based supervision. The last one has been chosen since it provides good data inputs for system diagnosis and state estimation whenever needed for the operation of advanced controllers. Multiple controllers are available for the supervisor to switch over depending on the functionality needed. These controllers are designed based upon different dynamic models which necessarily change according to the conditions that

the supervisor is prepared to treat. Having two controllers requires the presence of upper-level decision logic unit. The purpose of this unit is to switch from one controller to another whenever needed. This can be visualized as a concept in Figure 4.4. The supervisor should take the control input  $u$ , output  $y$  and difference between reference  $y$  and ideal/estimated  $\hat{y}$  as inputs to perform the mathematical operations needed to organize the switching between the two controller, and generate the needed variable control signal to handle the deviation of the output due to backlash in this study.

### 4.3.1. Tracking Control Design Techniques

#### 4.3.1.1. PID Controllers

During the contact phase, the system is considered operating to maintain the output signal within an acceptable steady-state error range with respect to the input reference. PID controllers have been seen mostly dominating machine tool feed drive system control literature due to the fact that the integral part highly enhances error readings when implemented to the system. The PID controller can be realized as a function of error as following:

$$u(t) = K_p e(t) + K_I \int e(t) dt + K_D \frac{d}{dt} e(t) \quad (4.6)$$

Where  $e(t)$  is the position error – difference between reference and measured values,  $K_p$  is the proportional gain,  $K_I$  is the integral gain, and  $K_D$  is the derivative gain. Usually, PI controllers are used in machine tool feed drives where the integral part compensate for the loading cutting forces, see Figure 4.5.

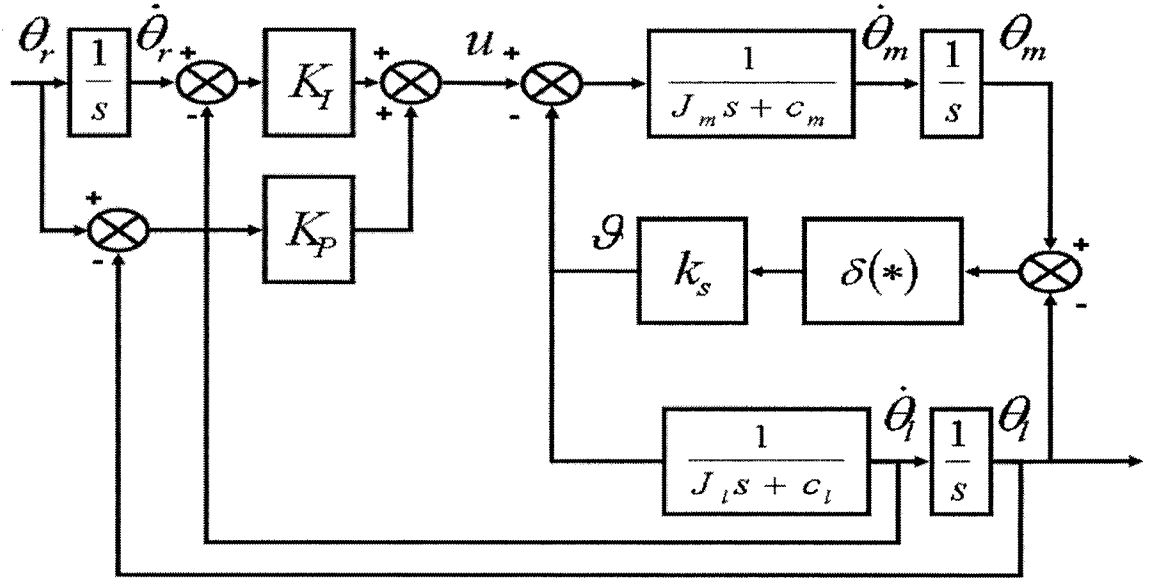


Figure 4.5. Proportional-Integral (PI) control law for a 2-DOF feed drive model.

Feed drive systems can be represented by state-space formulation depending the following equations of motion:

$$\begin{aligned} J_m \ddot{\theta}_m + c_m \dot{\theta}_m + k_s (\theta_m - \theta_l) &= T_m \\ J_l \ddot{\theta}_l + c_l \dot{\theta}_l + k_s (\theta_l - \theta_m) &= 0 \end{aligned} \quad (4.7)$$

Where the different states are:

$$x_1 = \theta_m$$

$$x_2 = \theta_l$$

$$x_3 = \dot{\theta}_m$$

$$x_4 = \dot{\theta}_l$$

$$\dot{x}_1 = x_3 = \dot{\theta}_m$$

$$\dot{x}_2 = x_4 = \dot{\theta}_l$$

$$\dot{x}_3 = \ddot{\theta}_m = -\frac{c_m}{J_m} \dot{\theta}_m - \frac{k_s}{J_m} (\theta_m - \theta_l) + \frac{T_m}{J_m} = -\frac{c_m}{J_m} x_3 - \frac{k_s}{J_m} (x_1 - x_2) + \frac{T_m}{J_m}$$

$$\dot{x}_4 = \ddot{\theta}_l = -\frac{c_l}{J_l} \dot{\theta}_l - \frac{k_s}{J_l} (\theta_l - \theta_m) = -\frac{c_l}{J_l} x_4 - \frac{k_s}{J_l} (x_2 - x_1)$$



Now, after defining all the states and its derivatives, we obtain a linear system in the form:

$$\dot{x}(t) = Ax + Bu \quad (4.8)$$

$$\begin{bmatrix} \dot{x}_1 \\ \dot{x}_2 \\ \dot{x}_3 \\ \dot{x}_4 \end{bmatrix} = \begin{bmatrix} 0 & 0 & 1 & 0 \\ 0 & 0 & 0 & 1 \\ -\frac{k_s}{J_m} + \frac{k_s}{J_l} & -\frac{c_m}{J_m} & 0 & 0 \\ +\frac{k_s}{J_l} & -\frac{c_l}{J_l} & 0 & -\frac{c_l}{J_l} \end{bmatrix} \begin{bmatrix} x_1 \\ x_2 \\ x_3 \\ x_4 \end{bmatrix} + \begin{bmatrix} 0 \\ 0 \\ 1 \\ 0 \end{bmatrix} u \quad (4.9)$$

Where  $u = T_m$ , the applied torque.

#### 4.3.1.2. Model-based Control for Contact Zone

The main purpose of using model-based control techniques is to compensate for the effect of backlash outside the region of backlash. Such a technique supports the usage of a specialized controller which handles backlash nonlinearity, and provides harmony to the controlled system while receiving control signal from two different controllers. Since it is model-based, then the backlash model should reflect on the controller and describe the resulting effects on the contact region by adding or subtracting the value of backlash off the input, according to the direction change of velocity.

In contact zone, the position controller that controls the motor-side position of the machine tool feed drive system. Reference signal to be used as a comparison domain, the control law depending on the previously explained technique is shown below:

$$u_{C_l} = J_m(\ddot{\theta}_{ref} - K_1(\dot{\theta}_m - \dot{\theta}_{ref} \pm \beta) - K_2(\theta_m - \theta_{ref} \pm \beta)) \quad (4.10)$$

Where  $K_1$  and  $K_2$  are tuning control gains.  $\beta$  changes sign according to  $\theta_m - \theta_l$  being negative or positive, respectively. Feedforward control can be implicitly contained within the controller as we can see above.

The motivation for the previously mentioned control law is that when  $k_s = \infty$  and  $\beta = 0$ , dynamics of machine tool feed drive reduce to:

$$J_m \ddot{\theta}_m = u \quad (4.11)$$

Which can be stabilized with any positive  $K_1$  and  $K_2$ . This controller has been implemented and tested on different studies dealing with machine tool feed drive systems and showed good performance [Tao research group publications].

In this study, we are going to deal with two new control laws to solve this problem. The two control laws are taken and derived from equation (4.10). The original equation (4.10) is taken as a reference study and is denoted as contact-zone controller I. The following two equations represent the two control laws, as denoted later by contact-zone controller II and III, which are developed with a certain belief of a better performance and improved accuracy when confine the effect of inertia to acceleration component and the addition of integral part to the control which showed after studying PI systems the vital effect on transients of feed drive systems:

$$u_{C_{II}} = J_m \ddot{\theta}_{ref} - K_{1'}(\dot{\theta}_m - \dot{\theta}_{ref} \pm \beta) - K_{2'}(\theta_m - \theta_{ref} \pm \beta) \quad (4.12)$$

$$u_{C_{III}} = J_m \ddot{\theta}_{ref}(t) - K_{1'}(\dot{\theta}_m(t) - \dot{\theta}_{ref}(t)) - K_{2'}(\theta_m(t) - \theta_{ref}(t) \pm \beta) - K_3 \int (\theta_m(t) - \theta_{ref}(t))dt \quad (4.13)$$

Where  $K_{1'}$ ,  $K_{2'}$  and  $K_3$  are tuning control gains.  $\beta$  changes sign according to  $\theta_m - \theta_l$  being negative or positive, respectively.

### 4.3.2. Dead-Zone Control Design Techniques

#### 4.3.2.1. Model-based Control for Backlash Zone

For the same advantages mentioned before, this type of control is used for backlash. A backlash controller that controls the motor's position with respect to load position since feed drive system load- and motor- sides become decoupled from each other when backlash takes place. Control law can be introduced in the following form:

$$u_{B_I} = J_m(\ddot{\theta}_l - K_4(\dot{\theta}_m - \dot{\theta}_l \pm \beta) - K_5(\theta_m - \theta_l \pm \beta)) \quad (4.14)$$

Where  $K_4$  and  $K_5$  are tuning control gains.  $\beta$  changes sign according to  $\theta_m - \theta_l$  being negative or positive, respectively. In general, this controller has the advantage of controlling position, velocity and acceleration of the output produced by machine tool feed drives.

In this study, same as the last subsection, we are going to deal with two new control laws to solve this problem. The two control laws are taken and derived from equation (4.14). The original equation (4.14) is taken as a reference study in the backlash zone and is denoted as backlash-zone controller I. The following two equations represent the two control laws, as denoted later by backlash-zone controller II and III:

$$u_{B_{II}} = J_m\ddot{\theta}_{ref} - K_{4'}(\dot{\theta}_m - \dot{\theta}_{ref} \pm \beta) - K_{5'}(\theta_m - \theta_{ref} \pm \beta) \quad (4.15)$$

$$u_{B_{III}} = J_m\ddot{\theta}_{ref}(t) - K_{4'}(\dot{\theta}_m(t) - \dot{\theta}_{ref}(t)) - K_{5'}(\theta_m(t) - \theta_{ref}(t) \pm \beta) - K_6 \int (\theta_m(t) - \theta_{ref}(t))dt \quad (4.16)$$

Where  $K_{4'}$ ,  $K_{5'}$  and  $K_6$  are tuning control gains.  $\beta$  changes sign according to  $\theta_m - \theta_l$  being negative or positive, respectively.

#### 4.3.2.2. Rendezvous Problem

When  $\beta > 0$ , tracking performance is limited due to the motor involvement in overcoming the backlash gap. The main goal of backlash compensation is to minimize time of disengagement  $t_\beta$ . Where  $t_\beta = t_f - t_0$ ;  $t_0$  and  $t_f$  are times at which the feed drive system enters and exits the backlash zone, respectively, see Figure 4.6.

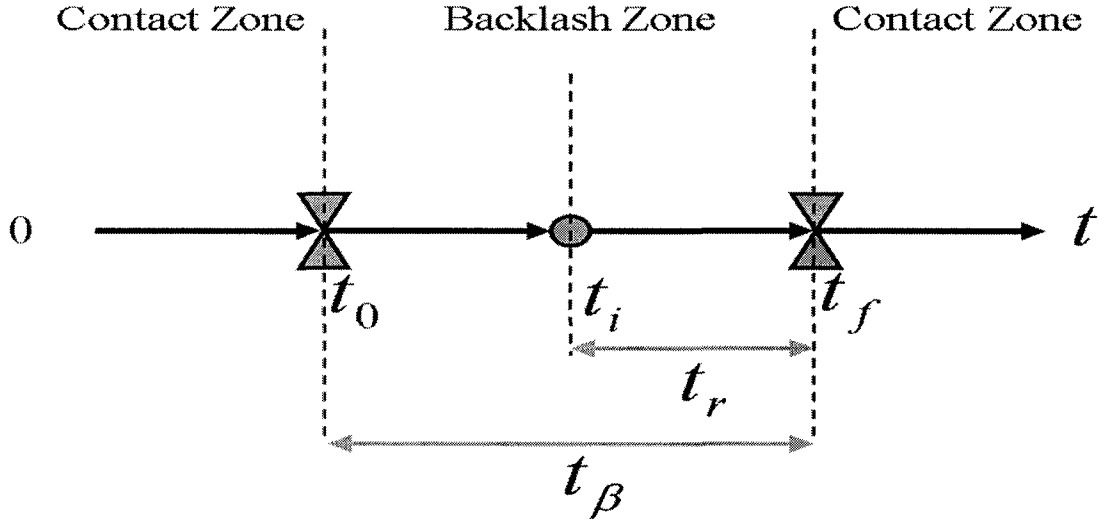


Figure 4.6. Switching occurrences along the timeline defining all time values related to backlash zone.

In addition to reducing time of disengagement, impact force attenuation should be taken into consideration when motor and load are in contact. For this reason,  $|\dot{\theta}_l(t_f) - \dot{\theta}_m(t_f)|$  should be very small at the instant of contact. Rendezvous problem that has been discussed in [Athans and Falb, 1966, Lee, Markus, 1967, Kirk, 1970, Carter, 1994, and Kokotović *et al.*, 1997] has ideally depicted the previous case in terms of force reduction at the instant of contact efficiently. When  $\mathcal{G}(t) = 0$ , system has just entered backlash phase and  $\mathcal{G}(t) = 0, \forall t \in [t_0, t_f]$ .

The objective during backlash zone is to minimize  $t_\beta$  taking into consideration the following boundary condition:

$$x_m(t_f) = x_l(t_f) + x_s \quad (4.17)$$

Where  $x_s^T = [\theta_s \ 0]$ , we select  $\theta_s$  relying on the previous action taken by the linear controller. This is obviously shown in the following equation:

$$\theta_s = \begin{cases} \beta + \varepsilon_1, & \text{if } u(t_o^-) > 0 \\ 0, & \text{if } u(t_o^-) = 0 \\ -\beta - \varepsilon_1, & \text{if } u(t_o^-) < 0 \end{cases} \quad (4.18)$$

Where  $u(t_o^-)$  is the value of the linear control input just before the system enters the backlash region. The design parameter  $\varepsilon_1 > 0$  is appropriately chosen to be large enough to overcome the critical disengagement area and that contact is definitely regained. The following mathematical formulation will depend on the assumption that  $\dot{x}_s = 0$  during the disengagement phase. Input is supplied confined with low frequency nature.

The optimal control objective is to reduce the penalty function  $J(u)$  as shown in following equation:

$$J(u) = \int_{t_0}^{t_f} [1 + \rho u^2(t)] dt$$

(4.19)

Subject to:

$$\begin{aligned} \dot{x}_m(t) &= A_m x_m(t) + B(u(t) - \mathcal{G}(t)) \\ \dot{x}_l(t) &= A_l x_l(t) + B_l \mathcal{G}(t) \\ x_m(t_f) &= x_l(t_f) + x_s \end{aligned}$$

The cost on control effort  $\rho$  is treated as a design parameter to guarantee achieving a reasonable range of gains for the controller.

The feedback control law can be obtained by solving for the optimal control problem mentioned above. The interval is transformed from  $[t_0, t_f]$  to  $[0, t_r]$  where  $t_r$  is

the remaining time for the system to return into coupling again. The control input in backlash region at  $t_i$ , where  $t_i$  is the instant time value within backlash region:

$$u(t_i) = -B^T M(0, t_r) [x_m(t_i) - \hat{x}_m(t_i)] \quad (4.20)$$

This feedback law depends on the instantaneous states of the motor  $x_m(t_i)$  and the load  $x_l(t_i)$ , and as well as the time remaining to contact  $t_r$ . The expected state value of the motor is estimated by the following equation:

$$\hat{x}_m(t_i) = e^{-A_m t_r} \{e^{-A_l t_r} x_l(t_i) + x_s\} \quad (4.21)$$

While  $M$  is the controllability gramian and can be evaluated by the following equation to be used to solve equation (4.20):

$$M^{-1}(0, t_r) = \int_0^{t_r} e^{-A_m \sigma} B B^T e^{-A_m^T \sigma} d\sigma > 0 \quad (4.22)$$

The remaining time to contact can be calculated by the following formula:

$$\hat{t}_r = \sqrt{\frac{-12x_\beta}{qw + \alpha^2 x_\beta / 5}} \quad (4.23)$$

Where  $x_\beta = \frac{x_{m1} - x_{s1}}{\gamma}$ ,  $\gamma = 1/J_m$ ,  $q = -\text{sgn}(x_\beta)$ ,  $w = 2\rho^{-1/2}$ ,  $\alpha = -b_m/J_m$ . The

estimated  $\hat{t}_r$  is calculated based on the fact that the system starts from rest. Usually,  $\hat{t}_r > t_r$  for cases of backlash happen after picking up from rest. This technique has been discussed thoroughly as an example in case Observer-based supervision is considered. This section is for demonstration by which no simulation validation for this concept has been tackled in this study.

#### 4.3.1. Switching Control

The control process can be discussed from the top down. Switching amongst various system structures is essential to fulfill the unique task of control by overcoming obstacles and barriers encountered when using linear control techniques. Stability of the whole system containing more than one controller is quite paramount condition for the whole structure to work in harmony and consistency. Separate stability conformance for switched entities is not enough for the entire system to be considered stable. In our case, the plant dynamics matrices  $A_i$ ,  $i = 1, \dots, M$  are stable, i.e., all eigenvalues of those matrices are in the left-half complex plane. If all the  $A_i$ 's share a common Lyapunov function  $V(x) = x^T P x$ , such that  $\dot{V}(x) = -x^T Q x$ ,  $Q > 0$ , where  $P$  and  $Q$ , are design matrices to assure that quadratic form of the state  $x$  is positive definitive, then the system is proved exponentially stable. Exponential stability can be realized via the following formula [DeCarlo *et al.*, 2000]:

$$|x(t)| \leq \alpha_1 e^{-\alpha_2 t} |x(0)| \quad (4.24)$$

The previous serves as conditions placed on  $V(x)$  which are equivalent to  $A_i^T P + P A_i = -Q$  for all  $i$ . To check for a common quadratic Lyapunov solution to prove the previously mentioned condition, the following two-inertia system can be envisaged as following:

$$\begin{aligned} \dot{x}_m &= A_m x_m + B(u - \mathcal{G}) \\ \dot{x}_l &= A_l x_l + B_l \mathcal{G} \end{aligned} \quad (4.25)$$

Where  $u$  is the control signal; i.e. the driving torque,  $\mathcal{G}$  is the torque produced due to torsion and internal damping; in this case we assumed internal damping equals to zero, other symbols are explained in Chapter 3, bearing in mind that model described above is realized using state-space formulation. The need for switching is called on by the presence of two different system characteristics that result in two different models of a machine tool feed drive system; i.e. when backlash occurs,  $\mathcal{G} = 0$ . Since we are dealing

with two-inertia system; i.e. from this point on, use of  $\theta$  substitutes that of  $x$  mentioned earlier. In case the control used here the position controller:

$$u = J_m(\ddot{x}_r - K_1(\dot{\theta}_m - \dot{\theta}_{ref}) - K_2(\theta_m - \theta_{ref})) \quad (4.26)$$

Where  $x_{ref}$  denotes the reference input.

$$\mathcal{G} = k_s(\theta_m - \theta_l) \quad (4.27)$$

And based on equation (4.7), the following equations can be deduced where  $T_m$  resembles the control signal  $u$  :

$$\begin{aligned} J_m\ddot{\theta}_m + c_m\dot{\theta}_m &= J_m(\ddot{x}_r - K_1(\dot{\theta}_m - \dot{\theta}_{ref}) - K_2(\theta_m - \theta_{ref})) - k_s(\theta_m - \theta_l) \\ J_l\ddot{\theta}_l + c_l\dot{\theta}_l &= k_s(\theta_m - \theta_l) \end{aligned} \quad (4.28)$$

Since the reference signal does not affect the system stability or its own characteristics, we have omitted terms associated with  $\theta_{ref}$  which leads to the following state-space realization for the problem  $\dot{x} = A_i x$ ,  $\forall i$  where  $A_i$  represent closed-loop matrix for model  $i$  :

$$A_1 = \begin{bmatrix} 0 & 0 & 1 & 0 \\ 0 & 0 & 0 & 1 \\ (-\frac{k_s}{J_m} - K_2) & -\frac{k_s}{J_l}x_2 & (-\frac{c_m}{J_m} - K_1) & 0 \\ +\frac{k_s}{J_l} & -\frac{k_s}{J_l} & 0 & -\frac{c_l}{J_l} \end{bmatrix} \quad (4.29)$$



$$A_2 = \begin{bmatrix} 0 & 0 & 1 & 0 \\ 0 & 0 & 0 & 1 \\ -K_2 & 0_2 & (-\frac{c_m}{J_m} - K_1) & 0 \\ 0 & 0 & 0 & -\frac{c_l}{J_l} \end{bmatrix} \quad (4.30)$$

Where:

$$x_1 = \theta_m$$

$$x_2 = \theta_l$$

$$x_3 = \dot{\theta}_m$$

$$x_4 = \dot{\theta}_l$$

$$\dot{x}_1 = x_3$$

$$\dot{x}_2 = x_4$$

$$\dot{x}_3 = \ddot{\theta}_m = (-\frac{k_s}{J_m} - K_2)x_1 + \frac{k_s}{J_m}x_2 + (-\frac{c_m}{J_m} - K_1)x_3$$

$$\dot{x}_4 = \ddot{\theta}_l = +\frac{k_s}{J_l}x_1 - \frac{k_s}{J_l}x_2 - \frac{c_l}{J_l}x_4$$

The above two matrices  $A_1$  and  $A_2$ , exhibit the closed-loop matrices for a machine tool feed drive system in contact and backlash zones, respectively.

## 5. TOOLS AND IMPLEMENTATION ISSUES

### 5.1. MATLAB/SIMULINK OVERVIEW

In order to understand more the effects of input/output relationships, we will employ the use of simulation. MATLAB is currently used intensively by Academia as well as the industry for simulation, and is widely recognized to be reliable. The simulation in MATLAB comprises of high-performance language for technical computing that includes functions for numeric computation, data analysis, system simulation, and application.

By using Simulink tool in MATLAB, the transient response in a controlled environment can be observed. In the process of simulation, the control settings can be changed and the transient response is displayed in a graphical format with variable loading to ensure better understanding of the output. In addition to transient response which is considered the “de facto” measure of stability in electromechanical systems, any form of output and its compliance with the reference signal can also measured and visualized in various aids of demonstration such as 2-D and 3-D graphs.

Simulink is an interactive tool for modeling, simulating, and analyzing dynamic, multi domain systems. It supports linear and non-linear systems, modeled in continuous time, sampled time or a hybrid of the two. It allows the user to build a block diagram, simulate the system's behavior, evaluate its performance, and refine the design. Simulink integrates seamlessly with MATLAB, providing an immediate access to an extensive range of analysis and design tools. These benefits make Simulink the tool of choice for control system design, DSP design, communications system design, and other simulation applications. To start, Simulink provides a graphical user interface (GUI) for easy modeling. Using simple method as click and drag, the user can easily create block diagrams. Blocks – such as sinks, sources, linear and non-linear components and connectors distributed on specialized block libraries - represent elementary dynamic systems that Simulink knows how to simulate. A block comprises one or more of the following: a set of inputs resembled by vector  $u$ , a set of states resembled by vector  $x$ ,

and a set of outputs resembled by vector  $y$ , see Figure 5.1. Different transfer functions can also be created easily to suit any type of simulation process. The results can be viewed in real-time or as directed by the user [The Mathworks inc.].

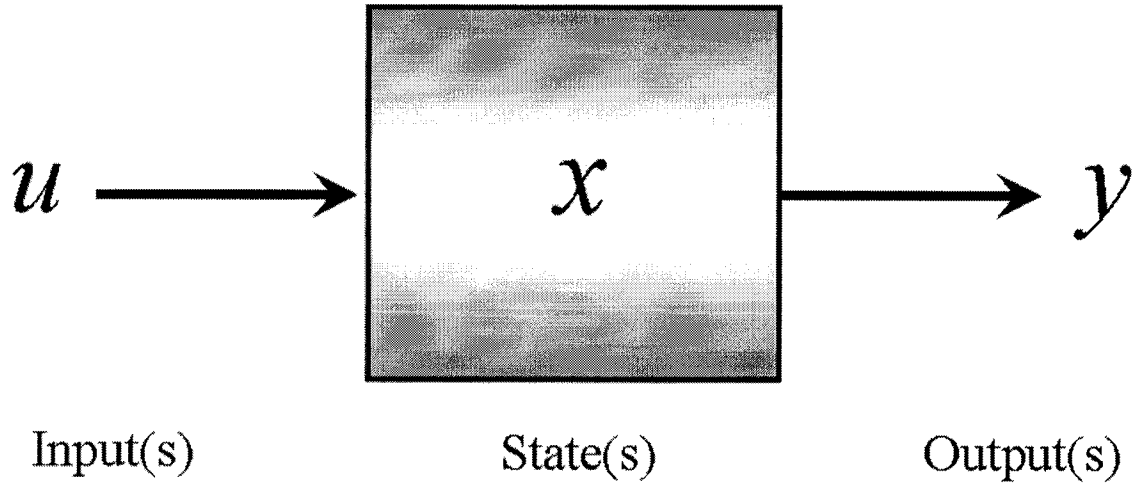


Figure 5.1. Simulink block structure.

The normal case –uncontrolled part of our study- is visualized where the linear controller is implemented solely to handle the machine tool feed drive system by means of the available block libraries found at Simulink toolboxes menu. While, Supervisory control and switching technique have been implemented in Simulink by means of extracting the available signals to a MATLAB function to perform the needed mathematical operations to determine the right moment to switch from one controller to another, apply observation theory and generate the needed control signal to be fed again into the system to compensate for the discrepancy of that system. The information transfer between Simulink and its encapsulating MATLAB occurs very smoothly and in a way that integrates the simulation process when user-customized functions are to be combined to achieve the desired goal of our study.

Simulink facilitates hierarchical top-down and bottom-up modeling approaches. By double-click on blocks the level of model detail is increased. However, if a Simulink model has a lot of blocks and a lot of levels, the model organization and how parts interact can become quit difficult to understand.

## **5.2. PROPOSAL FOR HARDWARE-IN-THE-LOOP SYSTEM IMPLEMENTATION**

RT-LAB is PC-based, real-time simulation software for dynamic systems and their associated control. It has been used by many industrial firms like GM, Ford, Bombardier, NASA, and many others.

RT-LAB, through its core engine, is specifically designed to address the needs of dynamics and control education. RT-LAB is a real-time, distributed simulation platform for MATLAB/Simulink, used for the design and control of complex industrial systems and products. Some of the features that guaranteed by RT-LAB are:

- Plant modeling and real-time simulation.
- Digital control design, with Hardware-in-the-Loop applications (HIL) (classical or model-based).
- Complex systems modeling and simulation acceleration using multiple sample rates.
- Available distributed parallel processing for model acceleration.
- Creates stand-alone embedded control systems.
- True multi-rate (multi-threaded) on reliable RTOS (QNX).
- Multi-command-station capability.
- Snapshot of model state vector.
- API to third-party GUI software.
- Supports multiple form-factors (ATX, SBC, VME, compact PCI, PXI, PC/104).

Hardware-in-the-loop (HIL) exhibits the most important tool in support of designing, testing and evaluating through electronic control units (ECU's) to provide doing a highly realistic simulation of the equipment/hardware in an operational (real-time) virtual environment, see Figure 5.2. Also, and to some extent, it helped industrial institutions in making early decision on specific design alternatives on a sound basis. HIL has evolved, thanks to revolutionary progress in mechatronics, by the encouragement of automotive and aerospace industries.

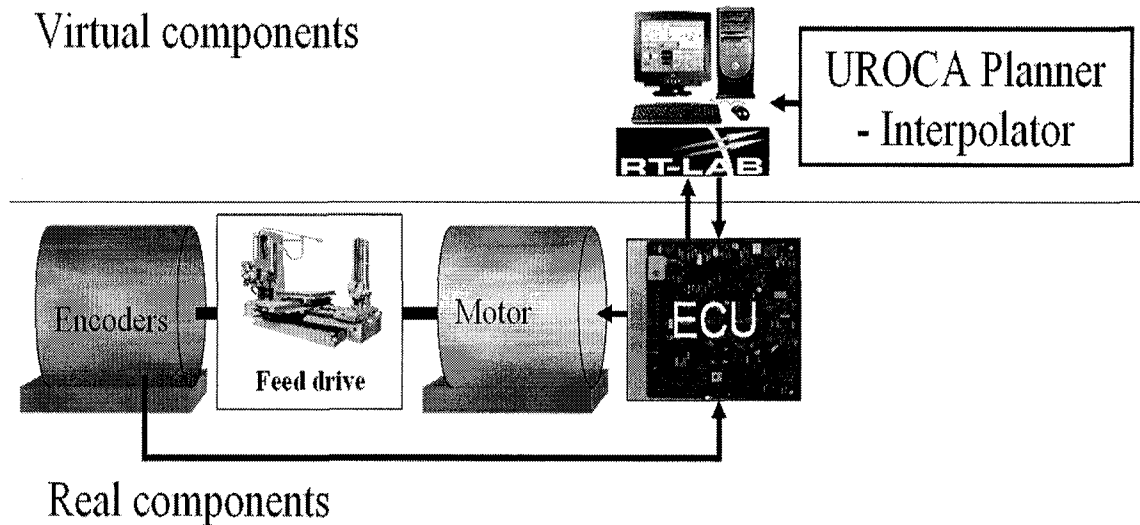


Figure 5.2. Hardware-in-the-Loop (HIL) vision for simulating a feed drive system within UROCA architecture.

RT-LAB is very flexible, offering many configuration options and topologies. As a general principle, RT-LAB distinguishes between, see Figure 5.3:

- Command Stations
  - Run a variant of the Windows® operating system.
  - Handle model development and offline simulations.
  - Run the human-machine interface of the model running under RT-LAB (simulation or real-time).
  - Perform some data acquisition functions.
- Computation nodes
  - Run the QNX® RTOS (real-time or simulation) or Windows® OS (simulation only)
  - Perform the computation of the mathematical models (as a single node or in a distributed fashion)
  - Integrate I/O interfaces for hardware-in-the-loop
  - Perform some data acquisition functions.

### RT-LAB Command Station

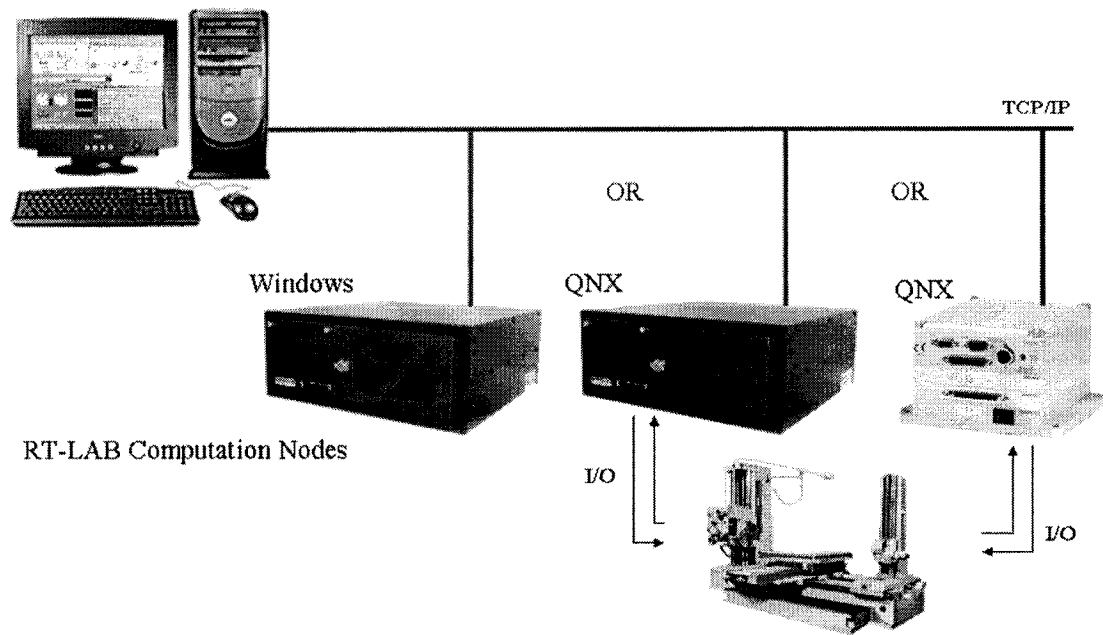


Figure 5.3. Plant control test distributed over several computation nodes.

Since MATLAB/Simulink is the base environment of simulating dynamic systems using RT-LAB tool, and this technology is based on distributed and hierarchical control, the model should be grouped and classified using the following criteria, see Figure 5.4:

#### Console subsystem

- Contains all user interface blocks (scopes, slider gains, manual switches).
- Will run asynchronously from the other subsystems.

#### Master subsystem

- Contains the computational elements of the controller.

#### Slave subsystem(s)

- Contains the computational elements of the plant model.

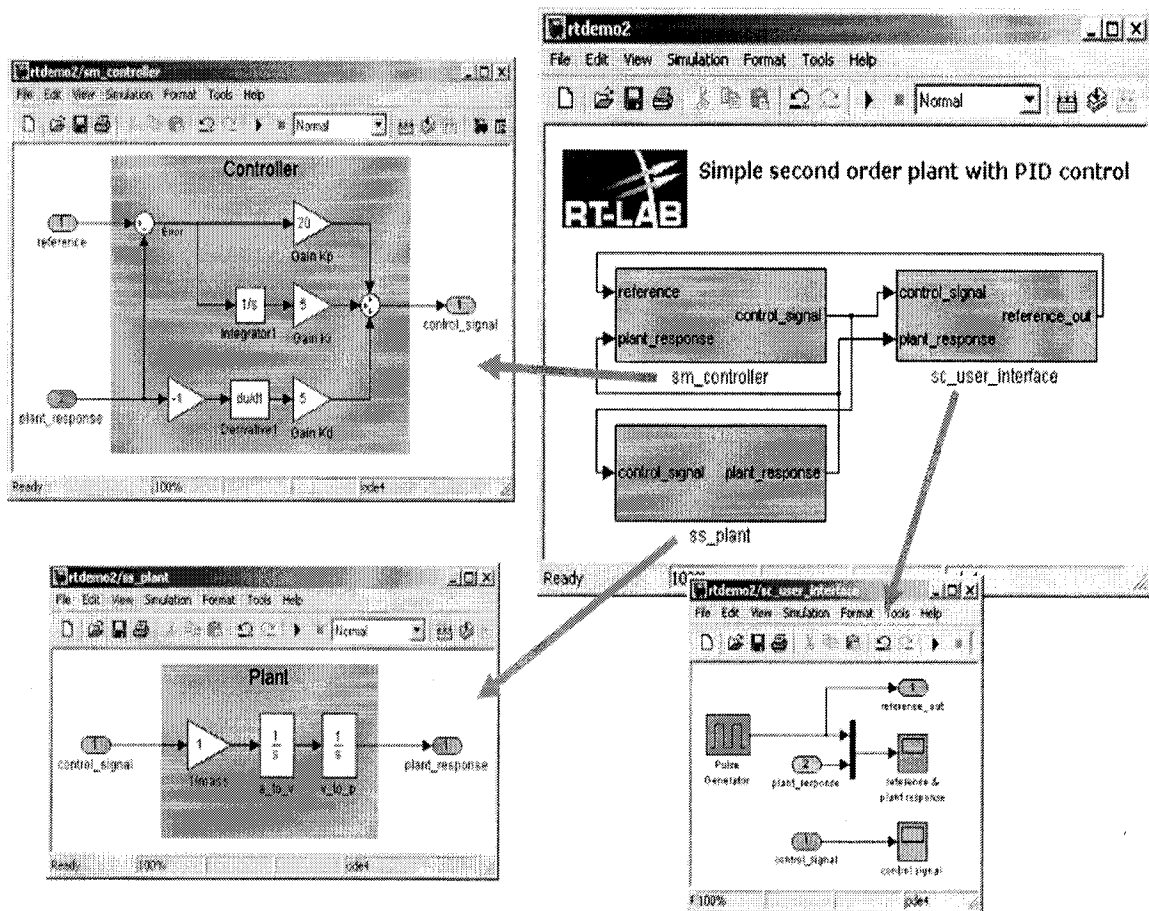


Figure 5.4. Categorization in Simulink model to be ready for RT-LAB usage.

Also, RT-LAB uses special blocks to facilitate operational communication, called OpComm blocks, to enable and to save communication setup information, and to let subsystems connected to other subsystems to adhere to real-time constraints. This includes both communication between the command station and computation nodes and communication between computation nodes in a distributed simulation scenario, see Figure 5.5. In the computation subsystems (master or slave subsystems):

- One OpComm receives real-time-synchronized signals from other computation subsystems.
- One OpComm receives signals asynchronously from the console subsystem.

In the console subsystem (console subsystem):

- One or more OpComm blocks may be inserted to receive signals from the computation nodes. Multiple OpComm blocks define unique “acquisition groups” with their own data acquisition parameters.

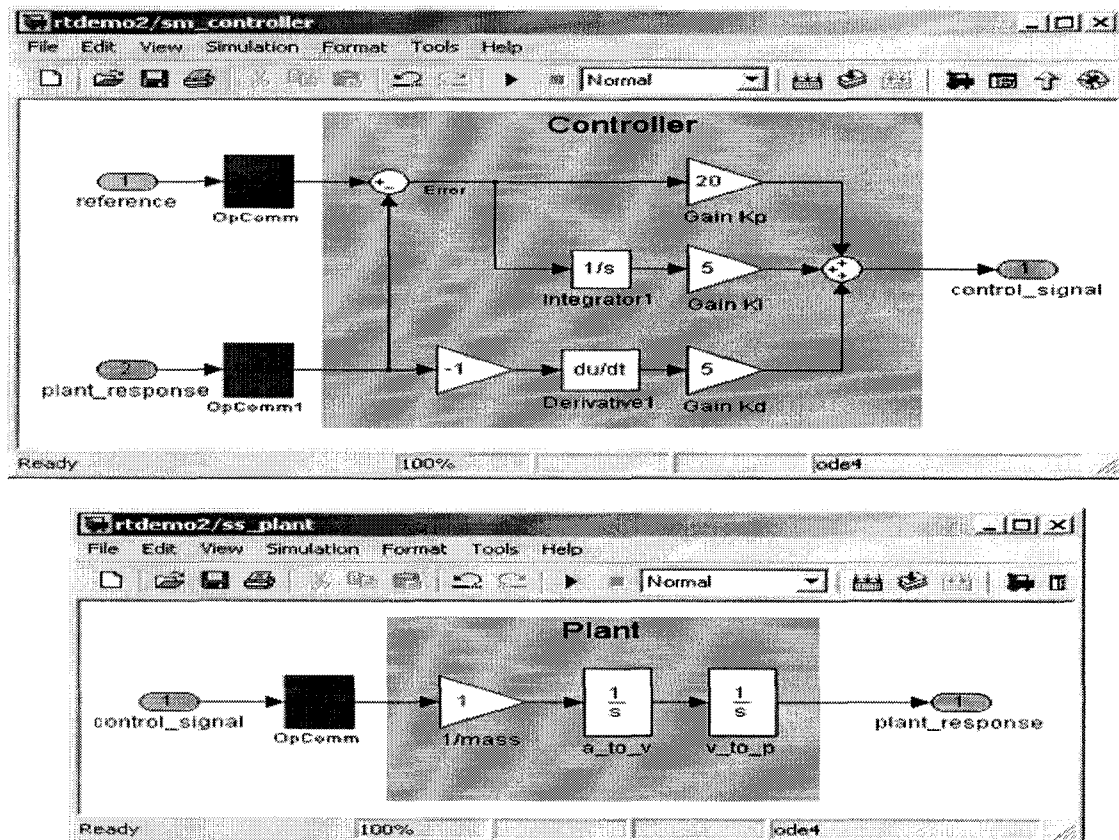


Figure 5.5. Addition of OpComm blocks to save Real-time communication setup.

The following are the steps to compile and execute a Simulink model within RT-LAB environment, after being reconditioned and categorized into subsystems according to RT-LAB requirements:

1. Load the file into RT-LAB, and choose the environment on which the hardware-in-the-loop is desired to be working on (QNX, Windows)



2. Model separation is where we divide the original model into as many separate models as there are top-level subsystems
3. Next, for each computation subsystem (Master and Slave), we call *Real-Time Workshop* to generate the C code for RT-LAB using a set of specific templates specific to the target OS.
4. We must transfer the newly generated C files to one of the computation nodes (called the development or compilation node) via the FTP protocol.
5. Next, for each computation subsystem (master and slave), we call the compiler (here *gcc*) to compile and link the C code into an executable file for RT-LAB.
6. We then retrieve the executable(s) via FTP. This allows us to load a subsystem on a different node than the compilation node.

Another essential implementation issue, is defining the in's and out's of the simulation model and the interconnectivity with the hardware, as such the loop will be closed and the model would be ready for testing. This can be achieved by the use of electronic control units (ECU's) which serves as a bridge between software and hardware in the loop, see Figure 5.6.

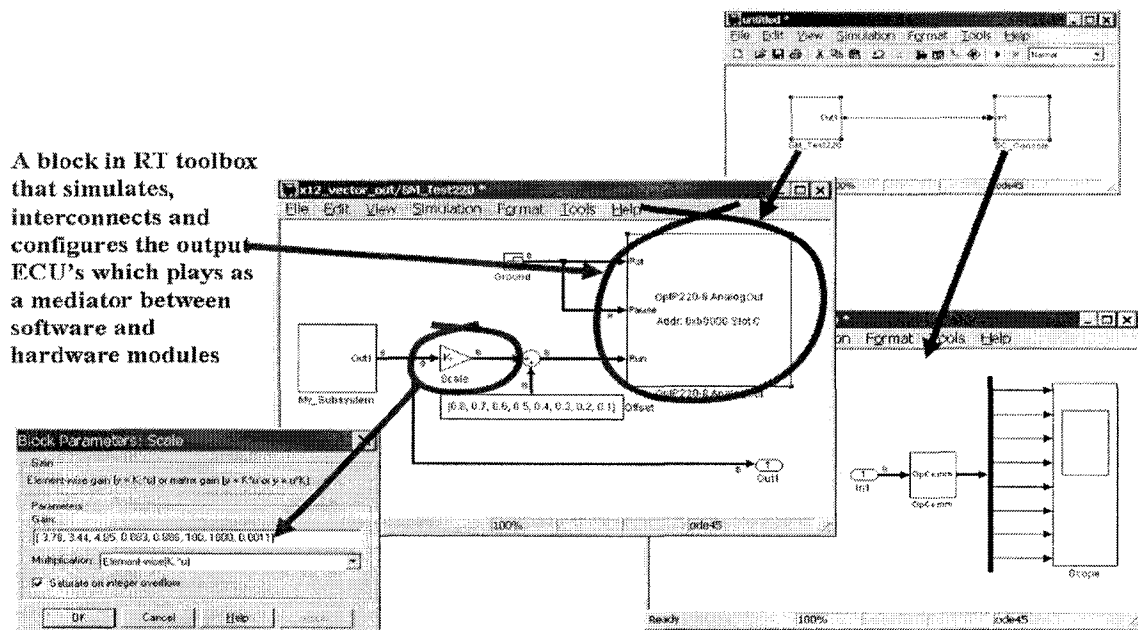


Figure 5.6. Specialized block to represent ECU as an implementation issue

These ECU's are used to serve as converters of engineering units – whatever the controlled values are – into raw voltage. For multi-pins binary ECU's, definition of each signal should be introduced at the Simulink model, pouring these signals into the specified ECU used which is chosen among a specialized library built in the RT-lab toolbox.

For more effective testing, partitioning the plant model into submodels will enhance the testability and verification for separate modules within the whole feed drive system. In such a case, feed drive system in a CNC machine tool can be separated into motor, shaft, ballscrew, table and load (cutting disturbances module) submodels. Also this will facilitate testing some parts of the feed drive system as real entities while the rest of the parts can be represented by virtual simulation submodels, see Figure 5.7.

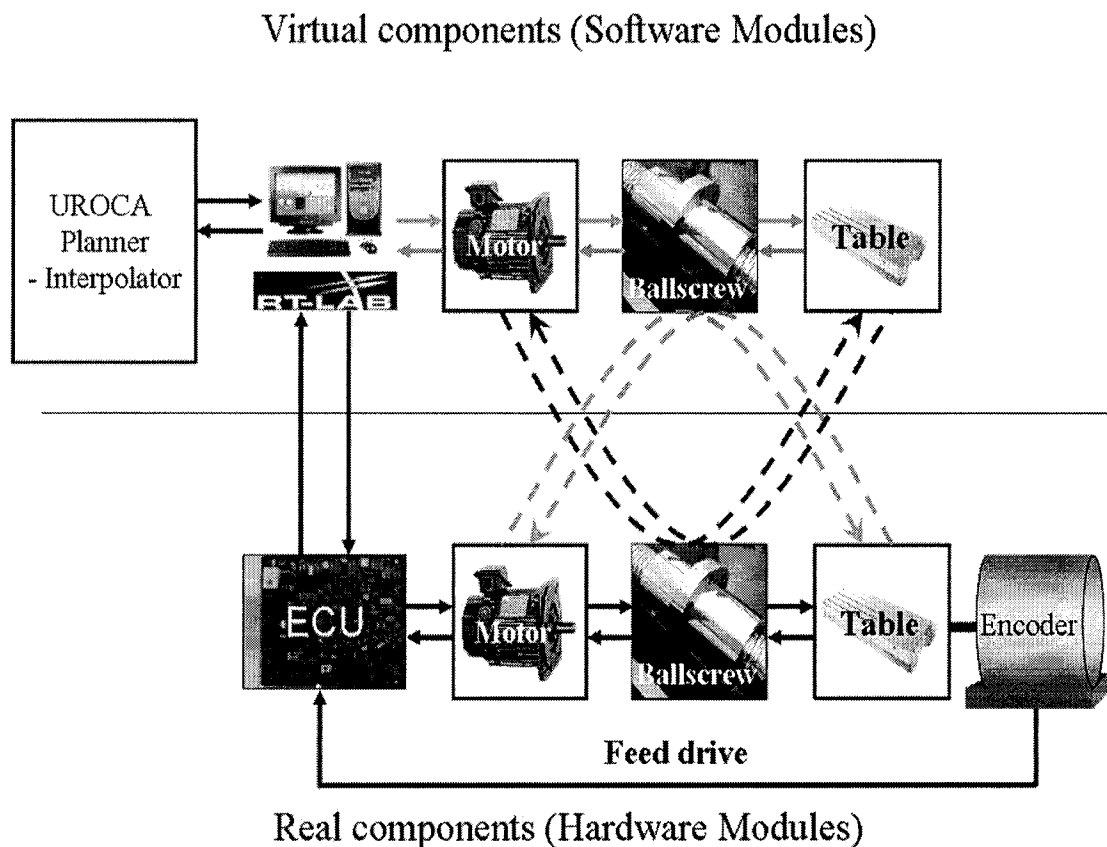


Figure 5.7. Different possibilities of partitioning feed drive model into submodels and different paths among these modules through simulation and/or real environments.

## 6. SIMULATION RESULTS

### 6.1. FEED DRIVE TESTING PROCEDURE

The following results are achieved using various techniques to check for validity of the supervisory control approach as a paramount part of the physical and control layers within UROCA architecture. Testing should resemble real-life applications the way the input is fed through in the system. Machine tool feed drives usually receive either linear, circular or spline interpolation points as input values. Reference input in cases of linear interpolation with a specific feedrate can be assigned to simulation by applying ramp signal with a slope value equals to the required feedrate. While reference input in cases of circular interpolation with specific feedrate can be assigned to simulation by having two sinusoidal signal sources having 90 degrees phase lag and identical amplitude equals the circular path radius. This can be interpolated as follows:

$$X = r \times \cos ((f / r / 60) \times t) \quad (6.1)$$

$$Y = r \times \sin ((f / r / 60) \times t) \quad (6.2)$$

The feed drive model used was a generic two-inertia system with a torsional stiffness in the middle [Matsubara *et al.*, 2000, Ebrahimi, 2000, Johnston *et al.*, 2001]. Disturbances of all kinds were excluded in simulation. Friction and damping were considered zero in order to only explore the backlash issue. A MATLAB-Simulink code was developed for conducting the simulation. Essentially, backlash generates limit cycles all over operation as one of the most important issues that have been noticed. The fluctuation in output occurs during the backlash zone and the limit cycles are induced even over the contact zone. The model, which is used here to describe the machine tool feed drive system, consists of two-inertia system as previously explained in Chapter 3 by equations (3.12). The same model was used in Chapter 4 for studying different control strategies. The dead zone model is used to represent the backlash nonlinearity as was previously explained in equations (3.13). The feed drive system parameters, where identical x- and y- axes are considered, are enlisted below:

$J_m$	:	$5.2 \times 10^{-3}$	$\text{kg} \cdot \text{m}^2$
$J_l$	:	$4.4 \times 10^{-3}$	$\text{kg} \cdot \text{m}^2$
$K_s$	:	950	$\text{N} \cdot \text{m/rad}$
$\beta$	:	50, 25, 12.5	$\mu\text{m}$
$r$	:	0.025	$\text{m}$
$l$	:	0.016	$\text{m/rev}$

When simulating feed drive systems with backlash, circular interpolation testing should be considered. To produce an arc or circle, both axes work concurrently with sinusoidal inputs. Our measure is the error between reference and output signals which also behaves the same way the velocity (feedrate) behaves. The feedrate indication is considered important due to the fact that inconsistency in feedrate would lead to a non-uniform surface quality and many other issues like tool wear.

## 6.2. PI CONTROL APPLICATION

Proportional-Integral (PI) controllers are dominant in the field of machine tool feed drive systems. The greatest control gain weight is done through the proportional component, while the integral part reduces system transients. For linear contouring, the feedrate has been varied over 500, 1000, 2000, 4000 and 8000 mm/min, and the results are shown in Figures 6.1, 6.2, 6.3, 6.4 and 6.5, respectively. For circular interpolation part, the feedrate has been varied over 4000, 6000 and 8000 mm/min, and the results are shown in Figures 6.6, 6.7 and 6.8, respectively. The (PID) control law that is depicted by equation (4.10) is used in these simulations. The controller gains are enlisted below:

$K_p$	:	200
$K_I$	:	25
$K_D$	:	0

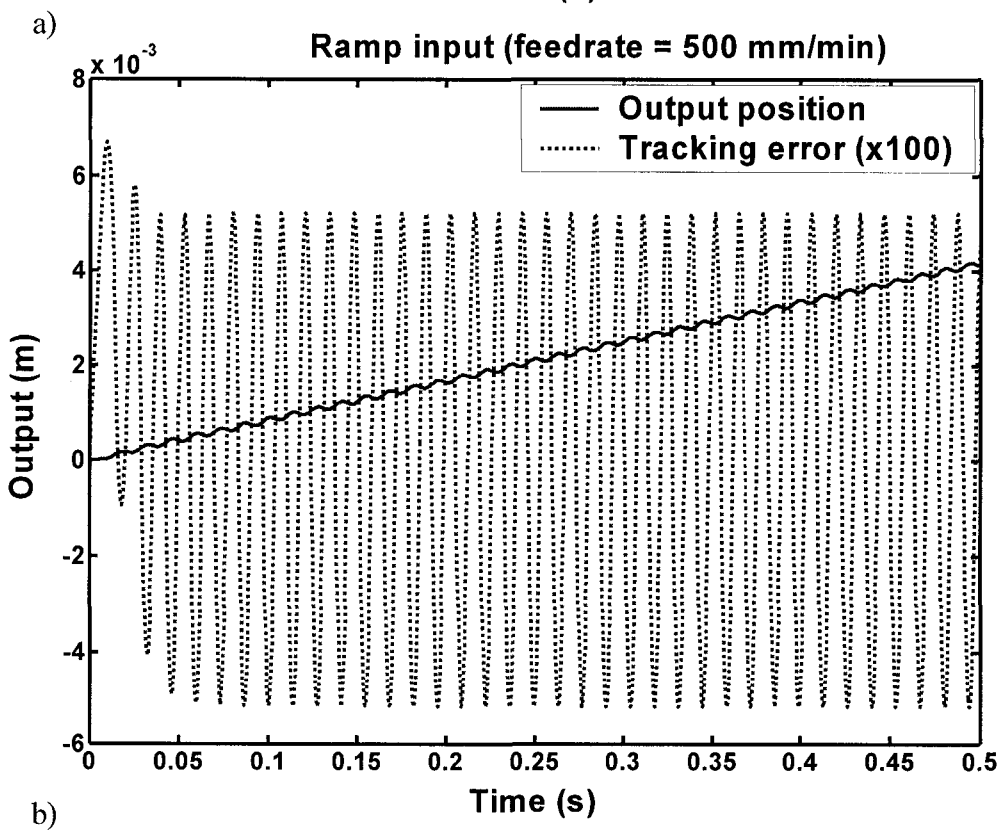
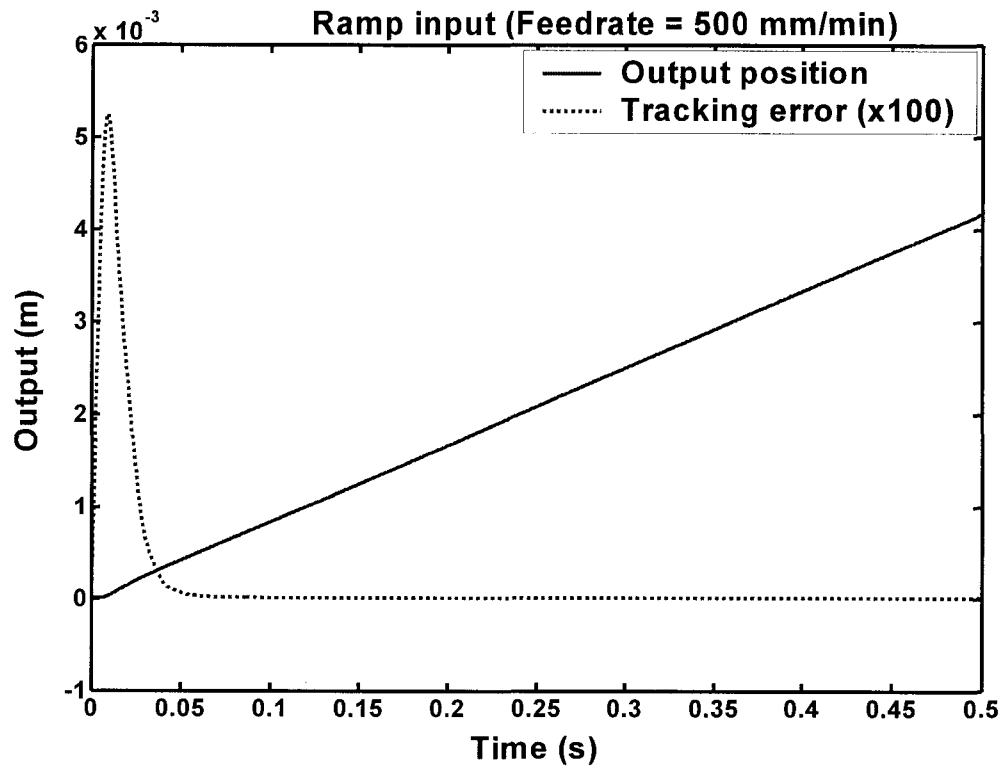
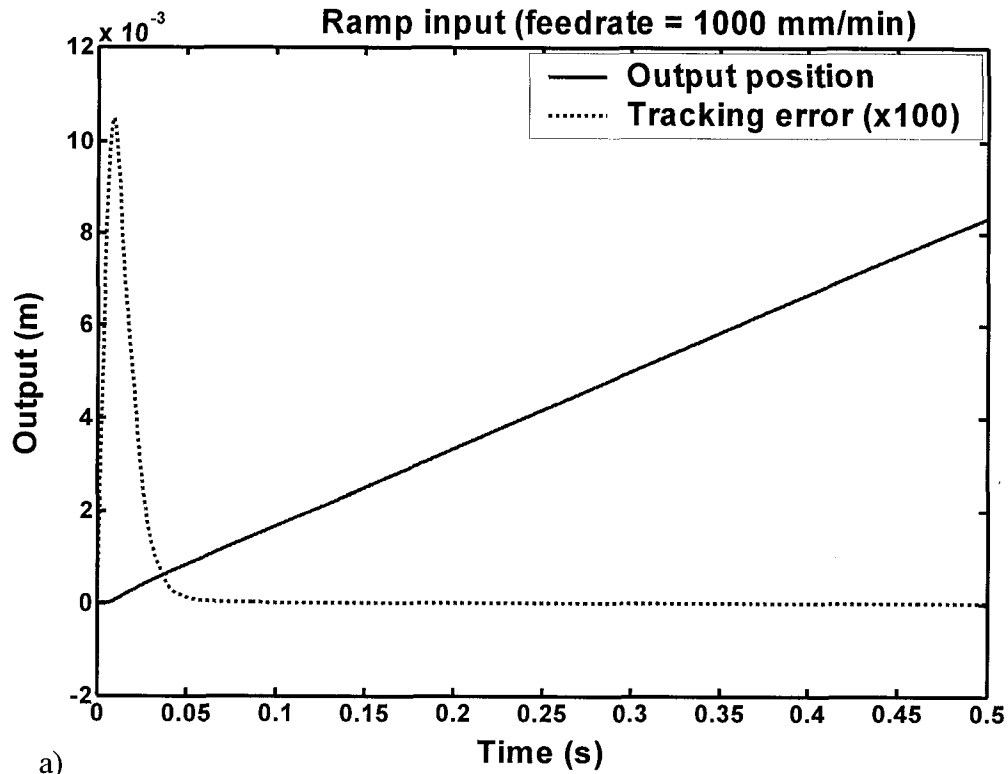
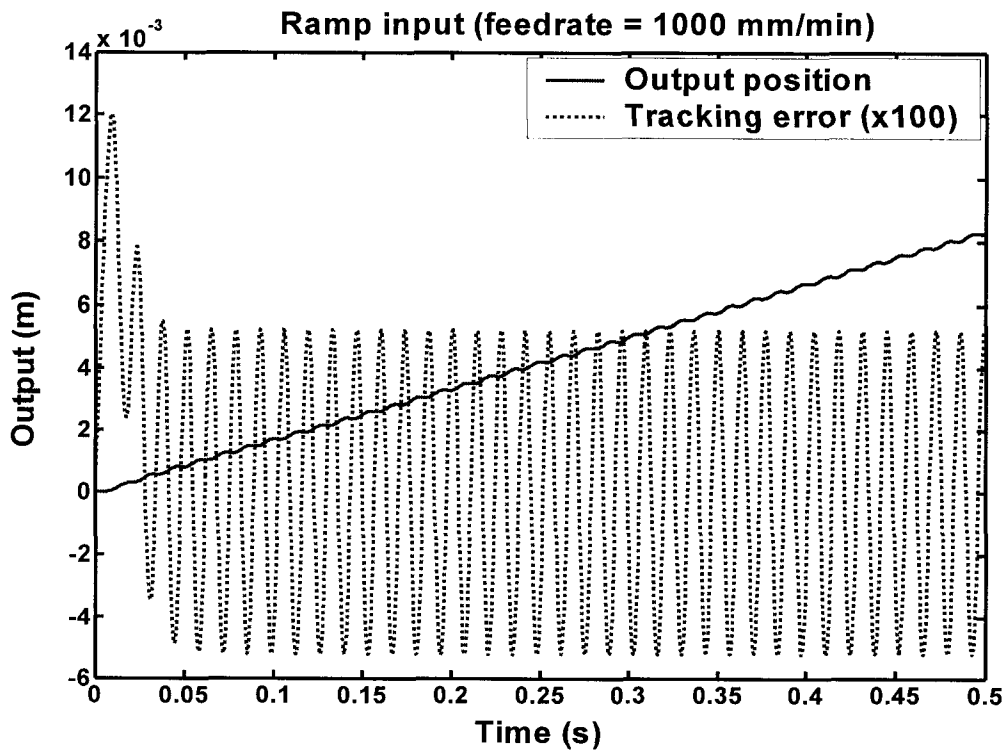


Figure 6.1. Feed drive transient response (ramp input = 500 mm/min): a) without backlash. b) with 50  $\mu$ m backlash.



a)



b)

Figure 6.2. Feed drive transient response (ramp input = 1000 mm/min): a) without backlash. b) with 50  $\mu$ m backlash.

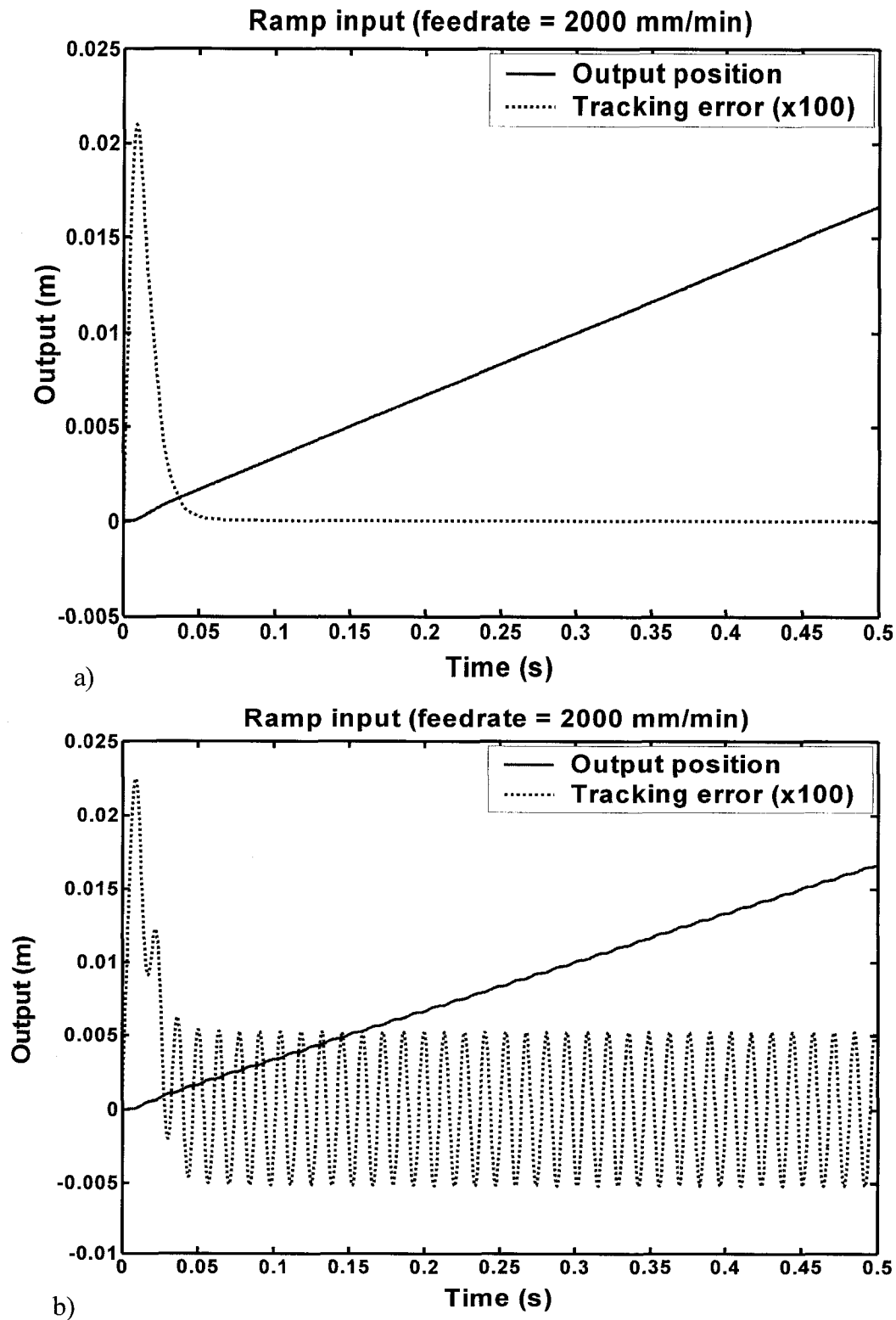


Figure 6.3. Feed drive transient response (ramp input = 2000 mm/min): a) without backlash. b) with 50  $\mu\text{m}$  backlash.

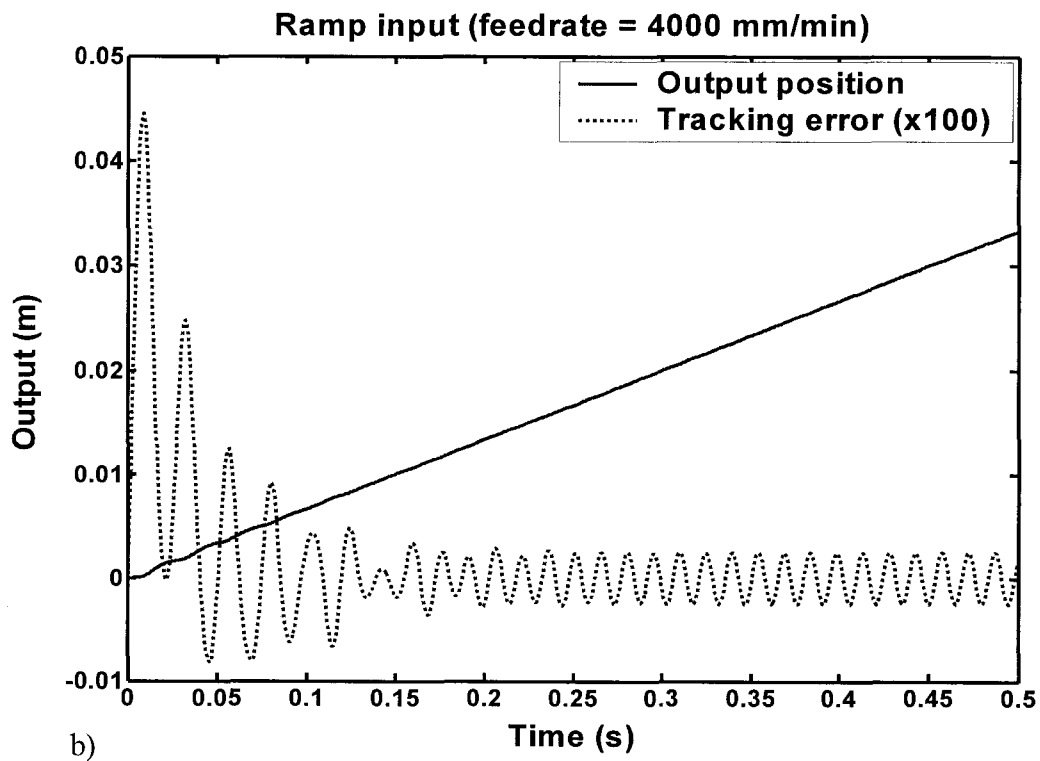
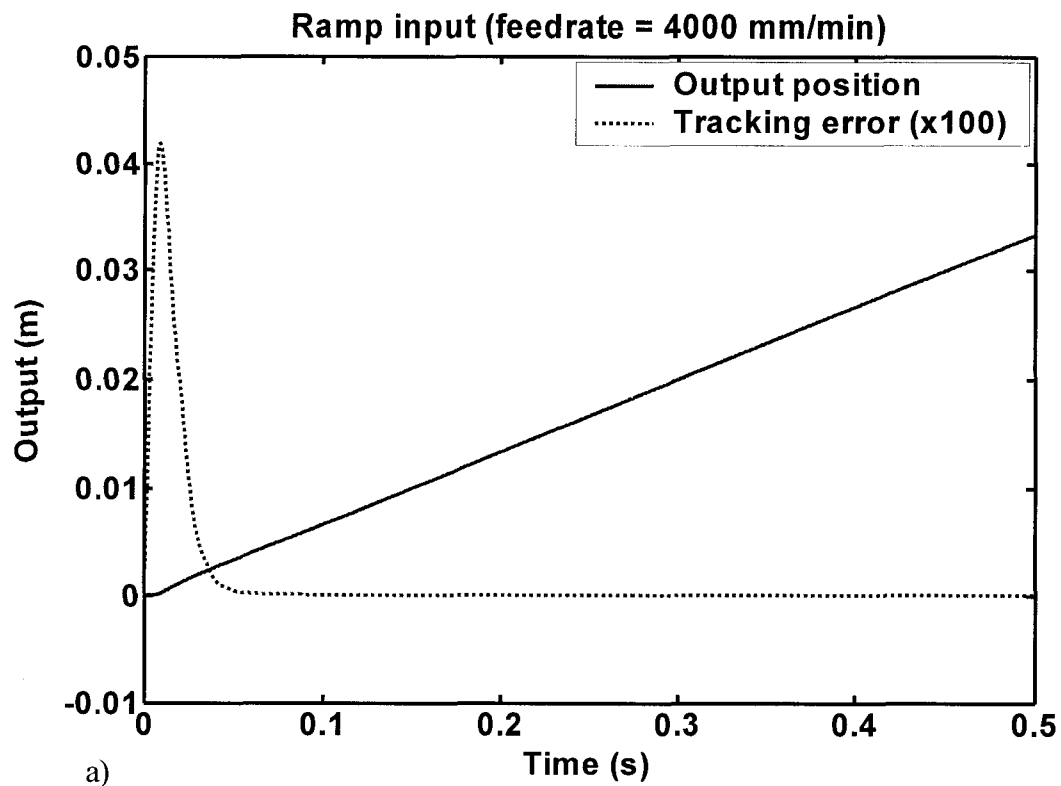


Figure 6.4. Feed drive transient response (ramp input = 4000 mm/min): a) without backlash. b) with 25  $\mu$ m backlash.



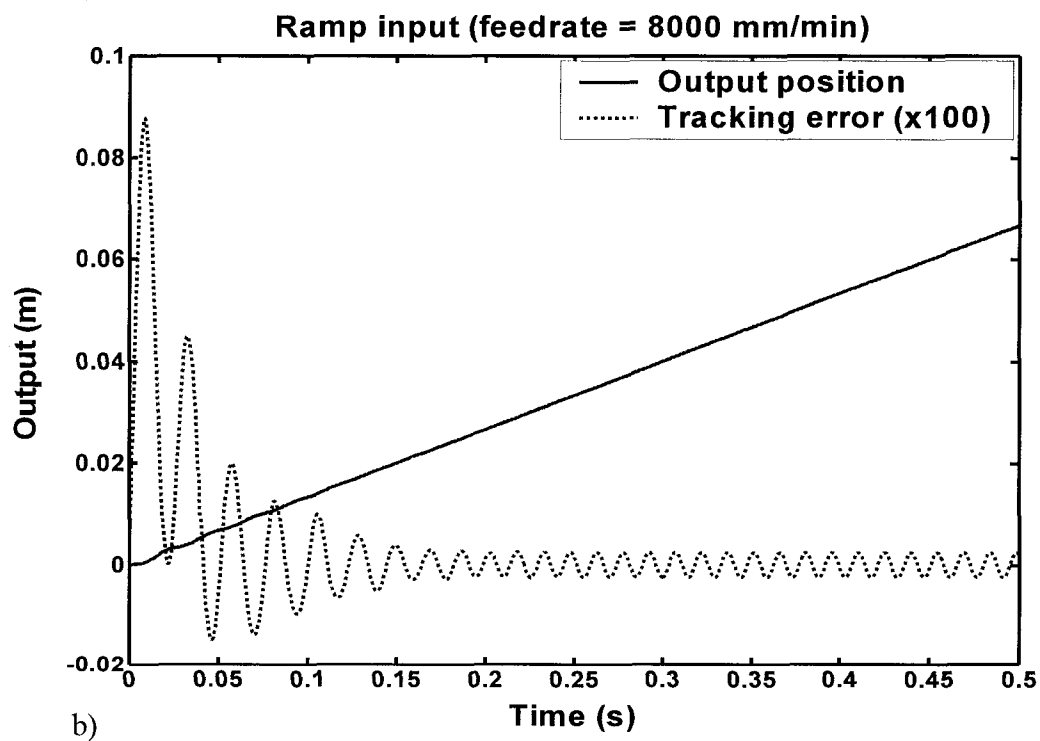
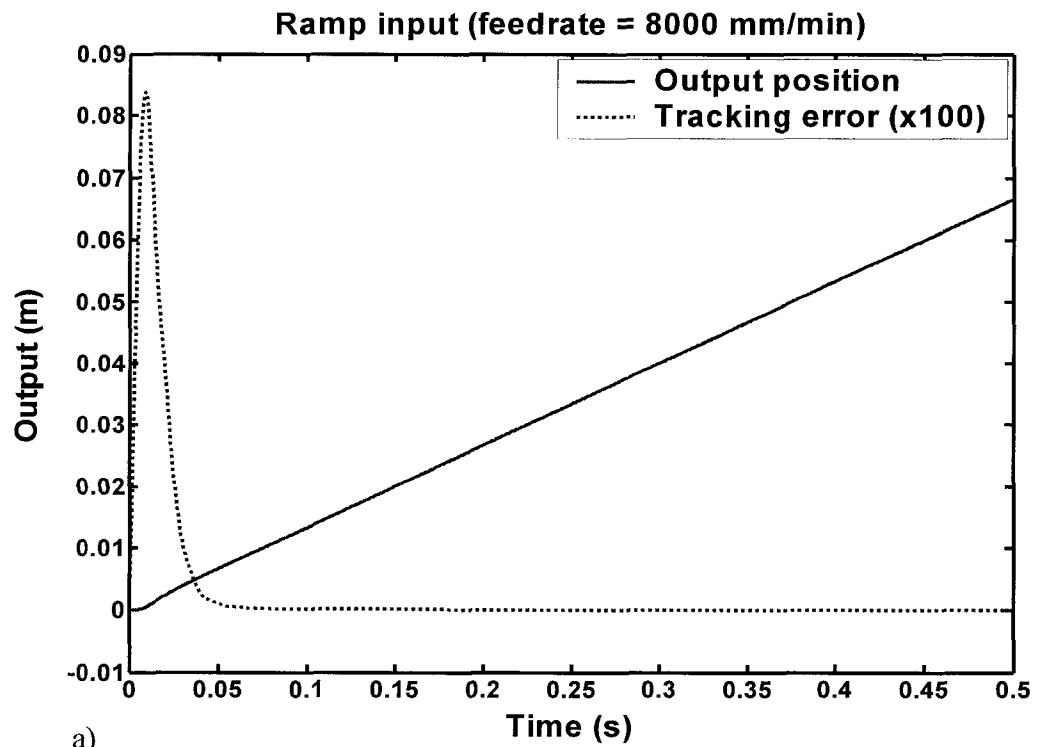


Figure 6.5. Feed drive transient response (ramp input = 8000 mm/min): a) without backlash. b) with 25  $\mu$ m backlash.

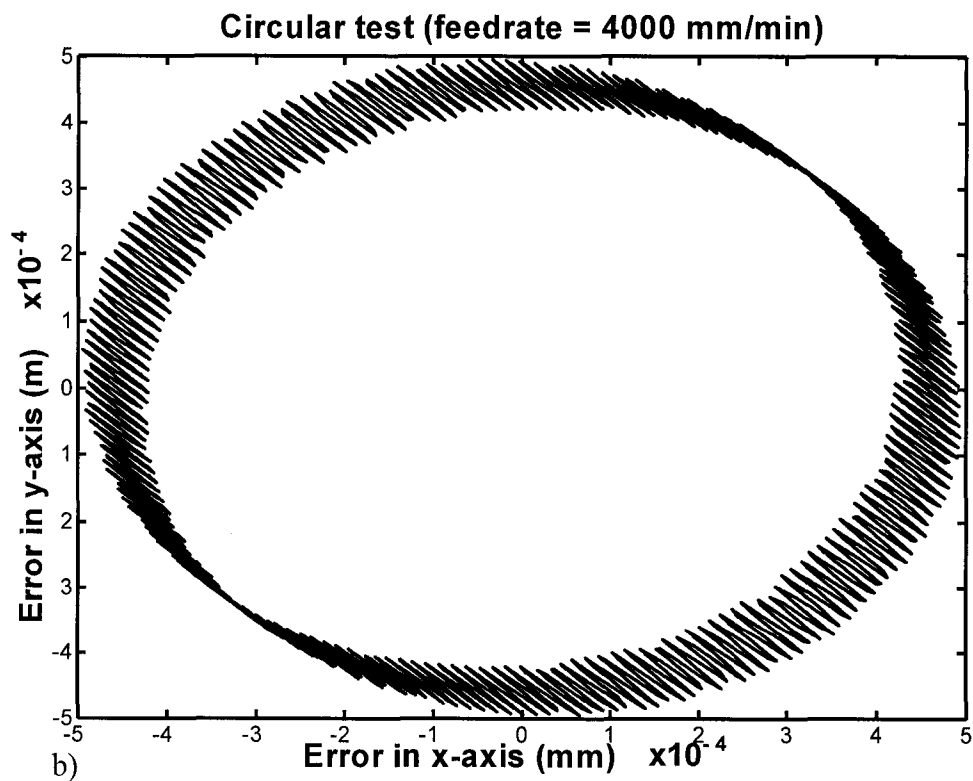
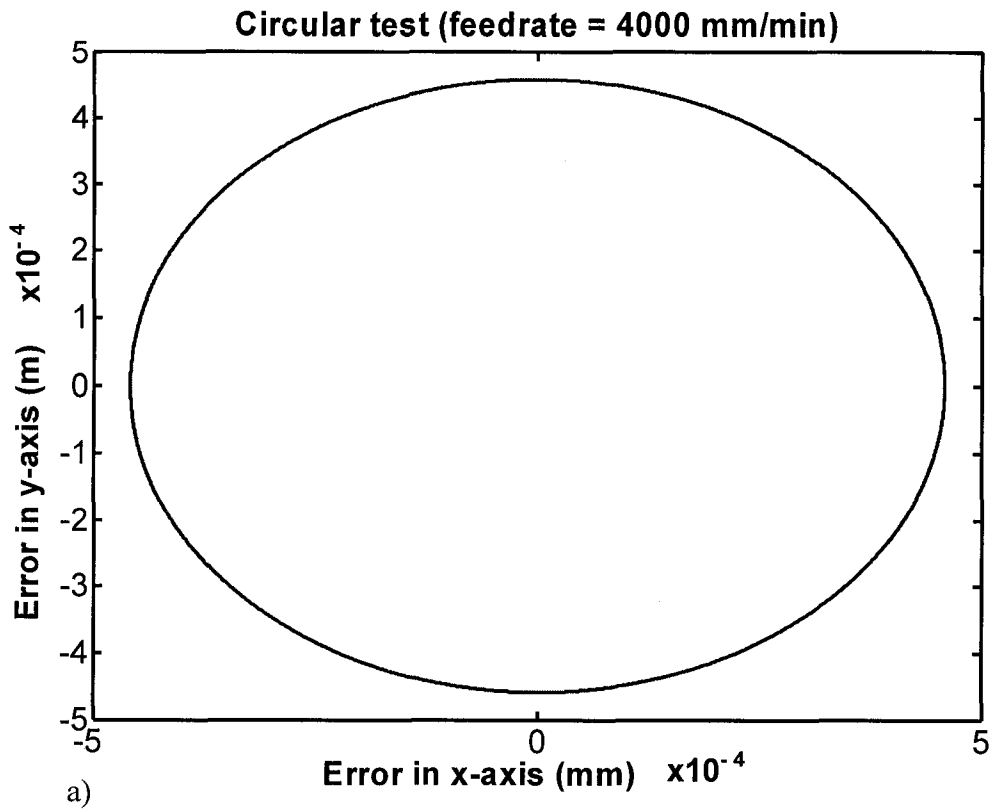
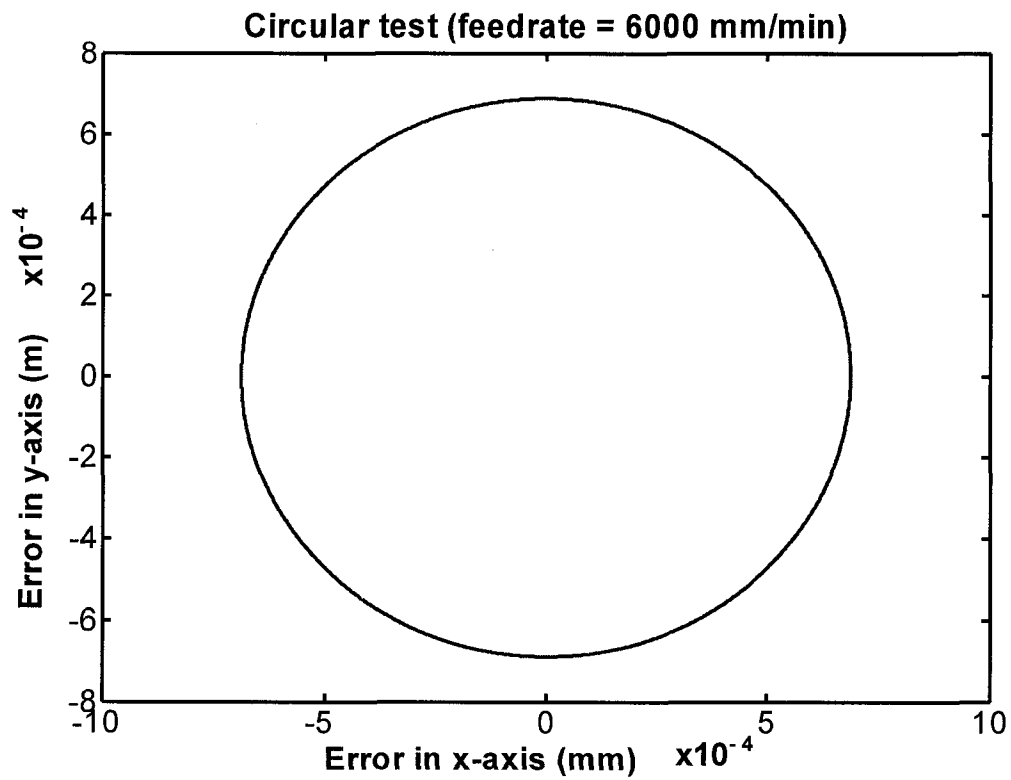
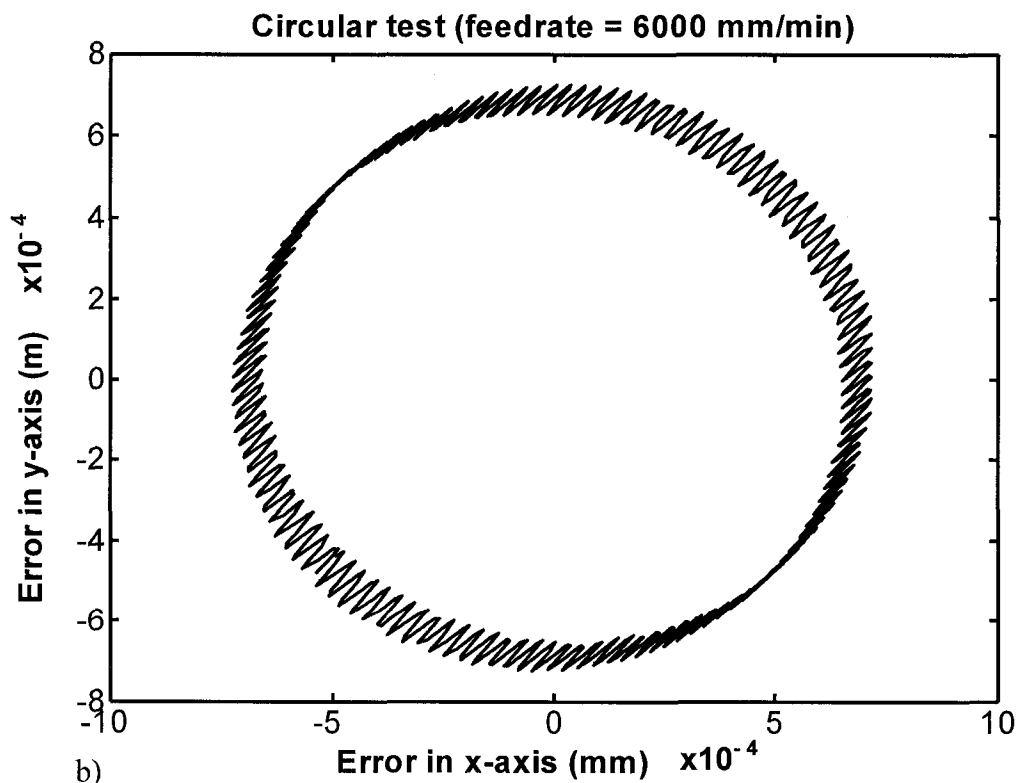


Figure 6.6. Feed drive circular test (feedrate = 4000 mm/min): a) without backlash. b) with 25  $\mu\text{m}$  backlash.

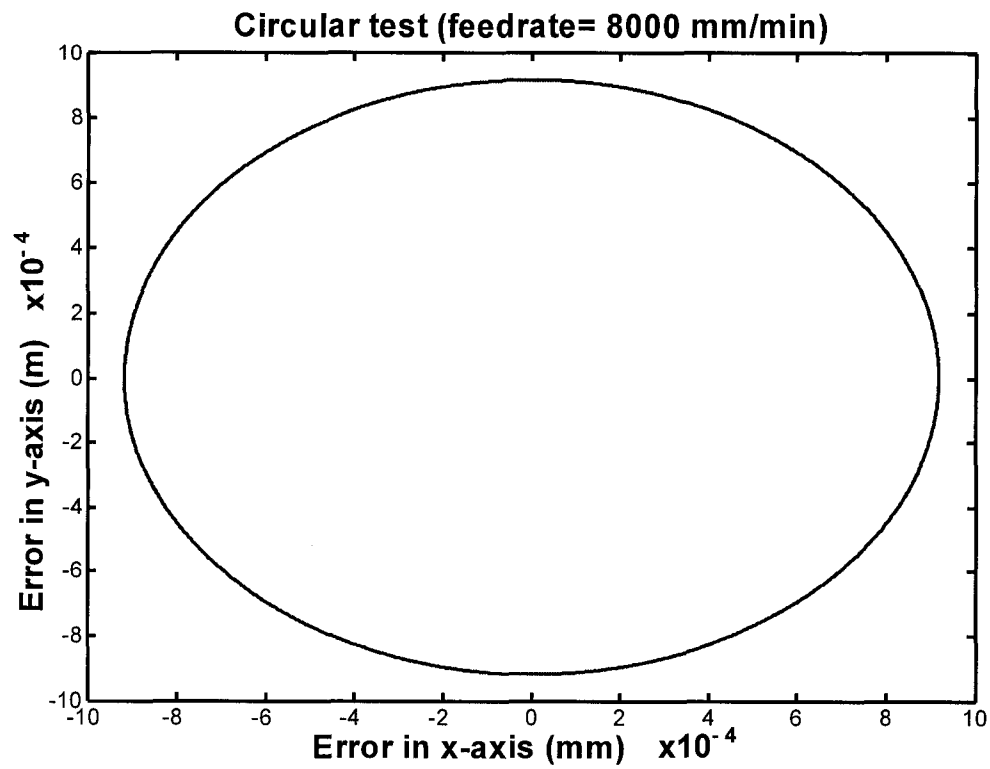


a)

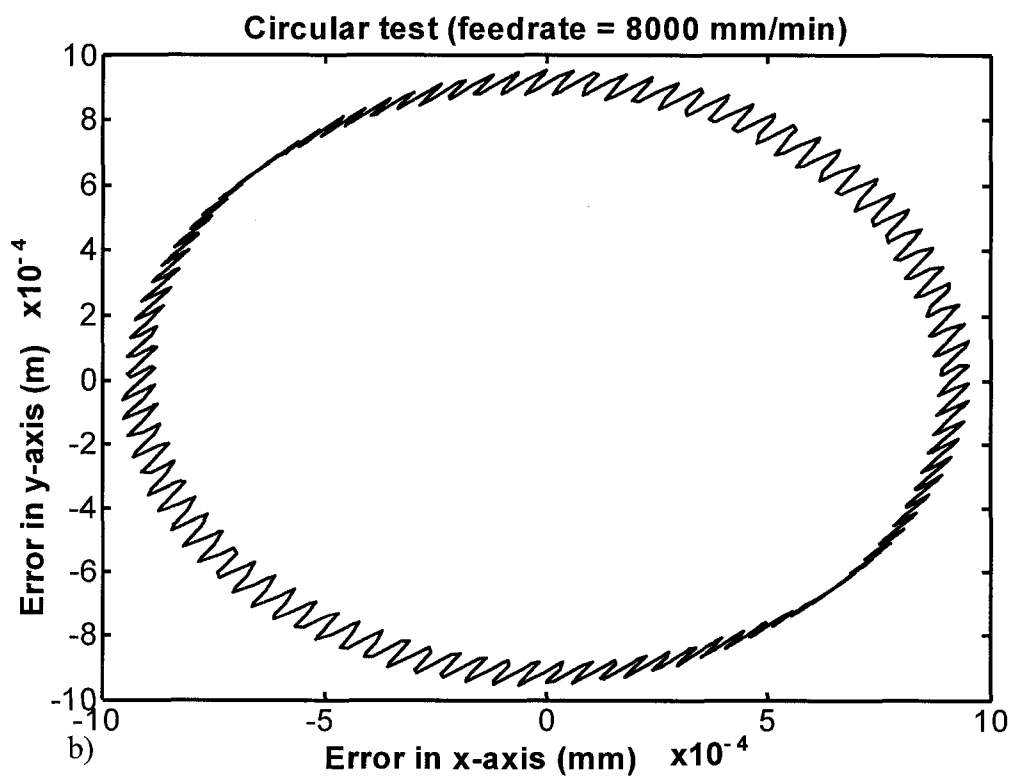


b)

Figure 6.7. Feed drive circular test (feedrate = 6000 mm/min): a) without backlash. b) with 25  $\mu\text{m}$  backlash.



a)



b)

Figure 6.8. Feed drive circular test (feedrate = 8000 mm/min): a) without backlash. b) with 25  $\mu$ m backlash.

For linear interpolation, error is fluctuating about the error value – which is quite infinitesimal as shown in those figures with no backlash – after entering the steady state region. Linear interpolation is considered insufficient to study the phenomenon of backlash, because in linear feeding, no change in direction happens to induce backlash to occur except the take-off moment of the system.

Noticeably, error margin increases with the increase in feedrate applied to the input. Also the value of peaks reached by the system while fluctuating about the no-backlash error value was found to be that same value of backlash; i.e. 50  $\mu\text{m}$  in Figures 6.1, 6.2 and 6.3; 25  $\mu\text{m}$  in Figures 6.4 and 6.5. Linear interpolation results have been introduced with wide range of input values to verify the fact that backlash effect shows minor discrepancy to feed drive systems. Henceforth, circular interpolation has been the only effective way to show the effect of backlash.

From the literature, we can see that the main measure to test feed drive systems under circular interpolation effect is that by graphing position error in  $x$ -axis versus position error in  $y$ -axis [Koren, 1984; Altintas, 2000]. The error produced from each of the two controlled axes of motion within a machine tool can be depicted idealistically by a circle with a constant radius; i.e., the two controllers should be tuned to result in identical amount of error – zero error cases are unreachable in control systems. Any deviation from that circle would mean that the system should be tuned in the first place to accomplish that condition; otherwise, serious change that requires applying other control techniques should be taken into consideration.

The difference between the two cases shown for each simulated feedrate is highly affecting the system to perform inconsistently regarding output feedrate which is indeed a bad reflection on surface quality, see Figure 6.8 as an example of feedrate fluctuation. Error in the previous example hits in between the interval  $\pm 0.936217\text{ m/min}$ , which yields 11.703% of error. For higher speeds, higher error percentages are believed to be the main cause of unsatisfactory surface quality.

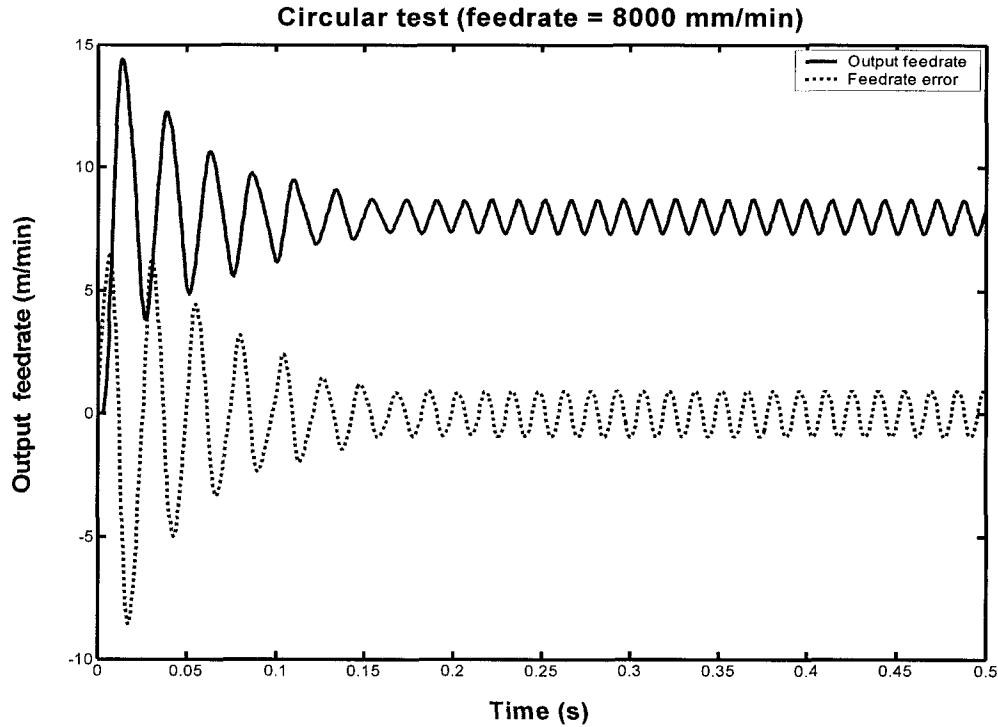


Figure 6.9. Feed drive circular test (feedrate = 8000 mm/min) with 25  $\mu$  m backlash.

### 6.3. MODEL-BASED CONTROL APPLICATION

The results in this section are achieved using the standard backlash compensation technique used in most backlash control literature [Tao and Kokotović, 1996; Ling and Tao, 1999; Ezal *et al.*, 1997]. This control law by itself is considered insufficient since it produces intolerable ranges of error. Results are shown here for demonstration only and to compare with the switching control criteria discussed in the next section. Friction and damping, also, were considered zero to study the backlash issue unaffected by other factors. Backlash value of 12.5  $\mu$  m is to deal with in this section. For circular interpolation, the feedrate has been varied over 4000, 6000 and 8000 mm/min, which are shown in Figures 6.10, 6.11, 6.12, 6.13, 6.14 and 6.15. The control law depicted by equation (4.14) is used for this section; the controller gains are:

$$K_1 : 10000$$

$$K_2 : 2000$$

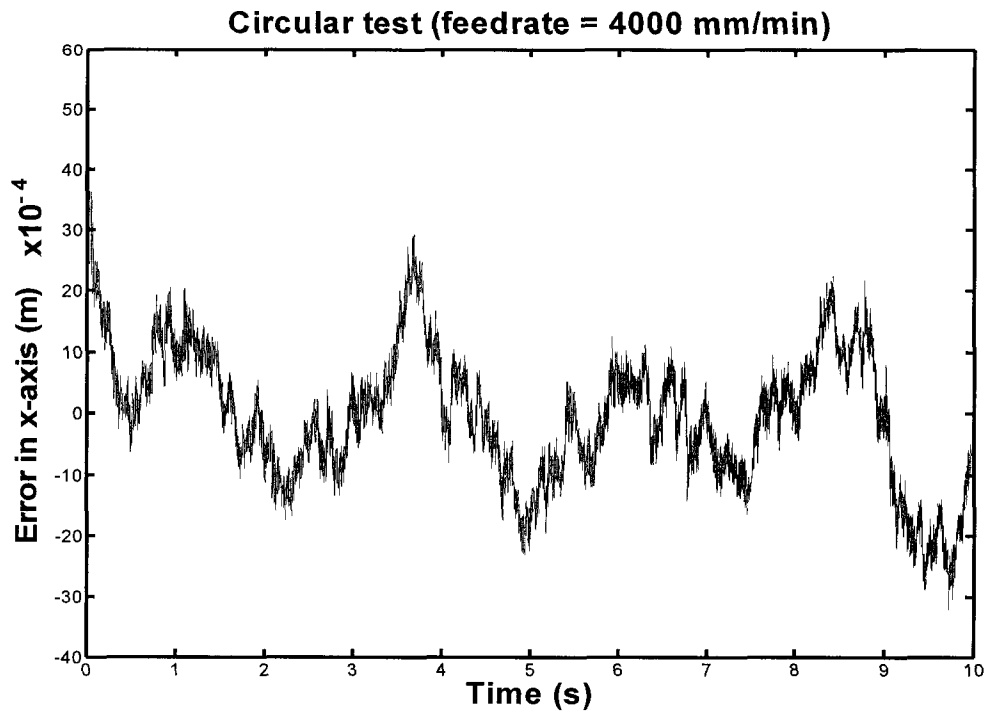


Figure 6.10. Position error of x-axis for a single controller set-up (no switching) with feedrate of 4000 mm/min.

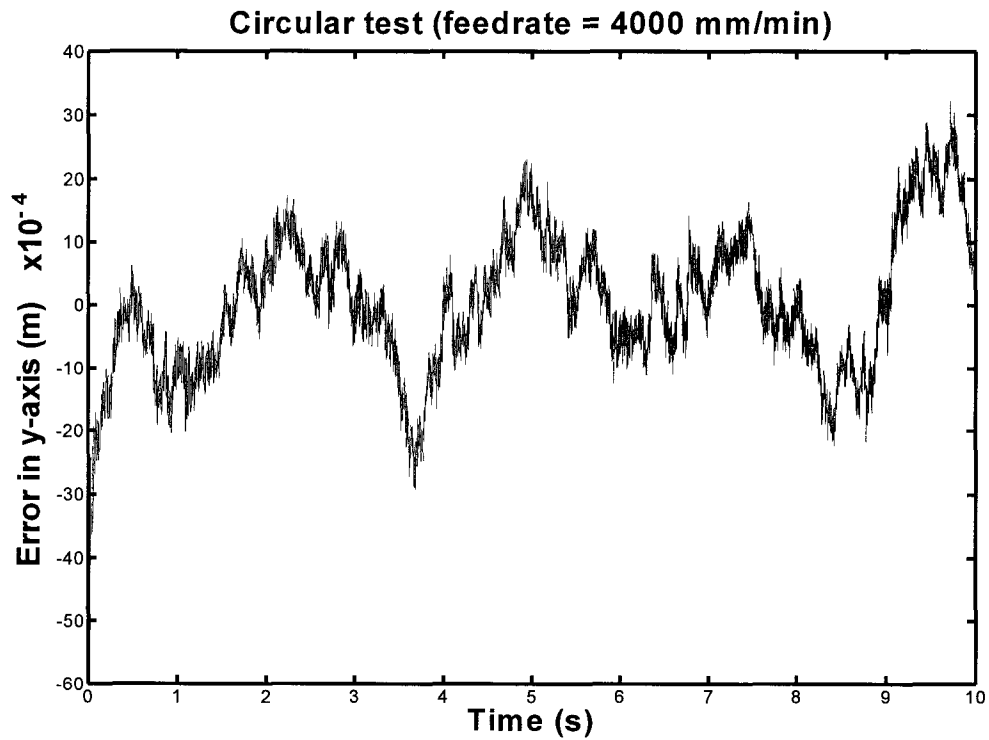


Figure 6.11. Position error of y-axis for a single controller set-up (no switching) with feedrate of 4000 mm/min.

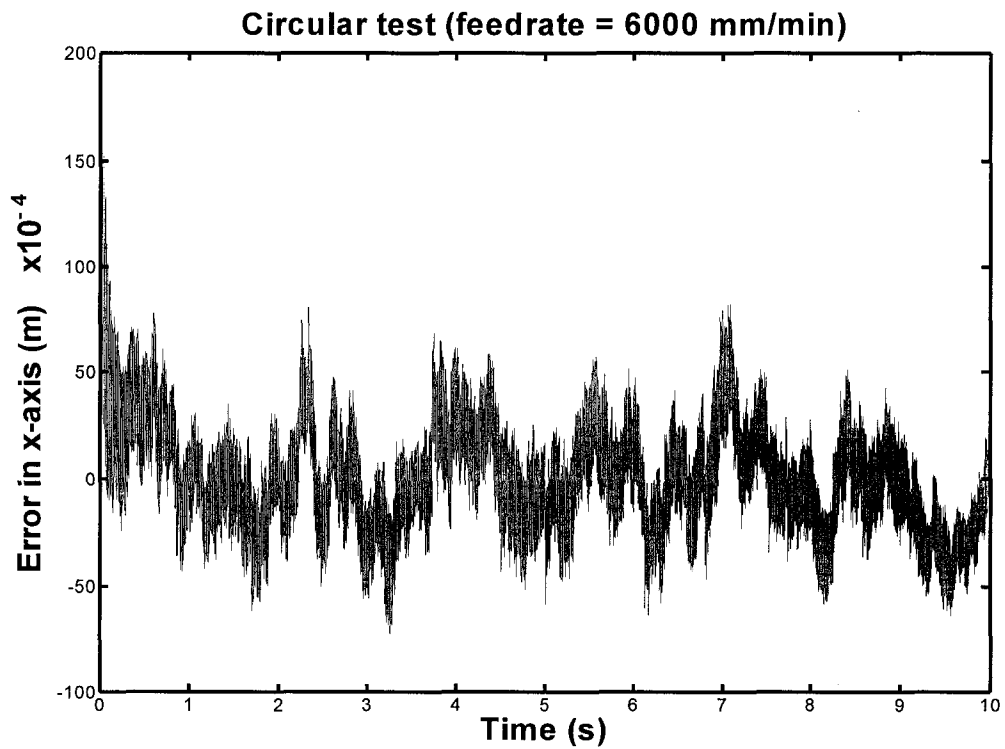


Figure 6.12. Position error of x-axis for a single controller set-up (no switching) with feedrate of 6000 mm/min.

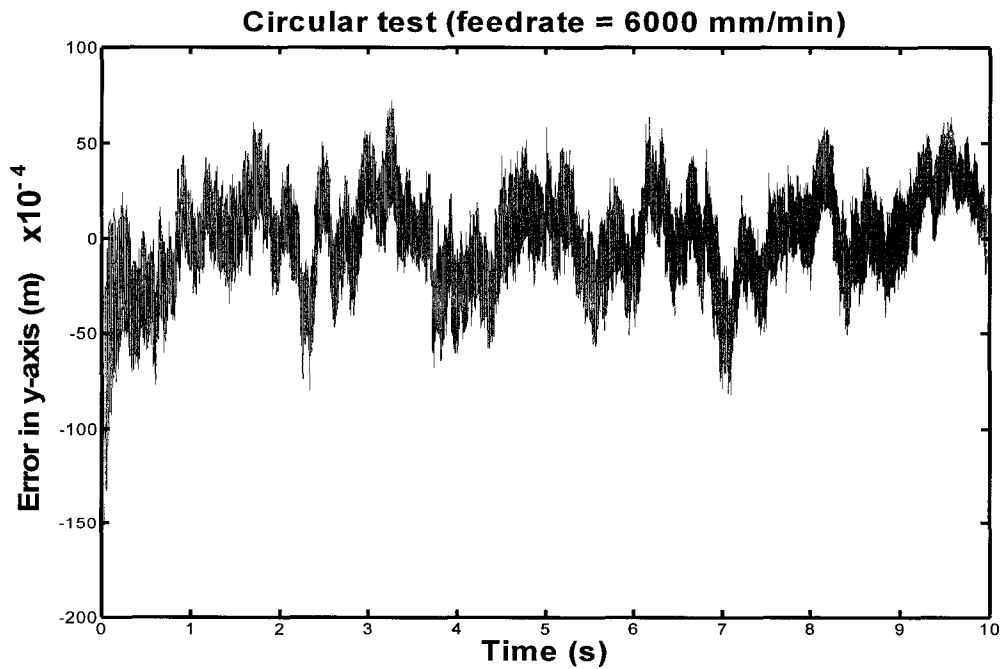


Figure 6.13. Position error of y-axis for a single controller set-up (no switching) with feedrate of 6000 mm/min.



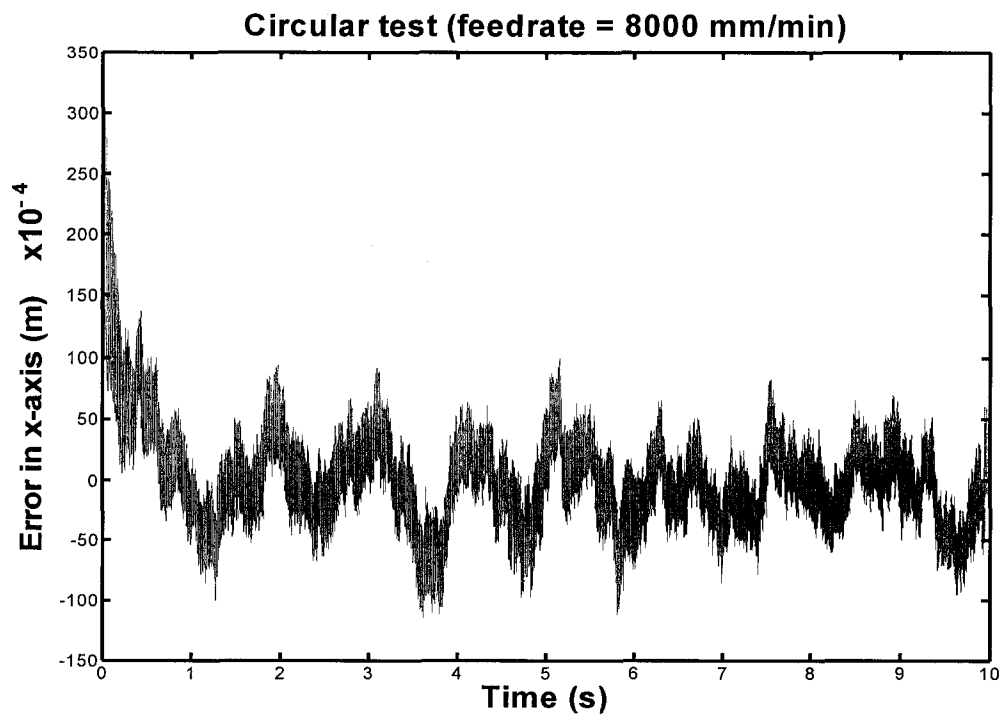


Figure 6.14. Position error of x-axis for a single controller set-up (no switching) with feedrate of 8000 mm/min.

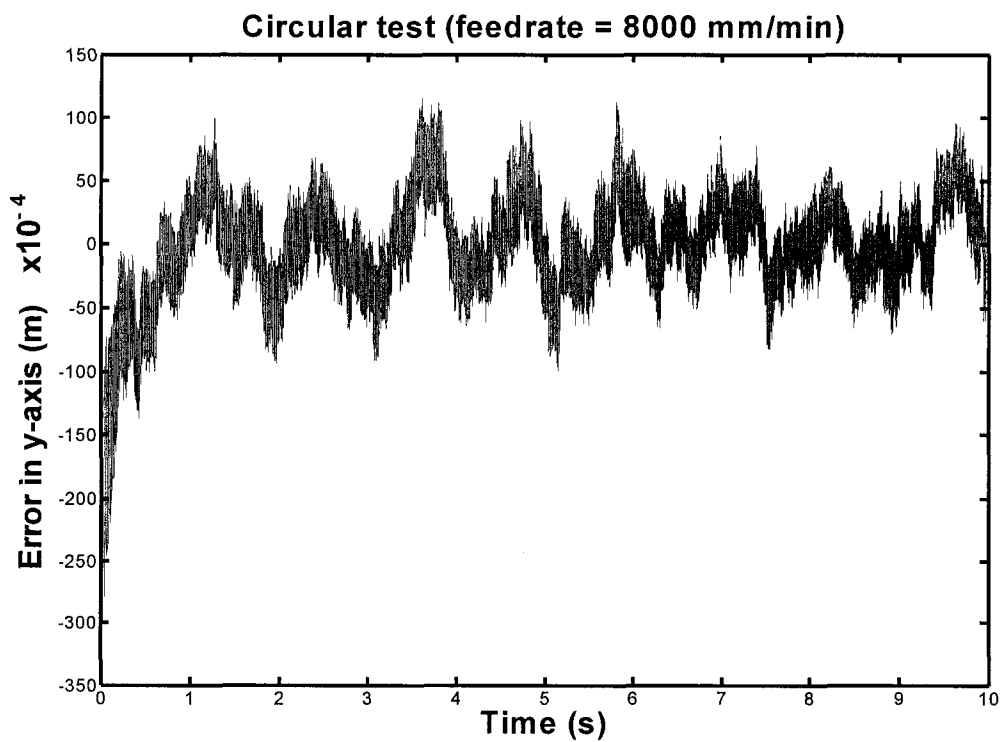


Figure 6.15. Position error of y-axis for a single controller set-up (no switching) with feedrate of 8000 mm/min.

As mentioned before, error ranges are quite high compared to those obtained by PI control technique. Also, the error functions among the different feedrates behave somehow in a quite disturbed manner. Model-based control technique has shown very low performance in fighting backlash nonlinearity as shown in the previous figures.

## **6.4. SWITCHING CONTROL APPLICATION**

### **6.4.1. Switching Control Scheme I**

The results in this subsection will be achieved using switching control decision unit with two controllers, each of which serves in a different region of operation: contact and backlash regions. Reference input signal will be assigned according to the type of test; tests undertaken in this subsection are similar of those of section 6.3. The feed drive model used is similar to that used previously. Friction and damping, also, were considered zero for the ease of calculation. The backlash value is 12.5  $\mu\text{m}$  in this subsection. For circular interpolation, the feedrate has been varied over 4000, 6000 and 8000 mm/min, which are shown in Figures 6.16, 6.17, 6.18, 6.19, 6.20 and 6.21. The control law for contact zone is depicted by equation (4.10), namely, contact-zone controller I, while the control law for backlash zone is depicted by equation (4.14), namely, backlash-zone controller I, is used for this subsection; the controller gains are:

$$\begin{array}{ll} K_1 & : \quad 10000 \\ K_2 & : \quad 2000 \\ K_4 & : \quad 10000 \\ K_5 & : \quad 2000 \end{array}$$

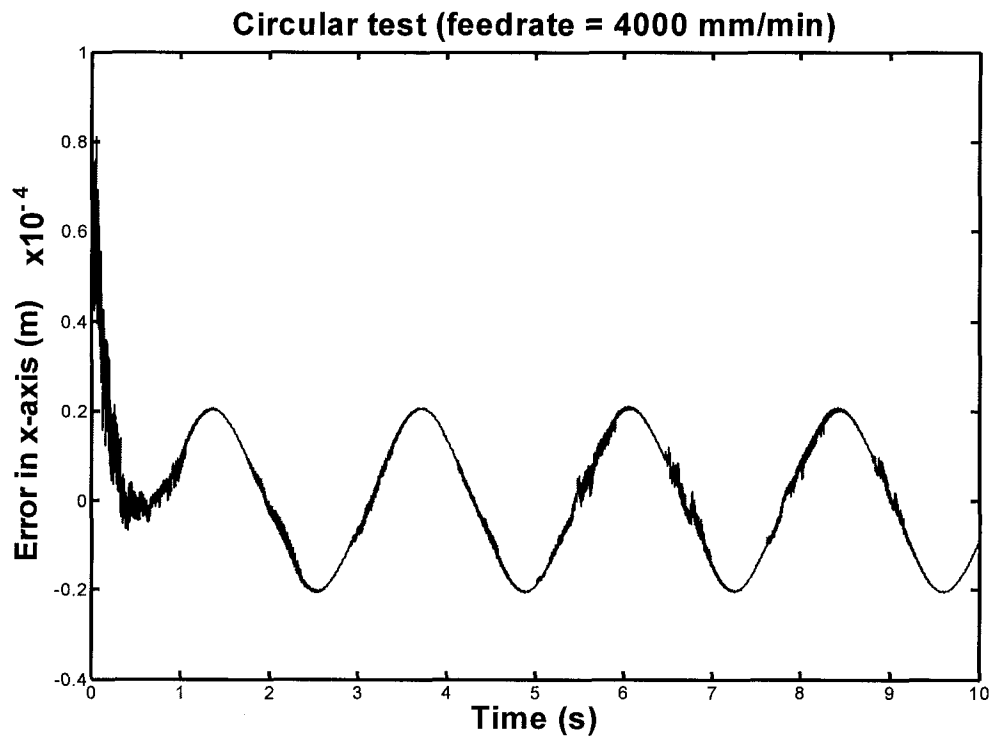


Figure 6.16. Position error of x-axis for switching control I set-up with feedrate of 4000 mm/min.

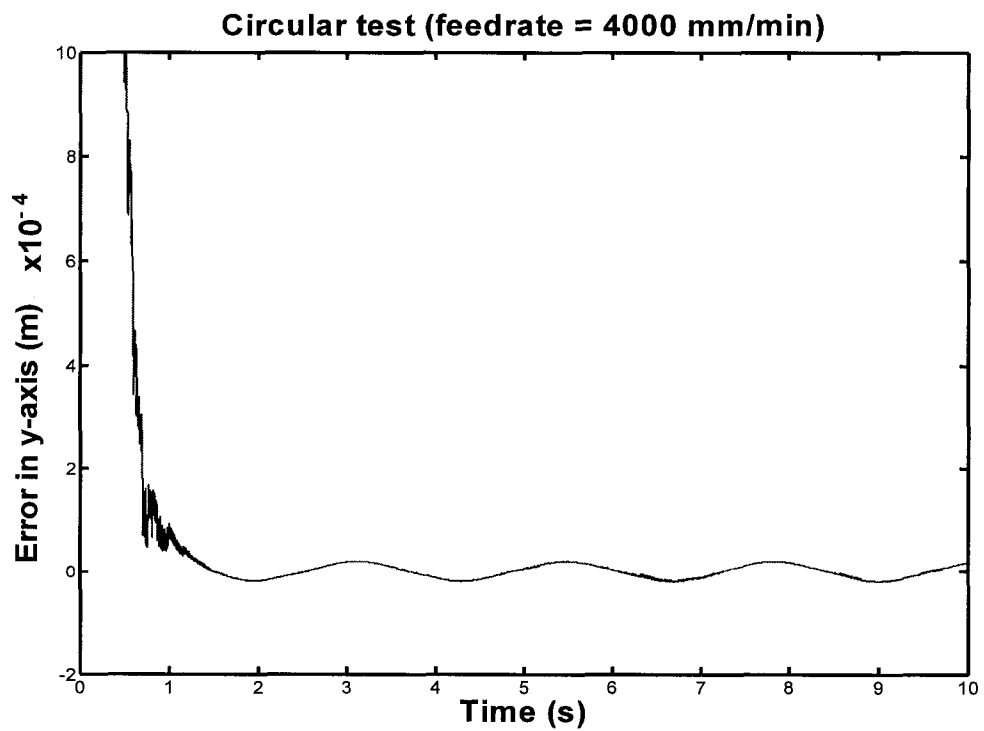


Figure 6.17. Position error of y-axis for switching control I set-up with feedrate of 4000 mm/min.

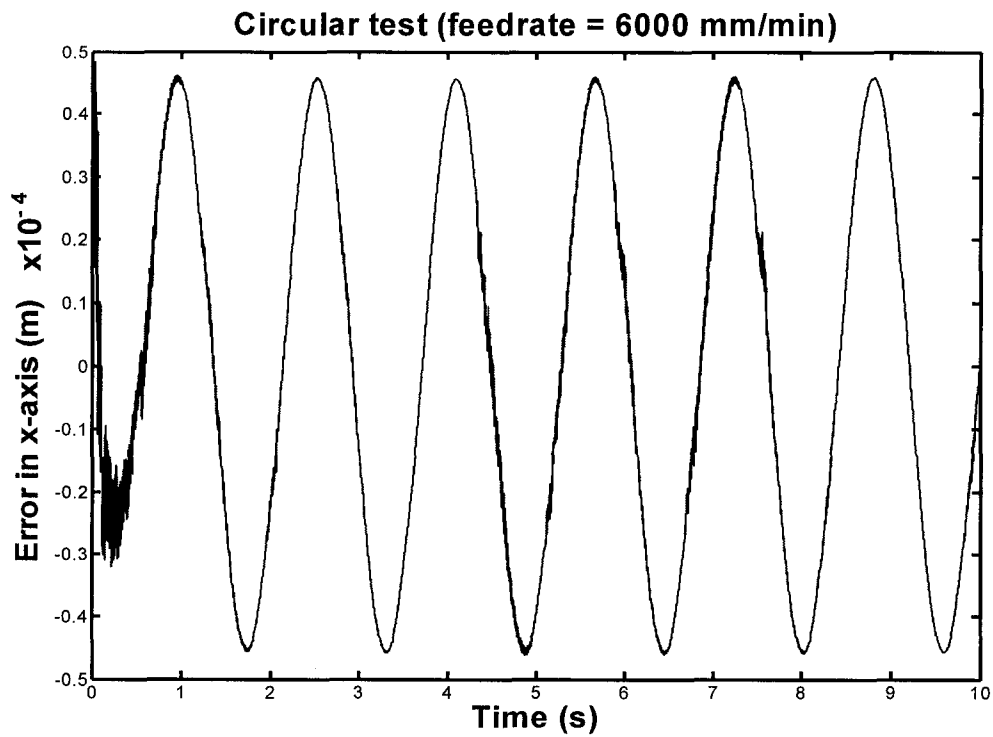


Figure 6.18. Position error of x-axis for switching control I set-up with feedrate of 6000 mm/min.

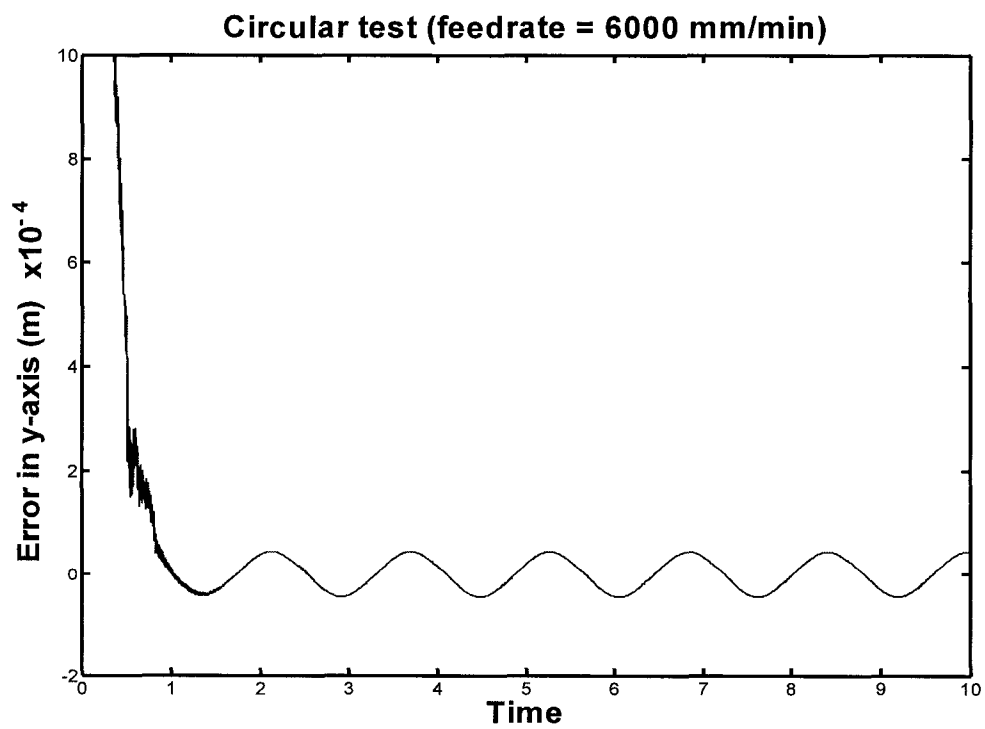


Figure 6.19. Position error of y-axis for switching control I set-up with feedrate of 6000 mm/min.

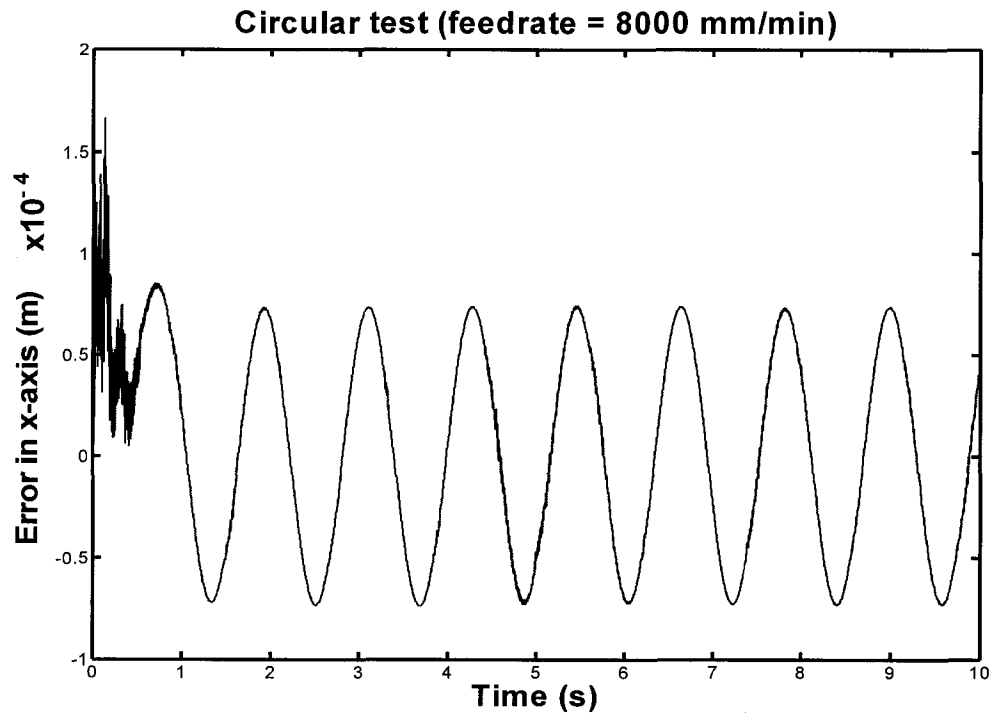


Figure 6.20. Position error of x-axis for switching control I set-up with feedrate of 8000 mm/min.

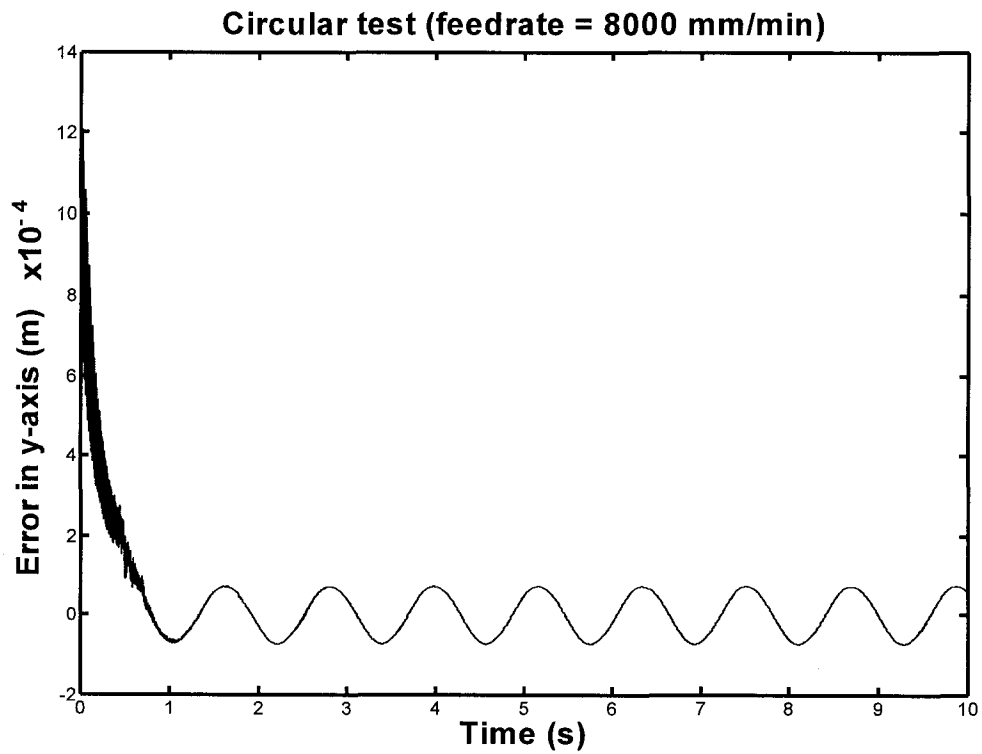


Figure 6.21. Position error of y-axis for switching control I set-up with feedrate of 8000 mm/min.

Now, we can see the sinusoidal nature of the error function is obtained back as the PI controller showed us before. However, this sinusoidal function is still considered inconsistent taking into consideration fluctuations in feedrate. Also, high transients noticed in the previous figures, especially in  $y$ -axis – due to the derivative of reference input for  $y$ -axis at  $t = 0$  does not equal zero – are considered a drawback against this switching scheme. Switching logic, between the two controllers, depends on measuring the difference between load and motor positions and compares it to the backlash value to assign the needed controller according to the rules explained and discussed thoroughly in Chapters 3 and 4. Error values, which have been produced from simulating this scheme for both identical  $x$ - and  $y$ - axes, of 20.4  $\mu\text{m}$ , 46.2  $\mu\text{m}$  and 71.6  $\mu\text{m}$  for feedrates of 4000, 6000 and 8000 mm/min, respectively.

#### 6.4.2. Switching Control Scheme II

The results in this subsection will be achieved using switching control decision unit with two controllers, each of which serves in a different region of operation: contact and backlash regions. The feed drive model used is similar to that used previously. Friction and damping, also, were considered zero in order to explore the backlash issue. The backlash value is 12.5  $\mu\text{m}$  in this subsection. For circular interpolation, the feedrate has been varied over 4000, 6000 and 8000 mm/min, which are shown in Figures 6.22, 6.23, 6.24, 6.25, 6.26 and 6.27. The control law for contact zone is depicted by equation (4.11), namely, contact-zone controller II, while the control law for backlash zone is depicted by equation (4.15), namely, backlash-zone controller II, is used for this subsection; the controller gains are:

$$\begin{aligned} K_{1'} & : 1000 \\ K_{2'} & : 200 \\ K_{4'} & : 1000 \\ K_{5'} & : 200 \end{aligned}$$

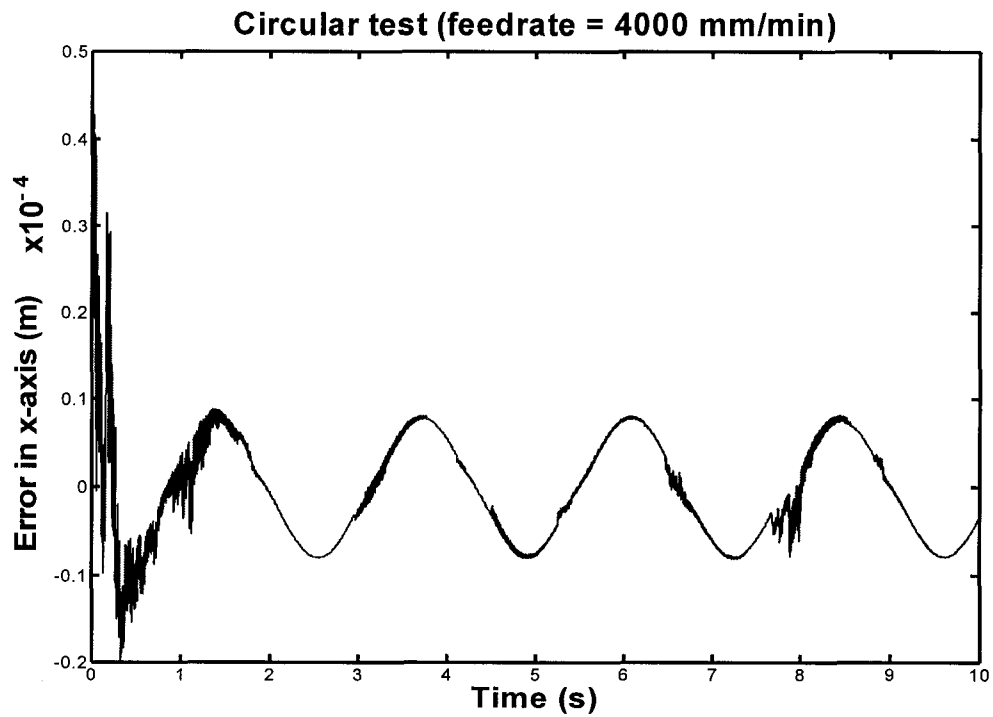


Figure 6.22. Position error of x-axis for switching control II set-up with feedrate of 4000 mm/min.

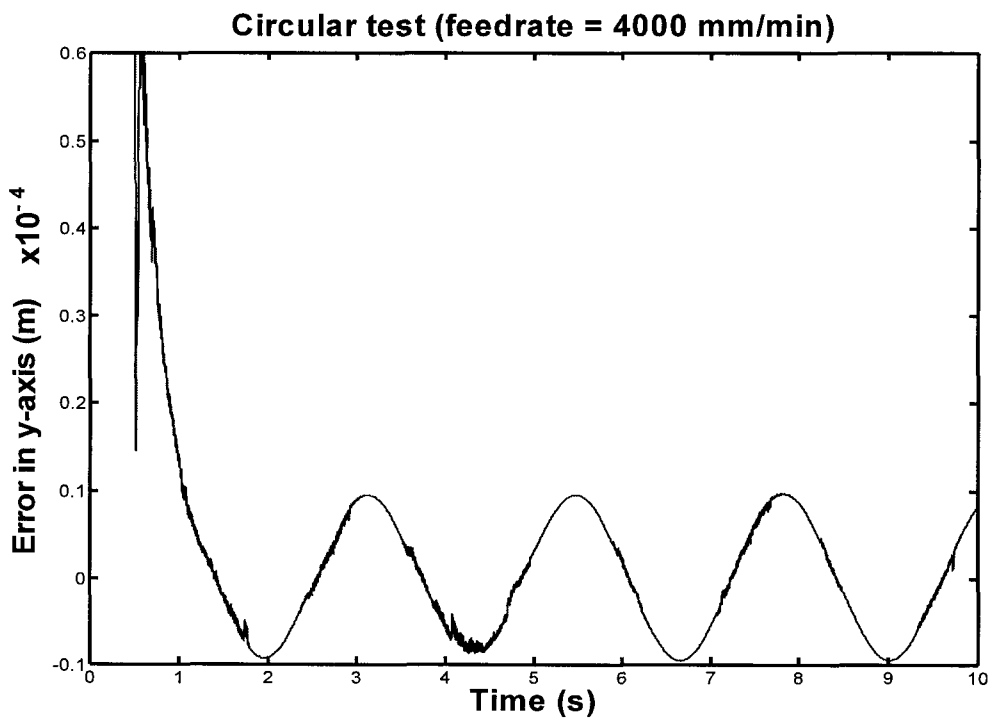


Figure 6.23. Position error of y-axis for switching control II set-up with feedrate of 4000 mm/min.

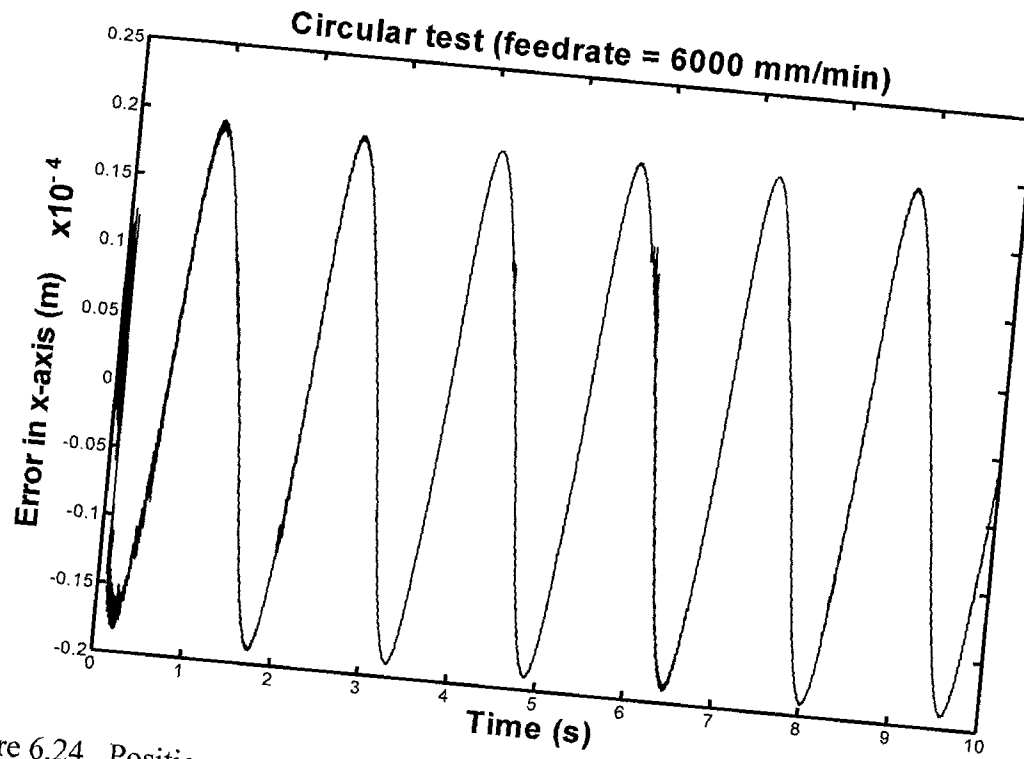


Figure 6.24. Position error of x-axis for switching control II set-up with feedrate of 6000 mm/min.

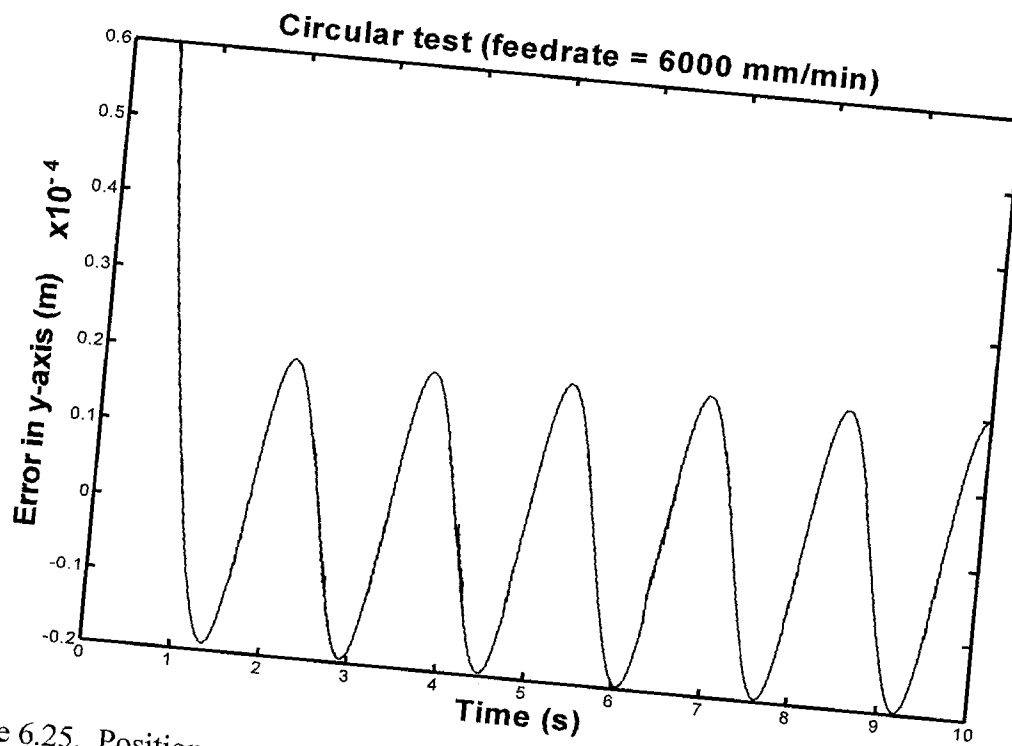


Figure 6.25. Position error of y-axis for switching control II set-up with feedrate of 6000 mm/min.



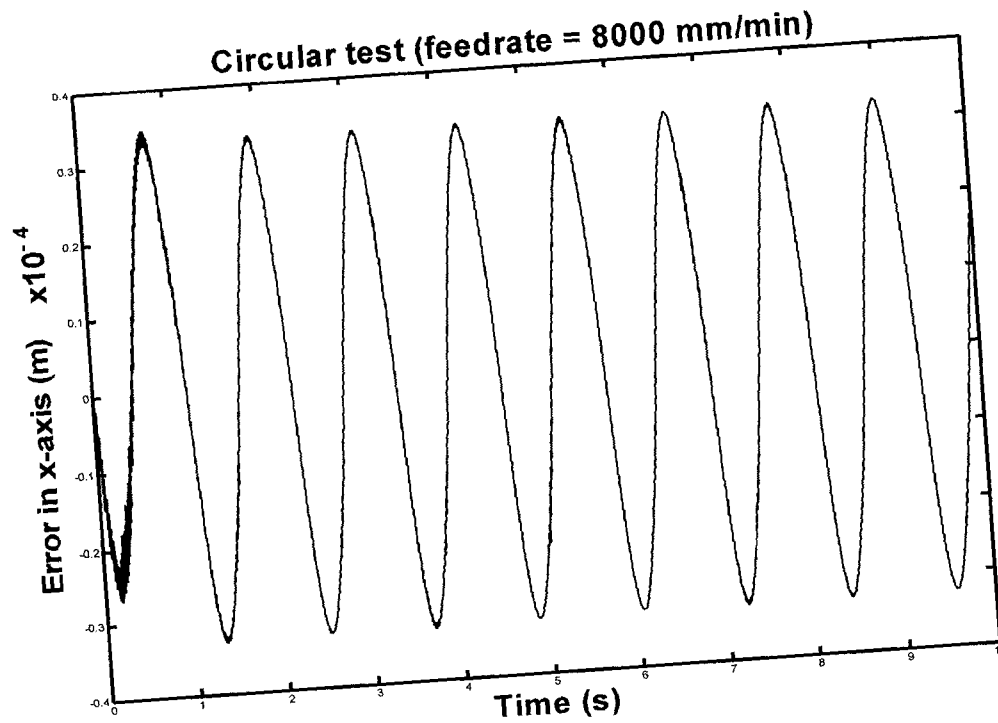


Figure 6.26. Position error of x-axis for switching control II set-up with feedrate of 8000 mm/min.

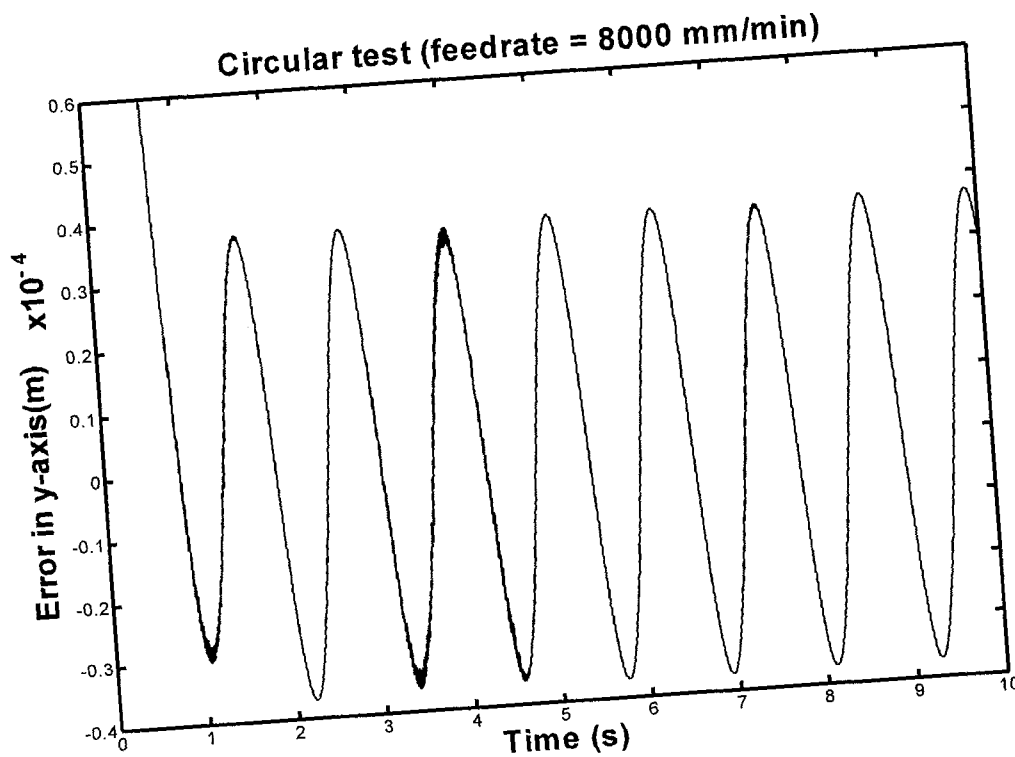


Figure 6.27. Position error of y-axis for switching control II set-up with feedrate of 8000 mm/min.

Also in this scheme, high transients are noticed in the previous figures, especially in  $y$ -axis – due to the derivative of reference input for  $y$ -axis at  $t = 0$  does not equal zero – are considered a drawback against this switching scheme. Switching logic, between the two controllers, depends on measuring the difference between load and motor positions and compares it to the backlash value to assign the needed controller according to the rules explained and discussed thoroughly in Chapters 3 and 4. Error values, which have been produced from simulating this scheme for both identical  $x$ - and  $y$ - axes, of  $9.59\text{ }\mu\text{m}$ ,  $19.7\text{ }\mu\text{m}$  and  $33.2\text{ }\mu\text{m}$  for 4000, 6000 and 8000 mm/min, respectively. Although, controllers' gains have been reduced ten times than those of switching scheme I, but error reduction has been obtained as 53%, 57.36% and 53.63%, for feedrates of 4000, 6000 and 8000 mm/min, respectively.

#### 6.4.3. Switching Control Scheme III

The results in this subsection will be achieved using switching control decision unit with two controllers, each of which serves in a different region of operation: contact and backlash regions. The feed drive model used is similar to that used previously. Friction and damping, also, were considered zero for the ease of calculation. Backlash value of  $12.5\text{ }\mu\text{m}$  is to deal with in this subsection. Reference input has been varied over 4000, 6000 and 8000 mm/min, respectively, using circular interpolation, which are shown in Figures 6.26, 6.27, 6.28, 6.29, 6.30 and 6.31. The control law for contact zone is depicted by equation (4.12), namely, contact-zone controller III, while the control law for backlash zone is depicted by equation (4.16), namely, backlash-zone controller III, is used for this subsection; the controller gains are:

$K_1$	:	1000
$K_2$	:	200
$K_3$	:	25
$K_4$	:	1000
$K_5$	:	200
$K_6$	:	25

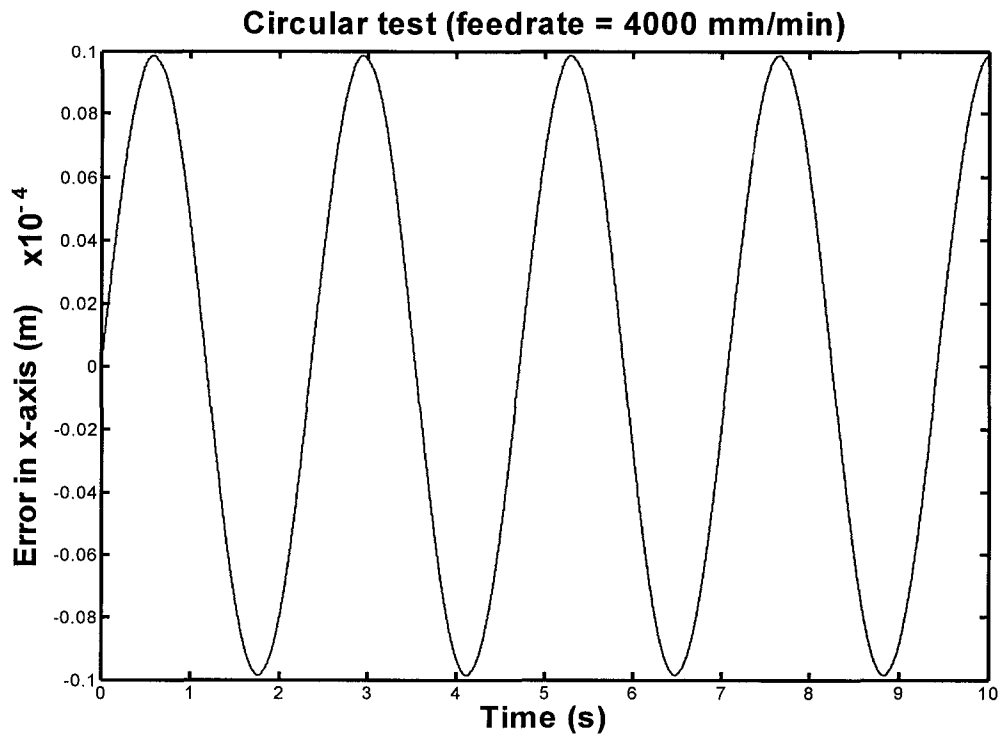


Figure 6.28. Position error of x-axis for switching control III set-up with feedrate of 4000 mm/min.

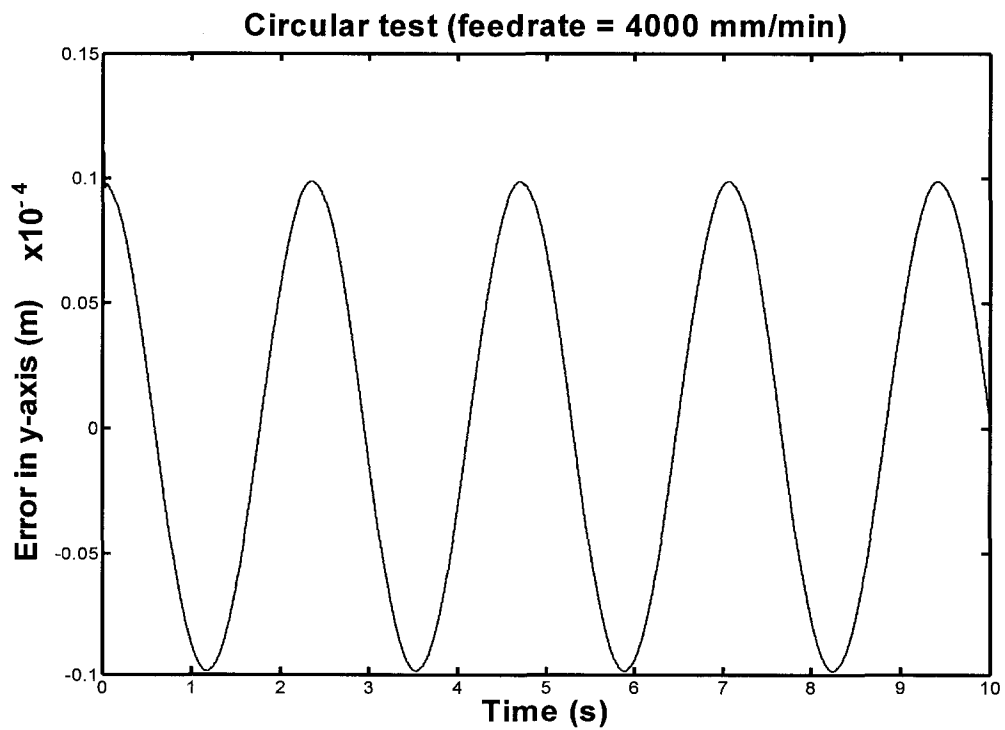


Figure 6.29. Position error of y-axis for switching control III set-up with feedrate of 4000 mm/min.

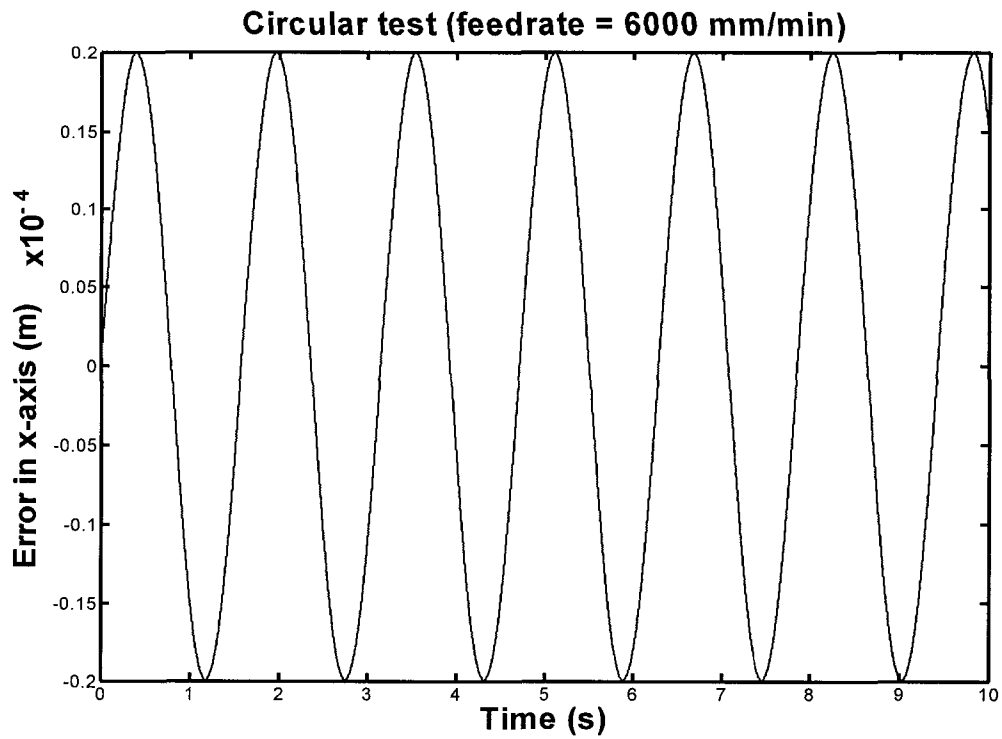


Figure 6.30. Position error of x-axis for switching control III set-up with feedrate of 6000 mm/min.

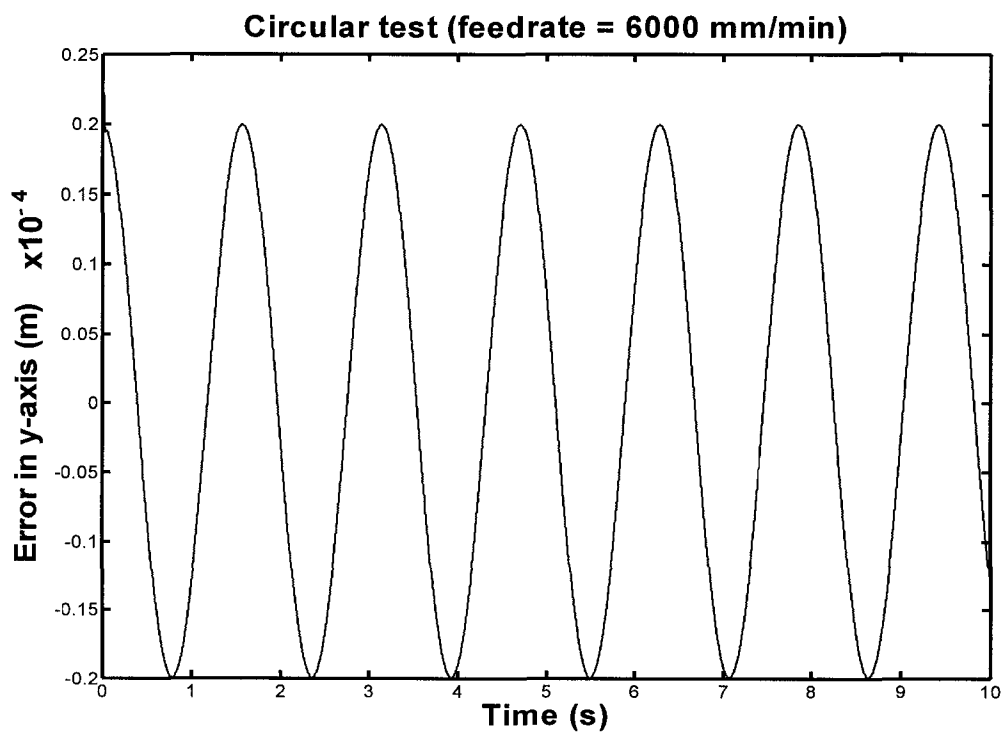


Figure 6.31. Position error of y-axis for switching control III set-up with feedrate of 6000 mm/min.

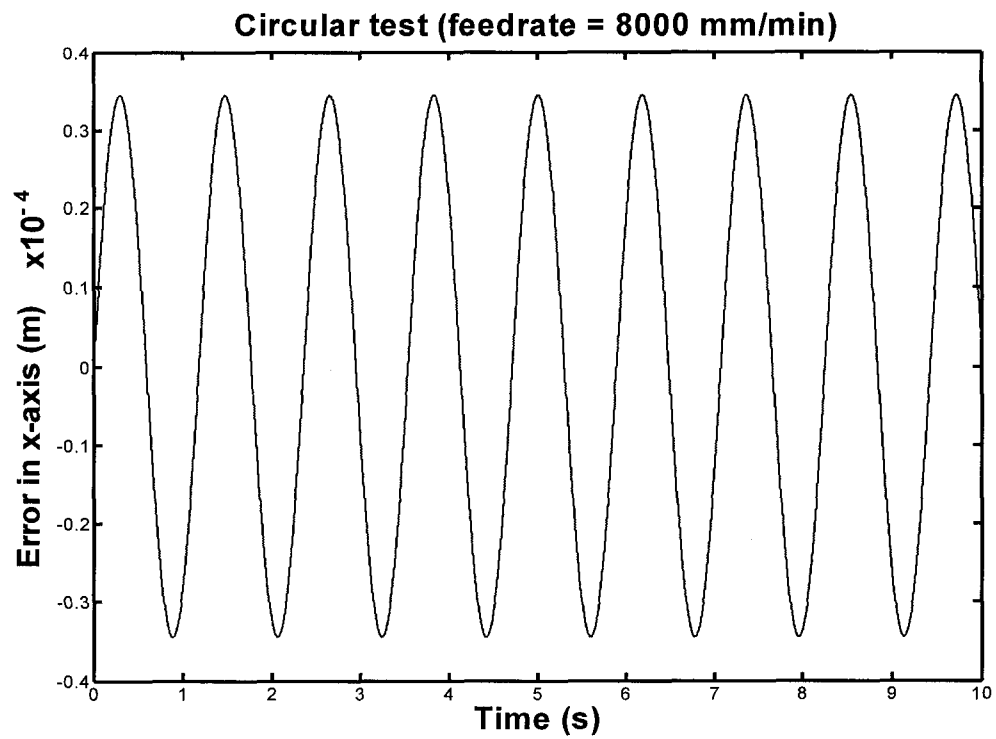


Figure 6.32. Position error of x-axis for switching control III set-up with feedrate of 8000 mm/min.

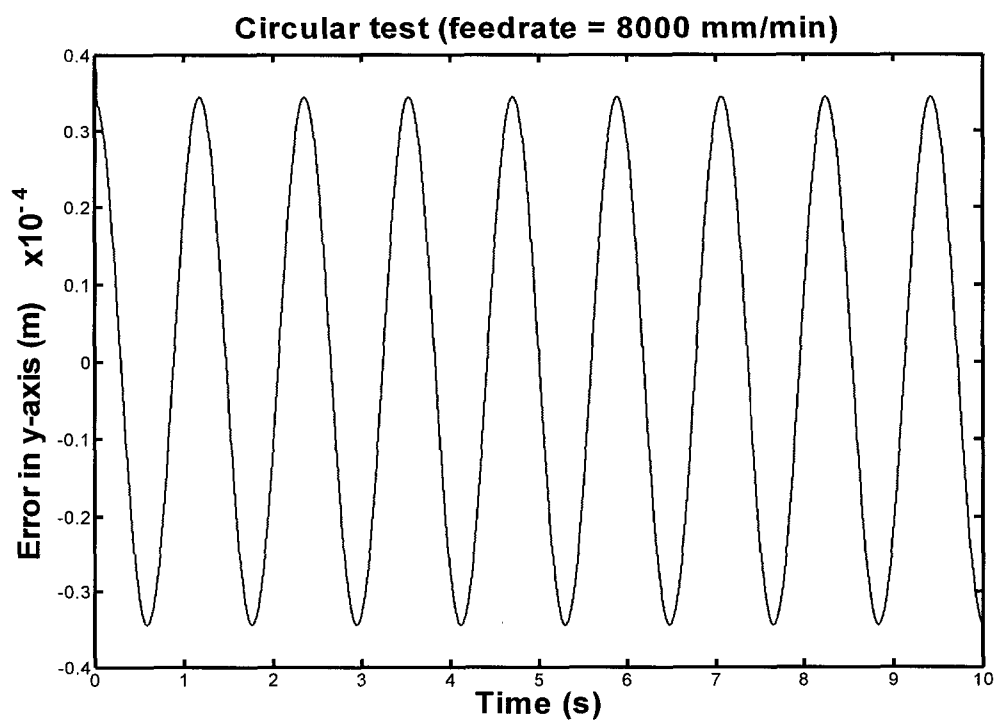


Figure 6.33. Position error of y-axis for switching control III set-up with feedrate of 8000 mm/min

Again in this scheme, switching logic, between the two controllers, depends on measuring the difference between load and motor positions and compares it to the backlash value to assign the needed controller. Error values, which have been produced from simulating this scheme for both identical  $x$ - and  $y$ - axes, are of  $9.21\text{ }\mu\text{m}$ ,  $18.9\text{ }\mu\text{m}$  and  $32.6\text{ }\mu\text{m}$  for 4000, 6000 and 8000 mm/min, respectively. Although, controllers' gains have the same values for of switching scheme II – except the integral part, but error reduction has been obtained by 54.9%, 59.1% and 54.5%, for 4000, 6000 and 8000 mm/min, respectively with respect to switching scheme I error values.

#### 6.4.4. Results Discussion and General Comparison

Comparisons among the three switching control schemes that have been discussed previously are shown using the error in  $x$ -axis plotted against  $y$ -axis, see Figure 6.34. Noticeably, switching schemes II and III show an error reduction by 53.6-54.5% with respect to switching scheme I.

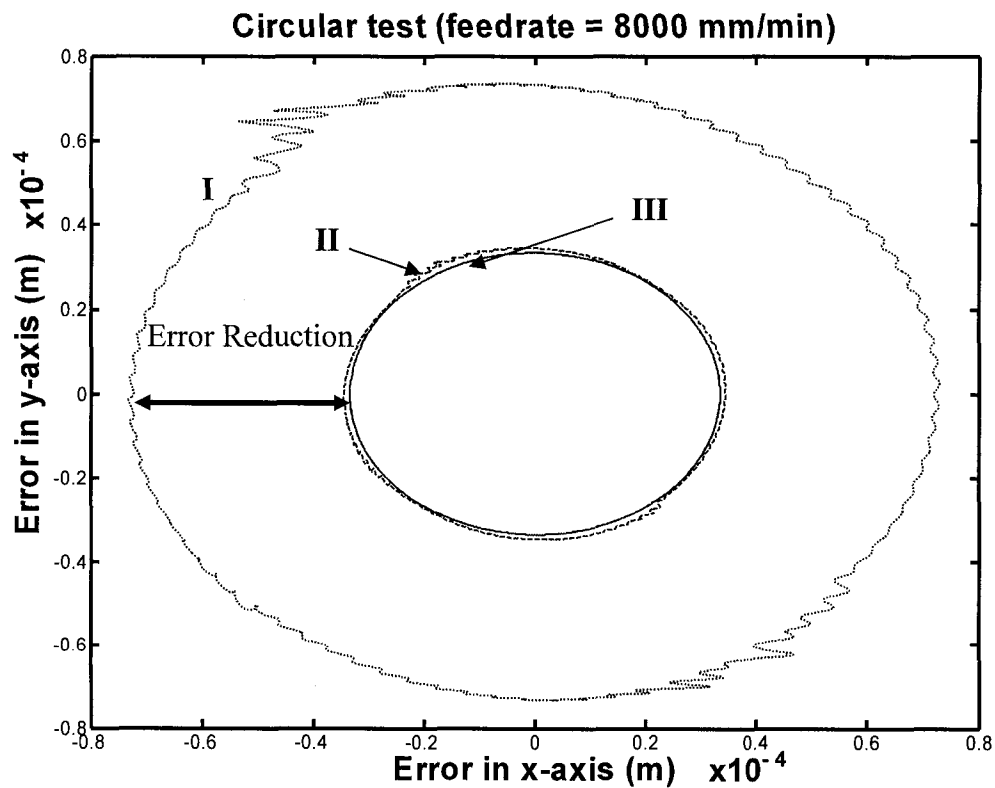


Figure 6.34. Comparison among the three switching schemes at a feedrate of 8000 mm/min

Zooming at switching scheme II and III in particular, see Figure 6.35, the fluctuations along both axes, produced while under switching scheme II, have been cleared out by the use of the integral action in switching scheme III.

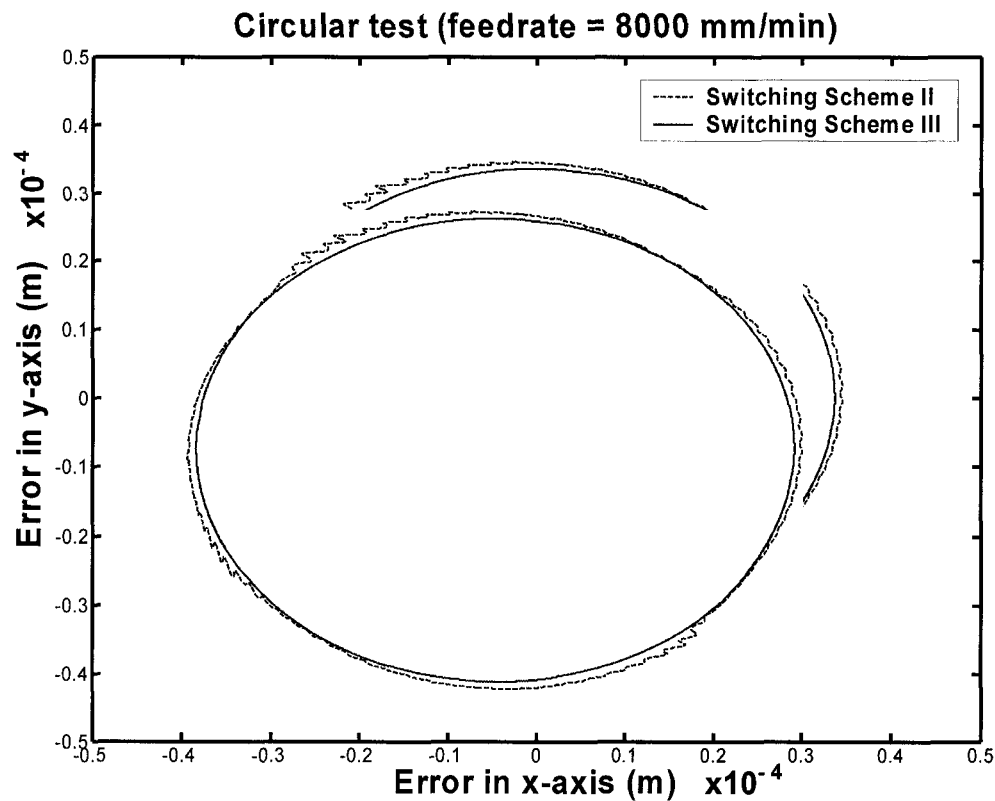


Figure 6.35. A zoomed view at switching schemes II and III at feedrate of 8000 mm/min.

As shown previously, another type of comparison was found to be essential; the output feedrate. The following Figures 6.37, 6.38 and 6.39 are showing output feedrate variations due to the effect of backlash; simulation time has been considered starting from 1 to 10 to neglect the transient effect. Best results have been achieved using switching scheme III as clearly shown by Figure 6.39. The effect of backlash has been reduced to the minimum and the output has had low-magnitude equally-spaced pulses along the feedrate function. This is explained by the exchange process of controllers – switching; A completely smooth switching process is impossible to reach. In switching schemes I and II, It seems that those virtual pulses propagate into higher-magnitude fluctuations without a tangible pattern causing feedrate variations.

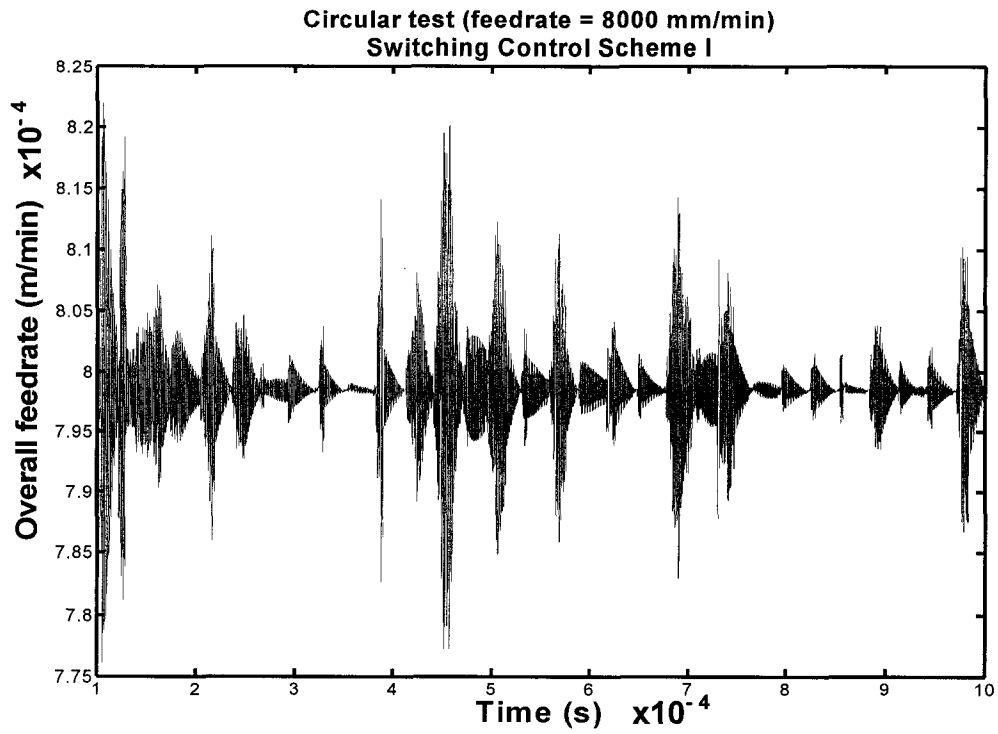


Figure 6.36. The overall feedrate output using switching scheme I.

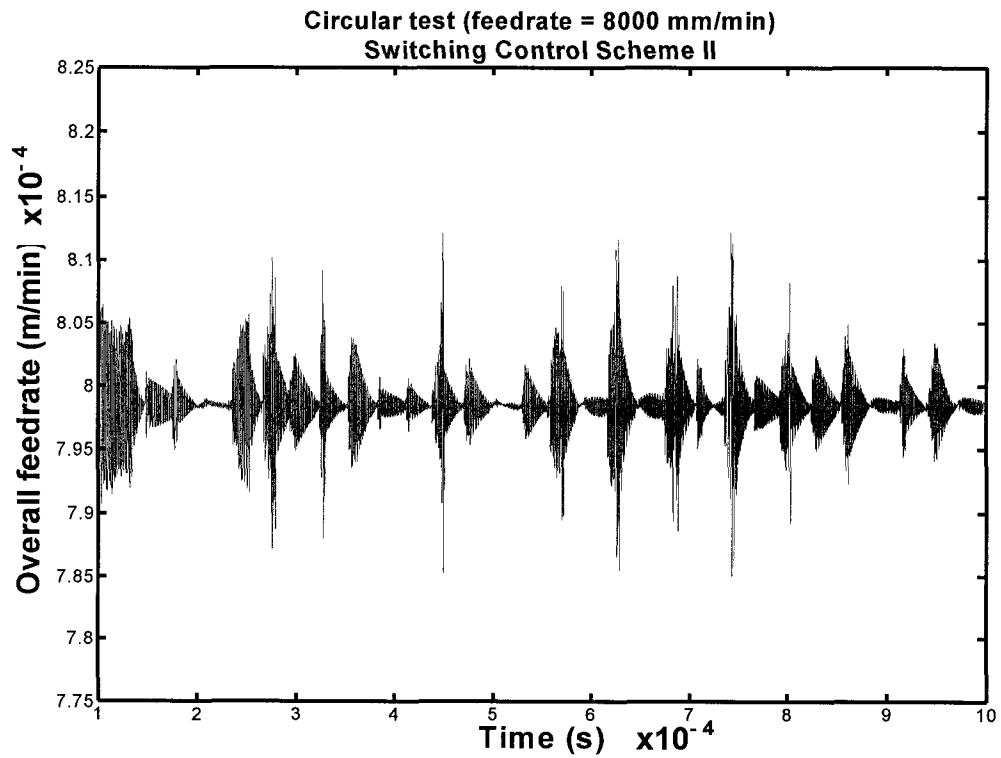


Figure 6.37. The output feedrate output using switching scheme II.



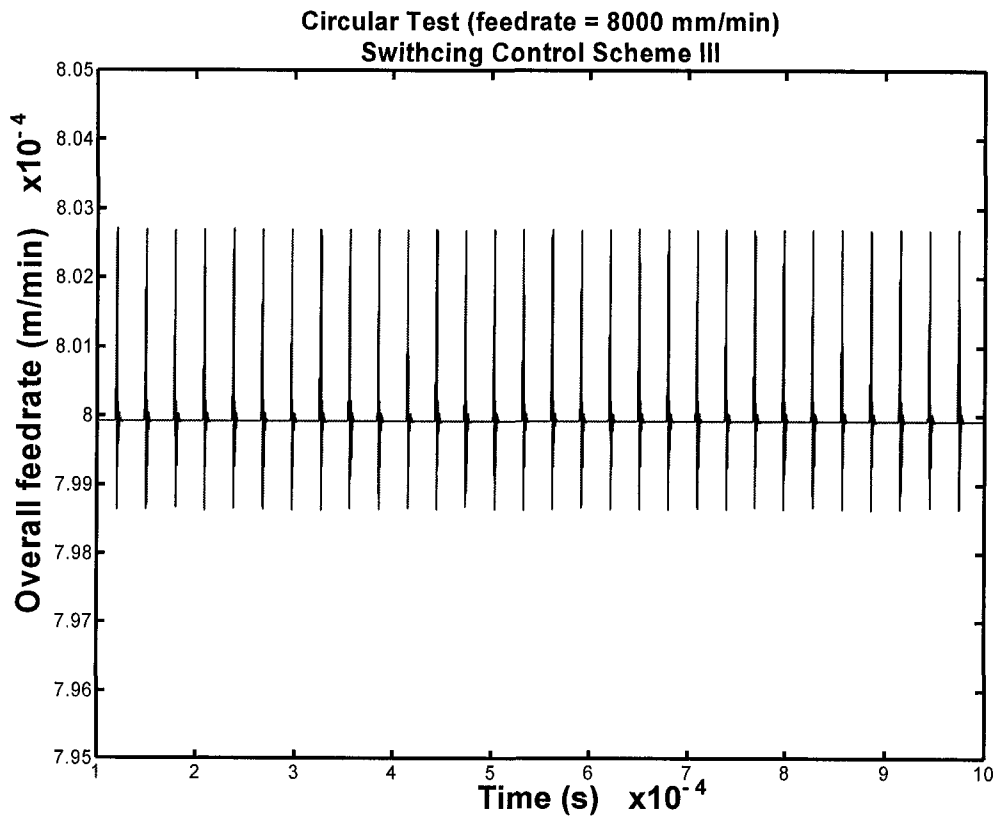


Figure 6.38. The output overall feedrate using switching scheme III.

After introducing the integral part in this scheme, transients were suppressed as discernibly perceived by the previous figures. Error values for the different feedrate inputs are quite the same as those of switching control scheme II. The produced feedrate is quite stable in magnitude with patterned pulse-like small variation (0.027 m/min compared to 0.25 m/min in scheme I). On the other hand, Machine tool feed drive system has been brought forth to steady state in a tremendously fast manner introducing an excellent and successful switching criterion to solve and compensate for the prominent problem of backlash.

## 7. CONCLUSION

Unified Reconfigurable Open Control Architecture (UROCA) is a research project, which aims at unifying the reconfiguration aspects and managing the interaction of individual machining control systems which perform in a reconfigurable manufacturing system. UROCA consists of two essential and integrated halves: deliberative left brain and reactive right brain. UROCA engulfs the idea of supervisory control as a mediator between machine-level entities and a high-level intelligent manager. The work of this thesis can be concluded as following:

1. A profound background has been initiated by undertaking a comprehensive survey about aspects of reconfiguration in machine tools and its reflections on the control process. The physical and control aspects mainly are the target of this study. Although, reconfiguration has numerous faces in this field, the study of implications on the control process by tackling the prominent problem of backlash.
2. A state-of-the-art study of machine tool feed drive systems' modeling and control has been undertaken. In particular, modeling and control of feed drive systems with backlash have been thoroughly investigated.
3. Application of supervisory control principles to earn improved results as expected outcomes of such an approach. This can be visualized by a stable and consistent process while changing from one controller to another due to change in needed functionality. Moreover, the performance of the supervisory control unit successfully switches from one controller to another according to signals measured, and based on that, mathematical operations are undertaken to decide when to switch on or off the backlash controller; hence, the required control signal is generated. Switching in Scheme III shows the optimal case, with regard to the instance of switching and its effect on the whole system, where reflections on feedrate are highly noticeable; i.e. Fluctuations are minimized drastically

compared to those in Scheme I and II. This is considered as an aspect of reconfiguration at the control level that satisfies the objectives of UROCA project at the physical and control layers. All of the proposed schemes have shown great improvement in comparison with the standard (PI) controller; i.e. 32.6  $\mu\text{m}$  compared to 946.3  $\mu\text{m}$ .

4. Different switching schemes, built on a performance-based manner, have been formulated, introduced and simulated to solve for the nonlinear phenomenon of backlash. Results were shown and discussed throughout the study.
5. In switching schemes we are proposing, an error reduction of 53.6-54.5% with regard of the control laws introduced by Tao and his associates in many publications [Tao and Kokotović, 1996; Ling and Tao, 1999; Ezal *et al.*, 1997; etc]. Also, highly-improved overall feedrate output has been achieved; less than 10% of feedrate fluctuations were attained. Scheme III has earned the best performance in position and feedrate outputs due to the applied control algorithm.
6. Such a centralized supervisory technique – a technique that is applied for each axis of motion separately, would prepare the feed drive system to be ready for decentralized control approaches, such as cross-coupling controllers.

All of the previous points emphasize that the output of this thesis depicts a reconfiguration aspect on the control process level for machine tools as perceived, investigated and resolved by the physical and control layers located at the left brain of UROCA architecture.

## **8. FUTURE WORK**

Nowadays, the study of reconfigurable control process for CNC machine tool feed drives is a major concern of academic researchers. Also, UROCA, as a project targeted at the unification of reconfiguration aspects in individual machining systems including both CNC machine tools and robotic systems, is believed to be one amongst many of those efforts spent to reach to a feasible outcome regarding this issue. The future work of mine is fortunately pivoted around the main principles of UROCA and can be summarized by the following points:

1. Investigating other problems and discrepancies, such as friction, that affect the movement of machine tool feed drives. Also, other important entities like cutting forces and viscous damping of machine tool components are to be considered within the feed drive model.
2. Investigating other aspects of reconfiguration and the influence amongst them towards each other.
3. The implementation of switching schemes on Hardware-in-the-Loop concept to verify simulation results using real-time experimentation. Proposal to that concept has been thoroughly discussed in Chapter 5.

## APPENDIX A: SWITCHING SCHEMES CONTROL ALGORITHMS

### Switching Scheme I Controllers Algorithm

Contact region  $x$ -axis controller:

```
function cc_Ix = contact_controllerx(u)

K1x = 2000;                % velocity gain
K2x = 10000;              % Position gain

Jmx = 0.0052;             % Inertia of motor

Thetamx = u(1);           % Measured motor position
Omegamx = u(2);           % Measured motor velocity
Thetalx = u(3);           % Measured load position
Omegalx = u(4);           % Measured load velocity
Thetarx = u(5);           % Reference position input
Omegarx = u(6);           % Reference velocity input
arx = u(7);               % Reference acceleration input

Thetab = 0.0004908738521234051935097880286;

% backlash angle =  $2\pi / l \times b$  where  $b$  is the value of backlash in (mm),  $l$  is the lead.

if (u(1)-u(3)) >= 0.0004908738521234051935097880286
    Thetab = -Thetab;
else
    Thetab = +Thetab;
end

cc_Ix = Jmx*(arx-K1x*(Omegamx-Omegarx+Thetab)-K2x*(Thetamx-
Thetarx+Thetab));

end
```

### Switching Scheme I Controllers Algorithm

Backlash region  $x$ -axis controller:

```
function bc_Ix = backlash_controllerx(u)

K4x = 2000;                % velocity gain
K5x = 10000;               % Position gain

Jmx = 0.0052;              % Inertia of motor

Thetamx = u(1);            % Measured motor position
Omegamx = u(2);            % Measured motor velocity
Thetalx = u(3);            % Measured load position
Omegalx = u(4);            % Measured load velocity
Thetarx = u(5);            % Reference position input
Omegarx = u(6);            % Reference velocity input
arx = u(7);                % Reference acceleration input

Thetab = 0.0004908738521234051935097880286;
% backlash angle =  $2\pi / l \times b$  where  $b$  is the value of backlash in (mm),  $l$  is the lead.

if (u(1)-u(3)) >= 0.0004908738521234051935097880286
    Thetab = -Thetab;
else
    Thetab = +Thetab;
end

bc_Ix = Jmx*(arx-K4x*(Omegamx-Omegalx+Thetab)-K5x*(Thetamx-Thetalx+Thetab));

end
```

### Switching Scheme I Controllers Algorithm

Contact region y-axis controller:

```
function cc_Iy = contact_controllery(u)

K1y = 2000;                % velocity gain
K2y = 10000;              % Position gain

Jmy = 0.0052;             % Inertia of motor

Thetamy = u(1);           % Measured motor position
Omegamy = u(2);           % Measured motor velocity
Thetaly = u(3);           % Measured load position
Omegaly = u(4);           % Measured load velocity
Thetary = u(5);           % Reference position input
Omegary = u(6);           % Reference velocity input
ary = u(7);               % Reference acceleration input

Thetab = 0.0004908738521234051935097880286;

% backlash angle =  $2\pi / l \times b$  where  $b$  is the value of backlash in (mm),  $l$  is the lead.

if (u(1)-u(3)) >= 0.0004908738521234051935097880286
    Thetab = -Thetab;
else
    Thetab = +Thetab;
end

cc_Iy = Jmy*(ary-K1y*(Omegamy-Omegary+Thetab)-K2y*(Thetamy-
Thetary+Thetab));

end
```

### Switching Scheme I Controllers Algorithm

Backlash region y-axis controller:

```
function bc_Iy = backlash_controllery(u)

K4y = 2000;                % velocity gain
K5y = 10000;               % Position gain

Jmy = 0.0052;              % Inertia of motor

Thetamy = u(1);            % Measured motor position
Omegamy = u(2);            % Measured motor velocity
Thetaly = u(3);            % Measured load position
Omegaly = u(4);            % Measured load velocity
Thetary = u(5);            % Reference position input
Omegary = u(6);            % Reference velocity input
ary = u(7);                % Reference acceleration input

Thetab = 0.0004908738521234051935097880286;
% backlash angle =  $2\pi / l \times b$  where  $b$  is the value of backlash in (mm),  $l$  is the lead.

if (u(1)-u(3)) >= 0.0004908738521234051935097880286
    Thetab = -Thetab;
else
    Thetab = +Thetab;
end

bc_Iy = Jmy*(ary-K4y*(Omegamy-Omegaly+Thetab)-K5y*(Thetamy-Thetaly+Thetab));

end
```



## Switching Scheme II Controllers Algorithm

Contact region  $x$ -axis controller:

```
function cc_IIx = contact_controllerx(u)

K1px = 200;                % velocity gain
K2px = 1000;              % Position gain

Jmx = 0.0052;              % Inertia of motor

Thetamx = u(1);            % Measured motor position
Omegamx = u(2);            % Measured motor velocity
Thetalx = u(3);            % Measured load position
Omegalx = u(4);            % Measured load velocity
Thetarx = u(5);            % Reference position input
Omegarx = u(6);            % Reference velocity input
arx = u(7);                % Reference acceleration input

Thetab = 0.0004908738521234051935097880286;

% backlash angle =  $2\pi/l \times b$  where  $b$  is the value of backlash in (mm),  $l$  is the lead.

if (u(1)-u(3)) >= 0.0004908738521234051935097880286
    Thetab = -Thetab;
else
    Thetab = +Thetab;
end

cc_IIx = Jmx*arx-K1px*(Omegamx-Omegarx+Thetab)-K2px*(Thetamx-
Thetarx+Thetab);

end
```

## Switching Scheme II Controllers Algorithm

Backlash region x-axis controller:

```
function bc_IIx = backlash_controllerx(u)

K4px = 200;                % velocity gain
K5px = 1000;               % Position gain

Jmx = 0.0052;              % Inertia of motor

Thetamx = u(1);            % Measured motor position
Omegamx = u(2);            % Measured motor velocity
Thetalx = u(3);            % Measured load position
Omegalx = u(4);            % Measured load velocity
Thetarx = u(5);            % Reference position input
Omegarx = u(6);            % Reference velocity input
arx = u(7);                % Reference acceleration input

Thetab = 0.0004908738521234051935097880286;
% backlash angle =  $2\pi / l \times b$  where  $b$  is the value of backlash in (mm),  $l$  is the lead.

if (u(1)-u(3)) >= 0.0004908738521234051935097880286
    Thetab = -Thetab;
else
    Thetab = +Thetab;
end

bc_IIx = Jmx*arx-K4px*(Omegamx-Omegalx+Thetab)-K5px*(Thetamx-
Thetalx+Thetab);

end
```

## Switching Scheme II Controllers Algorithm

Contact region  $y$ -axis controller:

```
function cc_Ily = contact_controllery(u)

K1py = 200;                % velocity gain
K2py = 1000;               % Position gain

Jmy = 0.0052;              % Inertia of motor

Thetamy = u(1);            % Measured motor position
Omegamy = u(2);            % Measured motor velocity
Thetaly = u(3);            % Measured load position
Omegaly = u(4);            % Measured load velocity
Thetary = u(5);            % Reference position input
Omegary = u(6);            % Reference velocity input
ary = u(7);                % Reference acceleration input

Thetab = 0.0004908738521234051935097880286;

% backlash angle =  $2\pi/l \times b$  where  $b$  is the value of backlash in (mm),  $l$  is the lead.

if (u(1)-u(3)) >= 0.0004908738521234051935097880286
    Thetab = -Thetab;
else
    Thetab = +Thetab;
end

cc_Ily = Jmy*ary-K1py*(Omegamy-Omegary+Thetab)-K2py*(Thetamy-
Thetary+Thetab);

end
```

### Switching Scheme II Controllers Algorithm

Backlash region  $y$ -axis controller:

```
function bc_Ily = backlash_controllery(u)

K4py = 200;                % velocity gain
K5py = 1000;               % Position gain

Jmy = 0.0052;              % Inertia of motor

Thetamy = u(1);            % Measured motor position
Omegamy = u(2);            % Measured motor velocity
Thetaly = u(3);            % Measured load position
Omegaly = u(4);            % Measured load velocity
Thetary = u(5);            % Reference position input
Omegary = u(6);            % Reference velocity input
ary = u(7);                % Reference acceleration input

Thetab = 0.0004908738521234051935097880286;
% backlash angle =  $2\pi/l \times b$  where  $b$  is the value of backlash in (mm),  $l$  is the lead.

if (u(1)-u(3)) >= 0.0004908738521234051935097880286
    Thetab = -Thetab;
else
    Thetab = +Thetab;
end

bc_Ily = Jmy*ary-K4py*(Omegamy-Omegaly+Thetab)-K5py*(Thetamy-
Thetaly+Thetab);

end
```

### Switching Scheme III Controllers Algorithm

Contact region x-axis controller:

```
function cc_IIIx = contact_controllerx(u)

K1px = 200;           % velocity gain
K2px = 1000;          % Position gain
K6x = 25              % Integral gain on position

Jmx = 0.0052;         % Inertia of motor

Thetamx = u(1);        % Measured motor position
Omegamx = u(2);        % Measured motor velocity
Thetalx = u(3);        % Measured load position
Omegalx = u(4);        % Measured load velocity
Thetarx = u(5);        % Reference position input
Omegarx = u(6);        % Reference velocity input
arx = u(7);           % Reference acceleration input
Thetamx_i = u(8);      % integral of measured motor position
Thetarx_i = u(9);      % integral of reference position input

Thetab = 0.0004908738521234051935097880286;

% backlash angle =  $2\pi/l \times b$  where  $b$  is the value of backlash in (mm),  $l$  is the lead.

if (u(1)-u(3)) >= 0.0004908738521234051935097880286
    Thetab = -Thetab;
else
    Thetab = +Thetab;
end

cc_IIIx = Jmx*arx-K1px*(Omegamx-Omegarx+Thetab)-K2px*(Thetamx-
Thetarx+Thetab)-K6x*(Thetamx_i-Thetarx_i);

end
```

### Switching Scheme III Controllers Algorithm

Backlash region  $x$ -axis controller:

```
function bc_IIIx = backlash_controllerx(u)

K4px = 200;           % velocity gain
K5px = 1000;          % Position gain
K6x = 25              % Integral gain on position

Jmx = 0.0052;         % Inertia of motor

Thetamx = u(1);       % Measured motor position
Omegamx = u(2);       % Measured motor velocity
Thetalx = u(3);       % Measured load position
Omegalx = u(4);       % Measured load velocity
Thetarx = u(5);       % Reference position input
Omegarx = u(6);       % Reference velocity input
arx = u(7);           % Reference acceleration input
Thetamx_i = u(8);     % integral of measured motor position
Thetarx_i = u(9);     % integral of reference position input

Thetab = 0.0004908738521234051935097880286;
% backlash angle =  $2\pi / l \times b$  where  $b$  is the value of backlash in (mm),  $l$  is the lead.

if (u(1)-u(3)) >= 0.0004908738521234051935097880286
    Thetab = -Thetab;
else
    Thetab = +Thetab;
end

bc_IIIx = Jmx*arx-K4px*(Omegamx-Omegalx+Thetab)-K5px*(Thetamx-
Thetalx+Thetab)-K6x*(Thetamx_i-Thetarx_i);

end
```

### Switching Scheme III Controllers Algorithm

Contact region  $y$ -axis controller:

```
function cc_IIIy = contact_controllery(u)

K1py = 200;           % velocity gain
K2py = 1000;          % Position gain
K6y = 25              % Integral gain on position

Jmy = 0.0052;         % Inertia of motor

Thetamy = u(1);        % Measured motor position
Omegamy = u(2);        % Measured motor velocity
Thetaly = u(3);        % Measured load position
Omegaly = u(4);        % Measured load velocity
Thetary = u(5);        % Reference position input
Omegary = u(6);        % Reference velocity input
ary = u(7);            % Reference acceleration input
Thetamy_i = u(8);       % integral of measured motor position
Thetary_i = u(9);       % integral of reference position input

Thetab = 0.0004908738521234051935097880286;

% backlash angle =  $2\pi/l \times b$  where  $b$  is the value of backlash in (mm),  $l$  is the lead.

if (u(1)-u(3)) >= 0.0004908738521234051935097880286
    Thetab = -Thetab;
else
    Thetab = +Thetab;
end

cc_IIIy = Jmy*ary-K1py*(Omegamy-Omegary+Thetab)-K2py*(Thetamy-
Thetary+Thetab)-K6y*(Thetamy_i-Thetary_i);

end
```

### Switching Scheme III Controllers Algorithm

Backlash region  $y$ -axis controller:

```
function bc_IIIy = backlash_controllery(u)

K4py = 200;           % velocity gain
K5py = 1000;          % Position gain
K6y = 25               % Integral gain on position

Jmy = 0.0052;         % Inertia of motor

Thetamy = u(1);        % Measured motor position
Omegamy = u(2);        % Measured motor velocity
Thetaly = u(3);        % Measured load position
Omegaly = u(4);        % Measured load velocity
Thetary = u(5);        % Reference position input
Omegary = u(6);        % Reference velocity input
ary = u(7);            % Reference acceleration input
Thetamy_i = u(8);       % integral of measured motor position
Thetary_i = u(9);       % integral of reference position input

Thetab = 0.0004908738521234051935097880286;
% backlash angle =  $2\pi/l \times b$  where  $b$  is the value of backlash in (mm),  $l$  is the lead.

if (u(1)-u(3)) >= 0.0004908738521234051935097880286
    Thetab = -Thetab;
else
    Thetab = +Thetab;
end

bc_IIIy = Jmy*ary-K4py*(Omegamy-Omegaly+Thetab)-K5py*(Thetamy-
Thetaly+Thetab)-K6y*(Thetamy_i-Thetary_i);

end
```



## REFERENCES

- Ahmad, S. [1985], "Second order nonlinear kinematic effects and their compensation," *Proceedings of CDC '85*, pp. 307-314.
- Alter, D. M. and Tsao, T.-C., [1996], "Control of linear motors for machine tool drives: Design and implementation of  $H_\infty$  optimal feedback control," *ASME J. Dyn. Sys., Meas., and Control*, Vol. 118, pp. 649-656, December 1996.
- Alter, D. M. and Tsao, T.-C., [1996], "Control of linear motors for machine tool feed drives: Experimental investigation of optimal feedforward tracking control," *ASME J. Dyn. Sys., Meas., and Control*, Vol. 120, pp. 137-142, March 1998.
- Altintas, Y., [2000], *Manufacturing automation: metal cutting mechanics, machine tool vibrations, and CNC design*, Cambridge University Press.
- Astrom, K. J., and Wittenmark, B., [1984], *Computer controlled systems: theory and design*, Englewood Cliffs, NJ: Prentice-Hall.
- Azenha, A. and Tenreiro Machado, J. R., [1996], "Variable structure control of systems with nonlinear friction and dynamic backlash," *Proceedings of IFAC World Congress*, San Francisco.
- Board on Manufacturing and Engineering Design, Commission on Engineering and Technical Systems, [1998], *Visionary Manufacturing Challenges for 2020*, National Research Council National Academy Press, Washington, D.C., 1998.
- Bohez, E. L. J., [2002], "Five-axis milling machine tool kinematic chain design and analysis," *International Journal Of Machine Tool and Manufacture*, Vol. 42, No. 4, pp. 505-520, 2002.
- Boneh, R. and Yaniv, O., [1999], "Reduction of limit cycle amplitude in the presence of backlash," *Journal of Dynamic Systems, Measurement and Control*, Vol. 121, pp. 278-284.
- Brandenburg, G. [1986], "Stability of a speed controlled elastic two-mass system with backlash and Coulomb friction and optimization by a load observer," *Symposium: Modelling and simulation for control of lumped and distributed parameter systems*, Lille, New Brunswick, NJ, pp. 107-113.
- Brandenburg, G. and Schafer, U., [1987], "Influence and partial compensation of backlash for a position controlled elastic two-mass system," *Proceedings of the European Conference on Power electronics and Applications*, Grenoble, France, pp. 1041-1047.

- Brandenburg, G. and Schafer, U., [1989], "Influence and adaptive compensation simultaneously acting backlash and Coulomb friction in elastic two-mass systems of robots and machine tools," *Proceedings of ICCON '89*, Jerusalem, NY, pp. WA-4-5.
- Brandenburg, G., [1987], "Stability of a speed-controlled elastic two-mass system with backlash and Coulomb friction and optimization by a disturbance observer," *Proceedings of the IMACS Conference on Applied Modelling and Simulation of Dynamical Systems, Sao Paolo, Brazil*, pp-243-255.
- Brandenburg, G., Geissenberger, S., Kink, C., Schall, N. -H. and Schramm, M., [1999], "Multi motor electronic line shafts for rotary printing presses: A revolution in printing machine techniques," *IEEE/ASME Transactions on Mechatronics*, Vol. 4, No. 1, pp. 25-31.
- Brandenburg, G., Unger, H. and Wagenpfeil, A., [1986], "Stability problems of a speed controlled drive in an elastic system with backlash and corrective measures by a load observer," *Proceedings of the International conference on Electrical Machines*, Munchen, Germany, pp. 523-527.
- Bredworth, D. D., Henderson, M. R. and Wolfe, P. M., *Computer-Integrated Design and Manufacturing*, McGraw-Hill, 1991.
- Brown, N. and Parkin, R. M., [1998], "A Mechatronics system for the improvement of surface form in planed and moulded timber components," *Proceedings of the 6th UK Mechatronics Forum International Conference (Mechatronics '98)*, pp. 173-179, New York City, September 9-11, UK Mechatronics Forum Centre for intelligent Automation.
- Chen, Y., Tlustý, J., [1995], "Effect of low friction guideways and lead-screw flexibility on dynamics of high-speed machines," *Annals of the CIRP*, Vol. 44/1, pp. 353-356.
- Chestnut, H., [1954], "Approximate frequency-response methods for representing saturation and dead band," *Transaction of the ASME*, pp. 1345-1363.
- Choi, G. -H, Nakamura, H. and Kobayashi, H., [1996], "Calibration of servo systems with redundant actuators," *Proceedings of IFAC world congress*, San Francisco, pp. 169-174.
- Chou, J. -J. and Yang, D. C., [1991], "Command generation for three-axis CNC machining," *ASME Journal of Engineering for Industry*, Vol. 113, No. 3, pp. 305-310, August 1991.

- Chou, J. -J. and Yang, D. C., [1992], "On the generation of coordinated motion of five-axis CNC/ CMM machines," *ASME Journal of Engineering for Industry*, Vol. 114, No. 1, pp. 15-22, February 1992.
- Cohen, M. and Cohen, I., [1994], "The use of worm gear transmissions in electromechanical systems: Analysis, digital control and application," *The 25<sup>th</sup> Israel Conference on mechanical engineering*, pp. 175-182.
- Dean, S. R. H., Surgenor, B. W. and Iordanou, H. N., [1995], "Experimental evaluation of a backlash inverter as applied to a servo-motor with gear train," *Proceedings of the IEEE Conference on Control Applications*, pp. 580-585.
- Desoer, C. A. and Shahrucz, S. M., [1986], "Stability of dithered non-linear systems with backlash or hysteresis," *International Journal of Control*, Vol. 43, No. 4, pp. 1045-1060.
- Dhaouadi, R., Kubo, K. and Tobise, M., [1994], "Analysis and compensation of speed drive systems with Torsional load," *IEEE Transactions on Industry Applications*, Vol. 30, No 3, pp. 760-766.
- Dubowsky, S. and Freudenstein, F., [1971A], "Dynamic analysis of mechanical systems with clearances – Part I: Formation of dynamic model," *ASME Jour. Eng. for Ind.*, Vol. 93, pp. 305-309, February 1971.
- Dubowsky, S. and Freudenstein, F., [1971B], "Dynamic analysis of mechanical systems with clearances – Part II: Dynamic response," *ASME Jour. Eng. for Ind.*, Vol. 93, pp. 310-316, February 1971.
- Ebrahimi, M., [2000], "Machine tool drivetrain modeling using computer-aided control system design," *International Journal of Computer Applications in Technology*, Vol. 13, Nos. 3/4/5, 2000.
- Ebrahimi, M., Whalley, R., [2000], "Analysis, modeling and simulation of stiffness in machine tool drives," *International Journal of Computers and Industrial Engineering*, Vol. 8, pp 93-105.
- ElBeheiry, E., ElMaraghy, W. and ElMaraghy, H., [2004], "The structured design of a reconfigurable Control Process," *14<sup>th</sup> CIRP Design Seminar 2004, Cairo Egypt May 14-18, 2004 – Design in the Global Village, section 7B-1*.
- Elijah Kannatey-Asibu, Jr., [1997], "New concepts on multi-sensor monitoring for reconfigurable machining systems." <http://eclipse.engin.umich.edu/Publications/PubFiles/TA3/ProjR2/MultiSensorModeling.pdf>
- Ezal, K., Kokotović, P. V. and Tao, G., [1997], "Optimal control of tracking systems with backlash and flexibility," *Proceedings of the 36<sup>th</sup> IEEE Conference on Decision and Control*, pp. 1749-1754.

- Freeman, E. A., [1957], "An approximate transient analysis of a second-order position-control system when backlash is present," *IEE Mono.*, Vol. 254 M, pp.61-68, September 1957.
- Freeman, E. A., [1959], "The effect of speed dependent friction and backlash on the stability of automatic control systems," *Transaction of the American IEE*, pp 680-691.
- Freeman, E. A., [1960], "The stabilization of control systems with backlash using a high-frequency on-off loop," *IEE Mono.*, Vol. 31, pp. 150-154, February 1960.
- Friedland, B., [1997], "Feedback control of systems with parasitic effects," *Proceedings of the American Control Conference*, Albuquerque, NM, USA, pp. 937-941.
- Gerdes, J. C. and Kumar, V., [1995], "An impact model of mechanical backlash for control system analysis," In *Proc. Amer. Control Conf. ACC*, pp. 3311-3315, June 1995.
- Golnaraghi, M. F., Lin, D.-C., and Fromme P., [1995], "Gear damage detection using chaotic dynamics techniques: A preliminary study. Cudney, H. H., editor. *ASME Proc. Eng. Tech.*, pp. 121-127, New York City, September 1995.
- Green, M. and Limebeer, D. J. N., [1995], *Linear robust control*, Prentice Hall, Englewood Cliffs.
- Harris, C. M. and Crede, C. E., editors, [1961], *Shock and Vibration Handbook*. Number §9 in McGraw-Hill Handbooks. McGraw-Hill, New York City, 1961.
- Hori, Y., Iseki, H. and Sugiura, K., [1994], "Basic consideration of vibration suppression and disturbance rejection control of multi-inertia system using SFLAC (state feedback and load acceleration control)," *IEEE Transactions on Industry Applications*, Vol. 30, No. 4, pp. 889-896.
- Horowitz, I. M., [1991], "Survey of quantitative feedback theory (QFT)," *International Journal of Control*, Vol. 53, No. 2, pp. 255-291.
- Indri, M. and Tornambè, A., [1997], "Application of a PD controller on two mating gears with elasticity and backlash," *Proceedings of the 36<sup>th</sup> conference on decision and control*, San Diego, NY, USA, pp. 4363-4368.
- Johansson, M. and Rantzer, A., [1997], "Computation of piecewise quadratic Lyapunov functions of hybrid systems," *Proceedings of the 30<sup>th</sup> conference on decision and control*, Sand Diego, NY, USA, Vol. 4, pp. 3515-3520.

- Johansson, M. and Rantzer, A., [1998], "Computation of piecewise quadratic Lyapunov functions for hybrid systems," *IEEE Transactions on Automatic Control*, Vol. 45, No. 4, pp. 555-559.
- Johansson, M., [1999], *Piecewise linear control systems*, Ph.D. thesis, Department of Automatic Control, Lund University, Sweden.
- Kao, J. Y. *et al.*, [1996], "A study of backlash on the motion accuracy of CNC lathes," *Int. J. Mach. Tools and Manuf.*, Vol. 36, No. 5, pp. 539-550, 1996.
- Kato, S., Sato, N., and Matsubayashi, [1972], T., "Some considerations on characteristics of static friction of machine tool slideway," *ASME J. Lub. Tech.*, Vol. 93, pp. 234-247, February 1972.
- Kokotović, P. V., Ezal, K. & Tao, G., [1997], "Optimal control of tracking systems with backlash and flexibility," *Proceedings of the 36<sup>th</sup> IEEE conference on decision and control*, San Diego, CA, pp. 1749-1754, 1997.
- Koren, Y. and Lo, [1992], "Advanced controllers for feed drives," *Annals of the CIRP*, Vol. 41, No. 2, pp. 689-698, 1992.
- Koren, Y., [1978], "Design of a digital loop for numerical control," *IEEE Transactions on Industrial Electronics and Control Instrumentation, IECI(3)*, pp. 212-217.
- Koren, Y., [1980], "Cross-coupled biaxial computer control for manufacturing systems," *ASME Journal of Dynamic Systems, Measurement and Control*, Vol. 102, No. 4, pp. 265-272, 1980.
- Koren, Y., [1984], *Computer Control of Manufacturing Systems*, McGraw-Hill.
- Koren, Y., Heisel, U., Jovane, F., Moriwaki, T., Pritchow, G., Van Brussel, H., Ulsoy, A.G., [1999], "Reconfigurable manufacturing systems," *Annals of the CIRP*, Vol. 48, No. 2, (*keynote paper*).
- Kulkarni, P., Sirnivasan K., [1991], "Identification of discrete time dynamic models for machine tool feed drives," *Modeling of machine tools, ASME, Pub. PED-45*, pp. 1-20.
- Lauderbaugh, L., Ulsoy, A., [1988], "Dynamic modeling for control of milling process," *ASME Journal for Industry*, Vol. 110, pp. 367-375.
- Lin, Z., [1997], "Global control of linear systems with saturating actuators," *Gang Tao, editor. J. IEEE Proc. Dec. Control*, pp. 4357-4362, New York City, December 1996.

- Ling, Y. and Tao, G., [1999], "Numerical design and analysis of backlash compensation for a multivariable nonlinear tracking system," *Proceedings of the American Control Conference*, San Diego, CA, USA, pp. 3539-3543.
- Lo, C.-C., [1998], "A New approach to CNC tool path generation," *Computer-Aided Design*, Vol. 30, No. 8, pp. 649.
- Ma, X. and Tao, G., [2000], "Adaptive actuator compensation control with feedback linearization," *IEEE Transactions on Automatic Control*, Vol. 45, No. 9, pp. 1705-1710.
- Macki, J. W., Nistri, P. and Zecca, P., [1993], "Mathematical models for hysteresis," *SIAM Rev.*, Vol. 35, No. 1, pp.94-123, March 1993. Survey paper.
- Matsubara A., Kakino, Y. and Watanbe, Y., [2000], "Servo performance enhancement of high speed feed drives by damping control," *Proceedings of the 2000 Japan-USA Flexible Automation Conference, July 23-26, 2000, Ann Arbor MI*.
- McKechnie, J. L., editor. [1983], *Merriam Webster's New Universal Unabridged Dictionary*. Simon and Schuster, New York City, fourteenth edition, 1983.
- Mehrabi, M., Ulsoy, A. and Koren, Y., [1998], "Reconfigurable manufacturing systems: Key to future manufacturing," in *The 1998 Japan-USA Symposium on Flexible Automation*, pp. 677--682, Otsu, Japan, July 1998.
- Mehrabi, M.G., Ulsoy, A.G., Koren, Y., [2000], "Reconfigurable manufacturing system and their enabling technologies," *International J. of Manufacturing Technology and Management*, Vol. 1, No. 1, pp. 113-130.
- Nakayama Y., Fujikawa, K. and Kobayashi, H., [2000], "A torque control method of three-inertia torsional system with backlash," *Proceedings of the IEEE International Workshop on Advanced Motion Control*, pp. 193-198.
- Nordin, M. and Gutman, P. O., [2000], "Nonlinear speed control of elastic systems with backlash," *Proceedings of the 39<sup>th</sup> IEEE conference on decision and control*, Sydney, New York, pp. ThP13-4.
- Nordin, M. and Gutman, P.-O., [1995], "A robust linear design of an uncertain two-mass system with backlash," *Proceedings of the IEEE International Workshop on Advanced Motion Control*, pp. 234-239.
- Nordin, M. and Gutman, P.-O., [2002], "Controlling mechanical systems with backlash – a survey," *Automatica*, vol. 38, No. 10, pp. 1633-1649, 2002.

- Nordin, M., [2000], *Nonlinear backlash compensation for speed controlled elastic systems*, Ph.D. thesis, Division of Optimization and Systems Theory, Royal Institute of Technology, 10044 Stockholm, Sweden.
- Nordin, M., Galić, J. and Gutman, P.-O., [1997], "New models for backlash and gearplay," *Int. J. Adaptive Control Sig. Proc.*, Vol. 11, pp. 49-63, May 1997.
- Odai, M., and Hori, Y., [1998], "Speed control of 2-inertia system with gear backlash using gear torque compensator," *Proceedings of the IEEE International Workshop on Advanced Motion Control*, pp. 234-239.
- Oldak, S., Bail, C., and Gutman, P. O., [1994], "Quantative design of a class of nonlinear systems with parameter uncertainty," *International Journal of Robust and Nonlinear Control*, 4, pp. 101-117.
- Olgac, N. and Iragavarapu, V. R., [1995], "Sliding mode control with backlash and saturation laws," *Int. J. Robot. Auto.*, Vol. 10, No. 2, pp. 49-55, 1995.
- Owen, E. W., [1959], "A phase-space and analogue computer study of some feedback control systems containing backlash and compensating nonlinearities," Master's thesis, Rensselaer Polytechnic Institute, Troy, New York, June 1959. C. H. Dunn, advisor.
- Pan, M. C. *et al.*, [1995], "Diagnosis of the joint backlash of a mechanism: Wigner-ville distribution combined with correlation techniques," Cudney, H. H., editor. *ASME Proc. Eng. Tech.*, pp. 1405-1412, New York City, September 1995.
- Parkin, R. M., Kallenbach, E. and Saffert, E., editors, [1997], *Control and Configuration Aspects of Mechatronics*, Institute of Microsystems Technology, Mechatronics and Mechanics, Postfach 100565, D-98684 Ilmenau, Thuringia, Deutschland, September 21-26, 1997. Euro Conference in Focused Aspects of Mechatronics, Tech. Uni.-Ilmenau, Faculty of Mech. Eng.
- Poo, R. P., Bollinger, J. G. and Younkin, W., [1972], "Dynamic errors in type 1 contouring systems," *IEEE Transactions on Industrial Applications*, Vol. IA-8, No. 4, pp. 477-484, 1972.
- Pritschow *et al.*, [2003], "Requirements for controllers in reconfigurable machining systems," *CIRP 2<sup>nd</sup> International Conference on Reconfigurable Manufacturing*, Ann Arbor MI, A20, August 2003.
- Pritschow, G., and Muller, J., [1997], "Object-oriented modeling of numerical control modules," *Production Engineering*, Vol. IV, pp.83-86.

- Recker, D. A., [1997], "Indirect adaptive non-linear control of discrete time systems containing a dead-zone," *Int. J. Adaptive Control Sig. Proc.*, Vol. 11, pp. 33-48, February 1997.
- Renton, D., Elbestawi, M., [2001], "Motion control for linear motor feed drives in advanced machine tools," *International Journal of Machine Tools & Manufacture*, Volume 41, pp 479-507.
- Schafer, U. and Brandenburg, G., [1991], "State position control for elastic pointing and tracking systems with gear play and Coulomb friction - a summary of results," *Proceedings of the European conference on power electronics and applications*, Firenze, Italy, pp. 596-602.
- Seidl, D. R. *et al.*, [1995], "Neural network compensation of gear backlash hysteresis in position-controlled mechanisms," *IEEE Trans. App. Ind.*, Vol. 31, No. 6, pp. 1475-1483, November/December 1995.
- Shahruz, S.M., [2000], "Performance enhancement of a class of nonlinear systems by disturbance observers," *IEEE/ASME Transactions on Mechatronics*, Vol. 5, No. 3, pp. 319-323.
- Slotine, J. J. and Li, W., [1991], *Applied nonlinear control*, Englewood Cliffs, NJ: Prentice-Hall International.
- Song, D.-J., "Monitoring and Compensating Spindle Bearing Compliance Using an electromagnetic Exciter", website: [http://batman.kjist.ac.kr/publication/paper/International\\_Proceeding/2000EUSPEN\\_Monitoring%20and%20Compensating%20Spin%20idle%20Bearing%20Compliance%20using%20an%20Electromagnetic%20Exciter.pdf](http://batman.kjist.ac.kr/publication/paper/International_Proceeding/2000EUSPEN_Monitoring%20and%20Compensating%20Spin%20idle%20Bearing%20Compliance%20using%20an%20Electromagnetic%20Exciter.pdf).
- Srinivasan, K. and Tsao, T. C., [1997], "Machine tool feed drives and their control – a survey of the state of the Art," *ASME Journal of Manufacturing Science and Engineering*, Vol. 119, pp. 743-748, November 1997.
- Stein, J. L. and Wang, C.-H., [1998], "Estimation of gear backlash: Theory and simulation," *ASME J. Dyn. Sys., Meas., and Control*, Vol. 120, pp. 74-82, March 1998.
- Stewart, D. E. and Trinkle, J. C., [1996], "An implicit time-stepping scheme for rigid body dynamics with inelastic collisions and Coulomb friction," *Int. J. Num. Meth. in Eng.*, Vol. 39, pp. 2673-2691, 1996.
- Su, C. -Y., Stepanenko, Y., Svoboda, J. and Leung, T. P., [2000], "Robust adaptive control of a class of nonlinear systems with unknown backlash-like hysteresis," *IEEE Transactions on Automatic Control*, Vol. 45, No. 12, pp. 2427-2432.



- Sugie, H., Iwasaki, T., Nakagawa, H., and Kohda, S., [2000], "Compensation for position-varying lost motion to improve the contouring Accuracy of NC Machine Tools," *Proceedings of the Industrial Electronics Conference*, Vol. 3, pp.2213-2218, 2000.
- Sun X., Zhang W. and Jin Y., [1992], "Stable adaptive control of backlash nonlinear systems with bounded disturbances," *J. IEEE Proc. Dec. Control*, pp. 274-275, New York City, December 1992.
- Suzuki, A. and Tomizuka, M., [1991], "Design and implementation of digital servo controller for high speed machine tools," In *Proc. Amer. Control Conf. ACC*, TA6, pp. 1246-1251. American Control Council, American Control Council, 1991.
- Tao G., [1999], "Hybrid control of sandwich systems with nonsmooth nonlinearities," *Proceedings of the 14<sup>th</sup> World Congress of IFAC*, vol. C, Beijing, China, pp. 97-102.
- Tao, G. and Kokotović, P. V., [1993], "Adaptive control of systems with backlash," *Technical report*, UC-Santa Barbara, Santa Barbara, California, 1993. Copy of presentation slides from 1993 SIAM conference.
- Tao, G. and Kokotović, P. V., [1995], "Discrete-time adaptive control of systems with unknown deadzones," *Int. J. Control*, Vol. 61, No.1, pp.1-17, 1995.
- Tao, G. and Kokotović, P. V., [1996], *Adaptive Control of Systems with Actuator and Sensor Nonlinearities*. Wiley Series on Adaptive and Learning Systems for Signal Processing, Communications, and Control. John Wiley & Sons, New York, London, Sydney, 1996.
- Tao, G. and Kokotović, V., [1993], "Adaptive control of systems with backlash," *Automatica*, Vol. 9, No. 2, pp. 323-335.
- Tao, G. and Kokotović, V., [1994], "Adaptive control of plants with unknown dead-zones," *IEEE Transactions on Automatic Control*, Vol. 39, No. 1, pp. 59-68.
- Tao, G. and Kokotović, V., [1995a], "Adaptive control of plants with unknown hystereses," *IEEE Transactions on Automatic Control*, Vol. 40, No. 2, pp. 200-212.
- Tao, G. and Kokotović, V., [1995b], "Adaptive control of systems with unknown output backlash," *IEEE Transactions on Automatic Control*, Vol. 40, No. 2, pp. 326-330.
- Tao, G. and Kokotović, V., [1995c], "Continuous-time adaptive control of systems with unknown backlash," *IEEE Transactions on Automatic Control*, Vol. 40, No. 6, pp. 1083-1087.

- Tao, G. and Kokotović, V., [1996], *Adaptive Control of Systems with Actuator and Sensor Nonlinearities*, Wiley, New York.
- Tao, G., [1996], "Adaptive control of systems with nonsmooth input and output nonlinearities," *IEEE Trans. Auto. Control*, Vol. 41, No. 9, pp.1348-1352, September 1996.
- Tao, G., Ma, M. and Ling, Y., [2001], "Optimal and nonlinear decoupling control of systems with sandwiched backlash," *Automatica*, Vol. 37, No. 2, pp. 165-176.
- Tarng, Y. S. and Cheng, H. E., [1995], "An investigation of stick-slip friction on the contouring accuracy of CNC machine tools," *Int. J. Mach. Tools and Manuf.*, Vol. 35, No. 4, pp. 565-576, 1995.
- Tarng, Y. S., Lao, J. Y. and Lin, Y. S., [1997], "Identification of and compensation for backlash on the contouring accuracy of CNC machining centers," *International Journal of Advanced Manufacturing Technology*, Vol. 13, No. 2, pp. 77-85.
- Taware, A. and Tao, G., [1999], "Analysis and control of sandwich systems," *Proceedings of the 38<sup>th</sup> IEEE Conference on Decision and Control*, Vol. 2, Phoenix, AZ, USA, pp. 1156-1161.
- Taware, A. and Tao, G., [2000], "Design and analysis of hybrid control schemes for sandwich nonlinear systems," *Proceedings of the American Control Conference*, Vol. 3, Chicago, IL, USA, pp. 1669-1673.
- Taylor, J. H. and Lu, J., [1993], "Robust nonlinear control system synthesis method for electromechanical pointing systems with flexible modes," *Proceedings of the American Control Conference*, vol. 1, Evanston, IL, USA, pp. 536-540.
- Taylor, J. H. and Strobel, K. L., [1985], "Nonlinear compensator syntheses via sinusoidal-input describing functions," *Proceedings of the American Control Conference*, pp. 1242-1247.
- The Math Work Inc, *The Student Edition of MATLAB, Version 5 User's Guild*, Englewood Cliff: Prentice Hall.
- Thomas, C. H., [1954], "Stability characteristics of closed loop systems with dead band," *Transactions of ASME*, pp. 1365-1382.
- Tornambè, A. and Valigi P., [1994], "A decentralized controller for the robust stabilization of a class of mimo dynamical systems," *ASME J. Dyn. Sys., Meas., and Control*, Vol. 116, pp. 293-304, June 1994.
- Tornambè, A., [1996], "Modelling and controlling one-degree-of-freedom impacts," *IEE Proc. Control Th. App.*, Vol. 143, No. 1, pp. 85-90, January 1996.

- Tsutsumi, M., et al., [1995], "Mathematical model of feed drive mechanical system and friction for CNC machine tools," *Journal of Japan Society of Precision Engineering*, Vol. 61, No. 10, pp. 1458-1463.
- Tung, E. D., Anwar, G. and Tomizuka, M., [1993], "Low-velocity friction compensation and feedforward solution based on repetitive control. *ASME J. Dyn. Sys., Meas., and Control*, Vol. 115, pp. 279-284, June 1993.
- Tung, E. D., Urushisaki, Y. and Tomizuka, M., [1993], "Low-velocity friction compensation for machine tool feed drives," In *Proc. Amer. Control Conf. ACC*, pp. 1932-1936, June 1993.
- Tustin, A., [1947A], "The effects of backlash and of speed-dependent friction on the stability of closed-cycle control systems," *IEE J.*, Vol. 94, No. 2A, pp. 143-151, 1947.
- Tustin, A., [1947B], "A method of analysing the effect of certain kinds of non-linearity in closed-cycle control systems. *IEE J.*, Vol. 94, No. 2A, pp. 151-160, 1947.
- University of Michigan, ERC-NSF webpage <http://erc.engin.umich.edu/about.htm>
- Weck, M., [1984], "Handbook of Machine Tools," Vol. 2 & 3, *John Wiley & Son*.
- Weng, S.-W. and Young, K.-Y., [1996], "An impact control scheme inspired by human reflex," *J. Rob. Sys.*, Vol. 13, No. 12, pp. 837-855, 1996.
- Yang, J. -H. and Fu, L. -C., [1996], "Nonlinear adaptive control for manipulator system with gear backlash," *Proceedings of the 35<sup>th</sup> IEEE Conference on Decision and Control*, Kobe, Japan, pp. 4369-4374.
- Yang, J. -S., [1992]. "Design of sampled-data control systems with one memoryless, time-invariant nonlinearity using QFT technique," *Proceedings of the American Control Conference*, Chicago, IL, USA, pp. 915-916.
- Yang, J.-H. and Fu, L.-C., [1996], "Nonlinear adaptive control for a manipulator system with gear backlash," *Gang Tao, editor. J. IEEE Proc. Dec. Control*, pp. 4369-4374, New York City, December 1996.
- Yang, S. and Tomizuka, M., [1987], "Adaptive pulse-width control for precise positioning under influence of stiction and Coulomb friction," In *Proc. Amer. Control Conf. ACC*, WA6, pp. 188-193. American Control Council, American Control Council, 1987.
- Yang, S. and Tomizuka, M., [1988], "Adaptive pulse width control for precise positioning under the influence of stiction and Coulomb friction," *ASME J. Dyn. Sys., Meas., and Control*, Vol. 110, pp. 221-227, September 1988.

- Youcef-Toumi, K. and Gutz, D. A., [1994], "Impact and force control: Modeling and experiments," *ASME J. Dyn. Sys., Meas., and Control*, Vol. 116, pp. 89-98, March 1994.
- Zhou, L, Rundensteiner, E. A., Shin, K. G., [1995], "OODB Support for real-time open-architecture controllers," Proceedings of the Fourth *International Conference on Database Systems for Advanced Applications (DASFAA'95)*, pp. 206-213, Singapore, April 1995.

## VITA AUCTORIS

NAME: Rami Shahin

PLACE OF BIRTH: Kuwait City, State of Kuwait

YEAR OF BIRTH: 1977

EDUCATION: Bishop's High School, Amman, Jordan  
1990-1995

Applied Science University, Amman, Jordan  
1995-2001 B.Sc.

University of Windsor, Windsor, Ontario  
2002-2004 M.Sc.